Vysoké učení technické v Brně
Fakulta strojního inženýrství
Ústav konstruování

Brno University of Technology
Faculty of Mechanical Engineering
Institute of Machine and Industrial Design

STUDY OF CORRELATION BETWEEN GREASE FILM FORMATIONS AND MECHANICAL LOSSES ON VARIOUS SURFACES

MEng. Kazumi Sakai
Autor práce
Author

prof. Ing. Ivan Křupka, Ph.D.
Vedoucí práce
Supervisor

Disertační práce
Dissertation Thesis

Brno 2018

STATEMENT

I hereby declare that I have written the PhD thesis *Study of Correlation between Grease Film Formations and Mechanical Losses on Various Surfaces* on my own according to advice of my supervisor prof. Ing. Ivan Křupka, Ph.D., and using the sources listed in references.

Brno, _____ _____

Kazumi Sakai

BIBLIOGRAPHICAL REFERENCE

SAKAI, K. *Study of Correlation between Grease Film Formations and Mechanical Losses on Various Surfaces*. PhD thesis. Brno University of Technology, Faculty of Mechanical Engineering, Institute of Machine and Industrial Design. Supervisor: prof. Ing. Ivan Křupka, Ph.D.

ACKNOWLEDGEMENT

I would like to appreciate my supervisor, prof. Ing. Ivan Křupka, Ph.D. and the head of Tribology research group, prof. Ing. Martin Hartl, Ph.D. for their support and advices during my whole doctoral study. Special thanks must be devoted to Ing. David Košťál, Ph.D. for his great assistance on my experiments and papers. Also, I would like to thank to prof. Motohiro Kaneta for the powerful recommendation and support for my overseas study in the Czech Republic. I would like to thank to all my colleagues at Institute of Machine and Industrial Design for friendly and positive atmosphere.

I would like to thank to my colleagues of our company, JXTG Nippon Oil & Energy Corporation, especially, Dr. Shitara, Mr. Komiya, Mr. Konishi, Mr. Sakamoto, Mr. Yaguchi, Dr. Hoshino, and our grease team for the support for my overseas study. The findings in this study should contribute to the development of the novel lubricants, I believe.

Finally, I would like to thank to my family. I appreciate the stiff support for my heart from my wife, Miyuki. I would like to thank to my daughters, Ruri and Midori for their innocent smiles. I would like to thank to my mother, Yoshiko for letting me go overseas study with patience.

ABSTRACT

In this dissertation thesis, radial ball bearing torque tendency was evaluated with Li type greases, considering base oil and thickener dependence. Analyses of the reason why each grease formulation provides the different bearing torque were conducted considering comprehensive grease properties, such as rheological parameter and thickener structure and friction and film thickness behaviors of EHL films. Observation of EHL film thickness measured by colorimetric interferometry has enabled detailed insight into the behavior of grease within smooth and dented surfaces. Investigating grease film thickness behaviors on non-smooth surfaces and discussing the influence on the bearing torque were novel approaches in this field. It was found that the film thickness behaviors seem to have a relationship with bearing torque at low rotation speeds and the yield stress and traction behaviors correlated with the bearing torque values at high rotation speed conditions. It was observed that the grease thickener entrainments to the contact areas influence on the film thickness at low speed and track pattern formations at the downstream of the contact areas, and starvation behaviors. The reason of the thickener entrainments exists on the chemical structure of thickeners. The high polarity of the hydroxyl group of the thickener promotes the entrainments to the contact surfaces. On the dented surfaces, the grease with the highest polarity showed the frequent entrainments to the dent areas. The obtained findings could be significant knowledge for the development of advanced greases featuring energy-saving performance of machine parts.

KEYWORDS

Grease, thickener, bearing torque, film thickness, colorimetric interferometry, surface texturing, EHL

ABSTRAKT

Tato disertační práce je zaměřena na studium vlivu vlastností základového oleje a zpevňovadla na velikost třecího momentu kuličkového ložiska mazaného plastickým mazivem s lithným mýdlem. Při posuzování příčin rozdílného průběhu třecího momentu v závislosti na složení plastického maziva byly zohledněny komplexní charakteristiky plastického maziva včetně reologických vlastností a struktury zpevňovadla a změny v tloušťce EHD mazacího filmu a velikosti tření. Změny v tloušťce mazacího filmu byly stanovovány pomocí kolorimetrické interferometrie, což umožnilo detailní studium chování plastických maziv mezi hladkými povrchy i povrchy s cíleně modifikovanou topografií. Zohlednění vlivu cílené modifikace topografie na tloušťku mazacího filmu při užití plastického maziva a detailní analýza průběhu třecího momentu ve valivém ložisku představují hlavní přínos této práce. Bylo zjištěno, že změny v tloušťce mazacího filmu lze vztahovat k velikosti třecího momentu ložiska při nízkých otáčkách a na základě meze toku plastického maziva a velikosti tření lze popsat chování třecího momentu ložiska za vysokých otáček. Dále bylo pozorováno, že schopnost zpevňovadla vstupovat do kontaktu má vliv na tloušťku filmu, vzhled kavitační oblasti na výstupu kontaktu a hladovění. Zda zpevňovadlo vstupuje do kontaktu souvisí zejména s jeho chemickou strukturou. Vysoká polarita hydroxylových skupin zpevňovadla podporuje jeho vtahování kontaktními povrchy. U maziva s nejvyšší polaritou byla na površích s cílenou modifikací topografie prokázána nejčastější přítomnost zpevňovadla v blízkosti důlků. Získané výsledky by mohly významně přispět k vývoji pokročilých plastických maziv navrhovaných s cílem snižování energetické náročnosti provozu strojních součástí.

KLÍČOVÁ SLOVA

Plastické mazivo, zpevňovadlo, třecí moment ložiska, tloušťka mazacího filmu, kolorimetrická interferometrie, cílená modifikace topografie povrchu, EHL

CONTENTS

1 INTRODUCTION

Use of lubricants featuring energy-saving property plays a significant role in reducing CO_2 emissions for prevention of the serious global warming. For instance, Holmberg et al. [1] have reported that 33% of fuel chemical energy is consumed by friction loss in the case of a passenger car driving at 60km/h. The impact is not small, therefore, not only liquid lubricants, such as motor oils and industrial lubricants, but also greases have been developed with improved energy-saving properties, such as low friction and torque properties. Greases are used for lubrication of more than 90% of rolling element bearings [2], therefore the industrial significance is high. Recently novel grease products effective in lowering energy consumption have been developed in some grease suppliers, but the detailed mechanisms have not been clarified. The mechanisms of the performance are quite important for not only the persuasion of customers but also further development of grease products. Therefore, the clarification of the influence of grease components on bearing torques is of crucial importance.

There are limited number of publications related to the bearing torque and grease components. In the study with the thrust ball bearings, Cousseau et al. [3, 4] reported commercial greases influence and they introduced a bearing friction model and decomposed a total friction torque into a rolling torque and a sliding torque. The rolling torque was high with greases containing higher viscosity base oils. While, the sliding torque was increased by greases with higher friction coefficient and lower film thickness. By investigating rheological parameters, it was shown that the rolling torque was dependent on the viscosity of the bleed oil and that the sliding torque depended on the specific film thickness with the bleed oil [5]. The following research by Goncalves et al. [6] was conducted for the polypropylene thickened greases. The rolling torque increased with increment of the bearing rotation speed, while the sliding torque decreased. In addition, the grease with large thickener content provided lower sliding torque. As the work on the cylindrical roller bearing, Wikstrom et al. [7] studied greases and operating parameters influences on bearing torques, especially focused on the low temperature region. Regarding grease parameters, base oil types and base oil viscosity were important factors, for instance, poly-alpha-olefin with superior viscosity index to naphthenes provided low starting torque.

For the study of radial ball bearing torque with greases, Oikawa et al. [8] suggested a relationship between the grease yield stress and the bearing torque. They used lithium (Li) type greases with different types of base oils and indicated a grease with higher yield stress caused the channeling in a bearing more easily, and that led to bearing torque reduction. Hokao et al. [9] reported a subsequent study, which indicated higher degree of dispersion of the thickener of the greases related to higher yield stress through the observation of thickener structures by using of AFM (Atomic Force Microscopy). Dong et al. [10] studied base oil viscosity dependence of Li type greases on radial ball bearing torque and the film thickness by using of the electrical potential method. It was confirmed that the grease forming higher film thickness reduced the bearing friction torque under the low bearing rotation speed due to higher viscosity base oil. Heyer et al. [11] measured the friction and the bearing torque for greases with different penetrations and temperatures using a modified low-temperature torque tester for ball bearings. The yield stress of greases influenced on the friction and the temperature effect for only one type grease was discussed for the

bearing torque. In the previous study, authors [12] investigated radial ball bearing torque with several types of greases with different types of base oils and thickeners. Higher film thickness formed the grease with thin and long thickener fiber structures reduced bearing torque. Also the tendency of thickener type corresponded to the grease flows observed by the fluorescence technique, Li complex type grease showed higher existence of lubricant in the inlet of EHL contact area.

Considering bearing operating conditions, the study of EHL under grease lubrication should be essential. Venner et al. [13, 14] estimated the central film thickness decay in ball and roller bearings by numerical simulations of grease flows. They observed that grease film thickness in a bearing decrease significantly and the bearing be operated under starved lubrication, therefore, film thickness under not only fully flooded but also staved conditions should be considered. Cann et al. [15] analyzed grease film thickness related rolling element bearings. Furthermore, Cann [16, 17] reported typical grease film thickness behaviors under fully flooded and starved conditions. Under fully flooded conditions and low speed area, grease thickener lumps pass through the contact and form greater film thickness than the base oil itself. Cousseau et al. [18] also indicated greases and bled oils from the greases form similar film thicknesses under fully flooded conditions. Recently, it was reported that polymer thickened greases show also quite thick film thickness in low-medium speed range [19]. Laurentis et al. [20] compared the film thickness and friction coefficient of commercial greases for bearing. The friction was governed by base oil types in the high speed region and depended on the thickener type in the low speed region. Kaneta et al. [21] investigated the film thicknesses for different types of urea greases. The thickness largely depended on thickener types and the thickener structures seemed to influence on grease movements related to starvations. Cen et al. [22] observed the film thicknesses of greases in a full bearing by using a capacitance method and obtained a good correlation with the results of a single contact condition of optical interferometry method.

As mentioned above, the overview of researches related with bearing torque with grease lubrication are shown. In the next chapter, the detailed explanations for each research fields will be conducted.

2 STATE OF THE ART REVIEW

2.1 Bearing torque under grease lubrication

The publications related to bearing torque can be roughly divided to thrust bearing and radial bearing types. Cousseau et al. [3, 5] investigated the influence of commercial greases on thrust bearing torque. Thrust ball bearings lubricated with several commercial greases were tested on a modified Four-Ball Machine, where the Four-Ball arrangement was replaced by a bearing assembly (Fig.1). A rolling bearing friction torque model was introduced and decomposed a total friction torque into a rolling torque and a sliding torque. The relationship each torque and grease parameters such as rheology and film thickness was evaluated.

The measured values of the bearing friction torque are plotted against the bearing rotational speed in Fig.2. Also, the SKF rolling bearing friction torque model (Eq.1) was introduced for the calculation of the ratios of rolling and sliding torque for total friction torque (Fig. 2). Greases containing higher viscosity base oils (MG1 and MG2) generated higher rolling torque.

$$M_{\text{total}} = \varphi_{\text{ish}}\varphi_{rs}\underbrace{(G_{rr}(vn)^{0.6})}_{M_{rr}} + \underbrace{(G_{sl}(\mu_{sl}))}_{M_{sl}} + \underbrace{(V_M K_{\text{ball}} d_m{}^5 n^2)}_{M_{\text{drag}}} + \underbrace{(K_{S1} d_s^{\beta} + K_{S2})}_{M_{\text{seal}}} \quad (1)$$

They also studied the influence of grease rheological parameter and proposed that the rolling torque was dependent on the viscosity of the bleed oil of the grease (Fig.3 left) and the sliding torque was dependent on the specific film thickness with the bleed oil (Fig. 3 right). That suggested that the sliding torque increased by higher friction coefficient and lower film thickness, especially related to contact replenishment and starvation. Even though the studies are related to thrust bearing type, they used the model to decompose the total friction torque into the rolling and the sliding ones, and suggested a trade-off relationship in reducing the both torque. Since using lowered viscosity base oil for a grease could reduce the rolling torque, however, that might increase the sliding torque due to lower film thickness and higher friction coefficient. In addition, they indicated that the essence of the bearing torque with greases exist on the bleeding oil of the grease not grease itself.

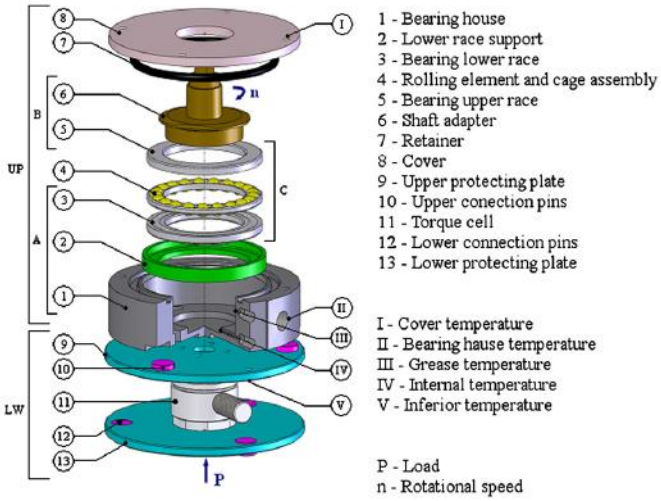

Fig. 1 Schematic view of the rolling bearing assembly with torque cell [3]

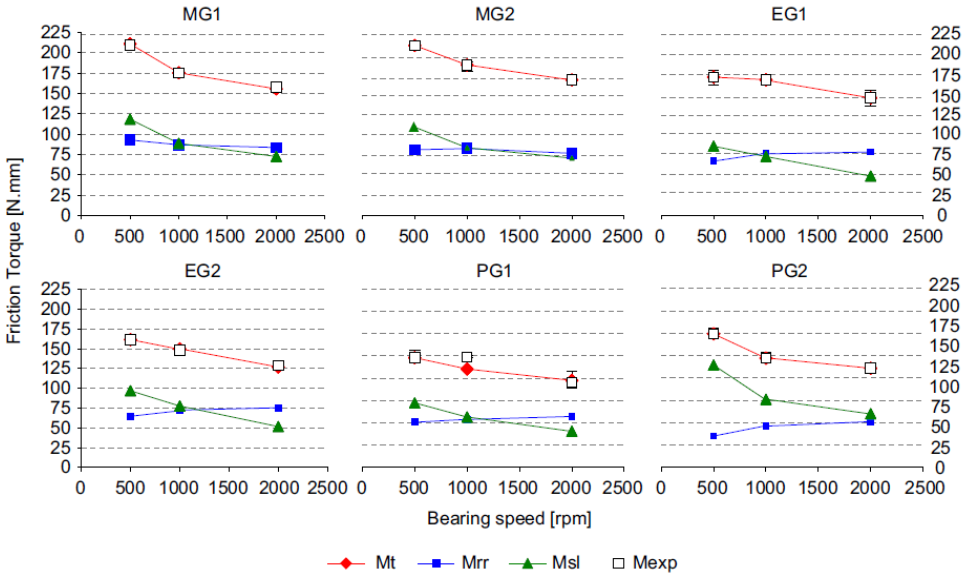

Fig. 2 Experimental torque (M_{exp}), rolling (M_{rr}), sliding (M_{sl}) and total torque (M_t) calculated vs. rotational speed [3]

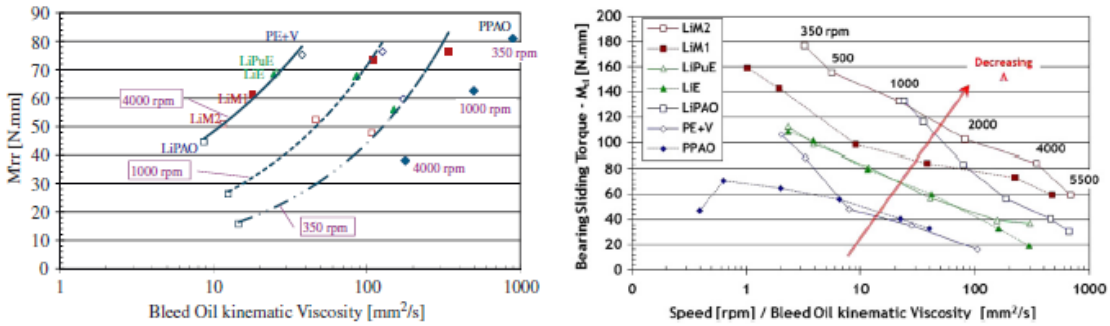

Fig. 3 (left) Bearing rolling torque vs. bleed oil viscosity [5].
Fig. 3 (right) Bearing sliding torque vs. speed / bleed oil viscosity [5].

As studies on radial ball bearing torque, Oikawa et al. [8] investigated the lithium (Li) type thickener greases with different base oils. Test greases were composed of lithium 12-hydroxystearate thickener and five types of base oils of poly alpha olefin (PAO), carbonate ester (COE), polyol ester (POE), and two types of poly alkylene glycol (PAG) with the same range of viscosity. Deep-grooved radial ball bearing 6305 were used and the initial torque and the steady-state torque were measured for the constant rotation speed. As shown in Fig. 4 left, PAO and PAG-3 greases showed lower initial torques and the torque values stayed almost flat. On the contrary, the torque with POE grease significantly decreased at the initial stage of the duration before it became constant. The torque decrease from initial torque is plotted in Fig.4 right. It shows that the grease with higher yield stress shows larger torque decrease and that the grease with higher yield stress tends to show channeling, which is effective in torque reduction.

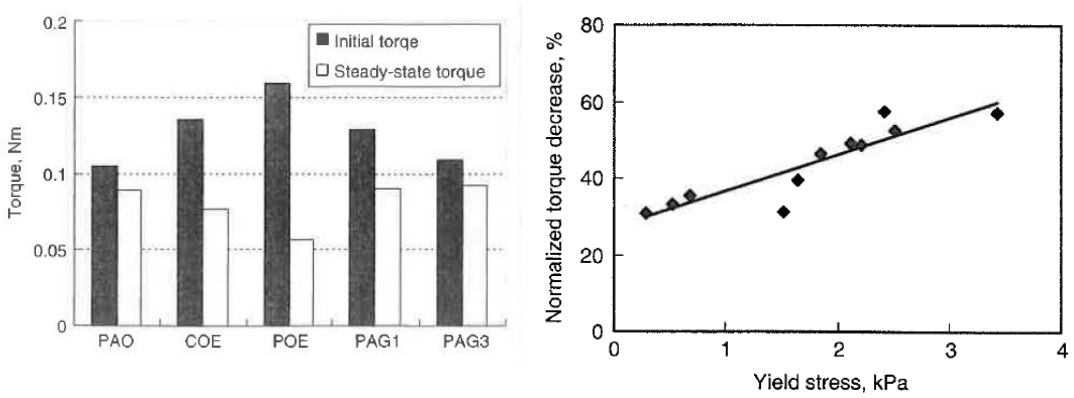

Fig. 4 (left) Initial torque and steady-state torque of tested greases [8]
Fig. 4 (right) Relationship between yield stress and torque decrease [8]

In the initial stage of the bearing operation, the grease is sheared by the moving parts and causes high bearing torque (or temperature increase) due to the drag losses [23, 24]. This is called churning phase. Through this phase, most of the grease is pushed away from the running track. Due to this grease clearing, the drag losses from grease shearing decrease. As a result, the bearing torque reaches at a steady low value, called the channeling phase. Hutton suggested the optimun clearability of grease is important for bearing operations as shown in Fig. 5.

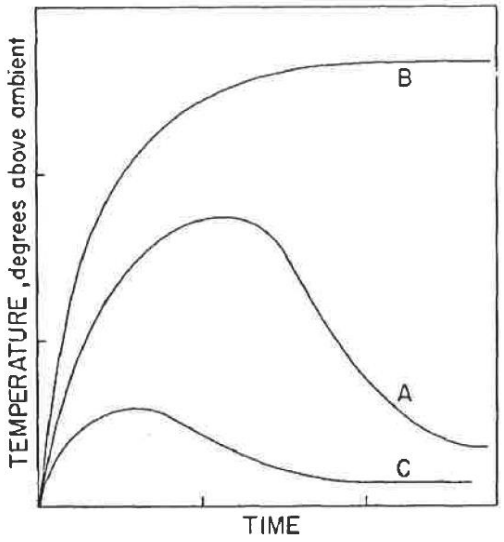

Fig. 5 Representative temperature profiles for bearing operation [23]
A: Optimum clearbility
B: Low clearability gives hot running
C: High clearability causes winding-out

Hokao et al. [9] investigated the correlation of the yield stress of the greases and other parameters, the thickener structures of greases were tested using atomic force microscope (AFM). The thickener structures of greases were observed by AFM (Fig. 6 left). As the parameters for AFM images, size, shape, number, density, and distribution were evaluated. The density and distribution related to the grease yield stress. In addition, the factor of grease dispersion showed good correlation with the yield stress (Fig. 6 right). These results indicates greases with a larger value of the degree of dispersion have higher yield stress.

Oikawa et al. proposed the yield stress of greases as an important factor for radial ball bearing torque. They emphasize the rheological parameter or the movement of grease itself, different from the bleed oil of greases as Seabra et al. proposed. However, the effect of the yield stress should be considered in different types of thickeners.

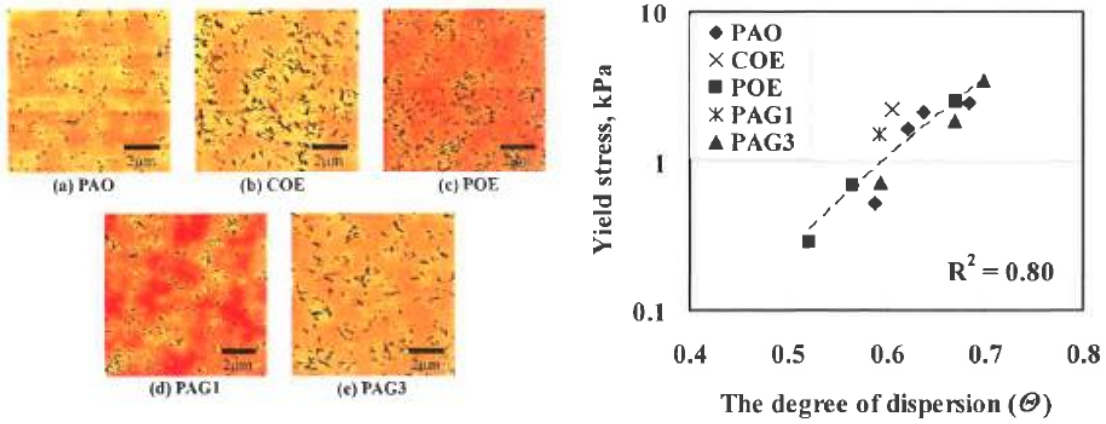

Fig. 6 (left) AFM images of the greases with different type of base oil [9]
Fig. 6 (right) Relationship between the degree of dispersion and yield stress [9]

Dong et al. [10] reported the dependence of base oil viscosity of Li type greases on the film thickness measured by the electrical potential method and bearing friction torque The dependence of base oil viscosity of Li type greases on film thickness was studied. The correlation with the radial deep-grooved ball bearing friction torque were confirmed with simultaneous monitoring of film thickness and bearing torque. 6204 radial deep grooved ball bearings were used for measurements. Figure 7 left shows the schematic image of measuring film thickness by the electrical potential method and measuring bearing friction torque. The tested grease composed of lithium 12-hydroxystearate thickener and PAO with different viscosity.

Figure 7 right shows that higher film thickness provided by the grease with higher viscosity oil under slow bearing rotation speed decrease the bearing friction torque. Under higher rotation speed range, the torque for each grease was similar. The results suggests that thick grease film thickness under slow rotation speed prevent metal contacts and reduce the sliding resistance. This is a reasonable finding but should be confirmed in different types of base oils and thickeners.

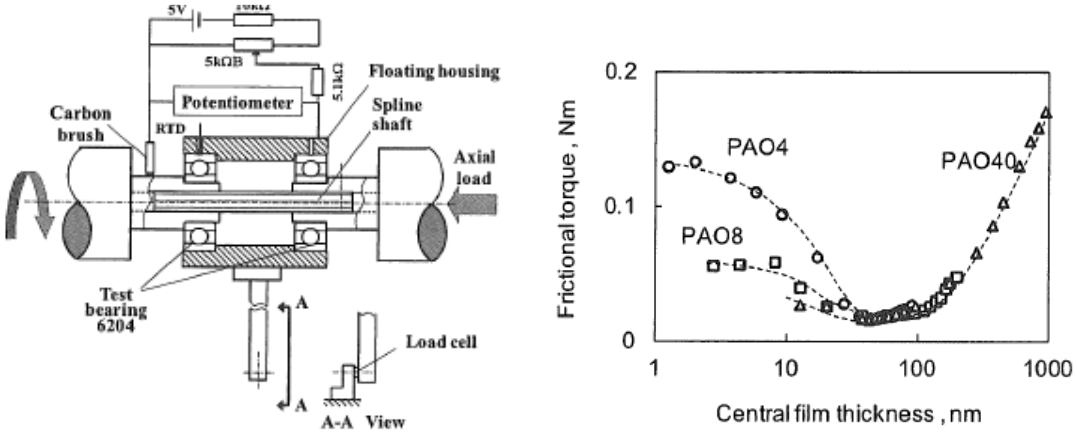

Fig. 7 (left) Schematic diagram of experimental apparatus [10]
Fig. 7 (right) Variation of frictional torque with film thickness [10]

Authors [12] investigated the effect of base oil and thickener types on radial ball bearing torque for Li type greases. For the clarification of the cause of the torque difference among greases, rheological parameters and film thickness were measured. The fluorescence technique was introduced for the observation of grease flow behaviors around EHL contact area.

The tested greases composed of mineral oil or PAO for the base oils, Li complex or single Li soap for the thickeners, and pyrene for the fluorescence dye. The bearing friction torque behaviors under grease lubrication for each bearing rotation speed are shown in Fig. 8 left. Grease-A (mineral oil and Li complex) showed the lowest torque especially under higher rotation speed. After the measurement of the film thickness for each grease, it seemed that grease with higher film thickness related to the lower bearing torque as shown in Fig. 8 right. In addition, grease flow behaviors were observed by fluorescence technique. Grease-A (Li-complex) showed the higher lubricant existence in the EHL inlet area under dynamic conditions compared with Grease-B (single Li soap), as shown in Fig. 9. The reason might exist on the thickener fiber structure. In other words, thin and long fibers of Li complex enable the grease to be entrained to the contact vicinity.

The present results suggest that the bearing torque depended on the grease base oil and thickener types. Grease film thickness and around EHL region seem important. The fluorescence observation demonstrated that Grease-A, G-I base oil and Li-complex thickener, which provides lower bearing torque, showed higher film thickness and superior flow behavior especially in the inlet of EHL region. The thin and long fiber structure of Li-complex thickener contributed to the improvement of film thickness and flow behaviors as the grease was entrained into the contact area.

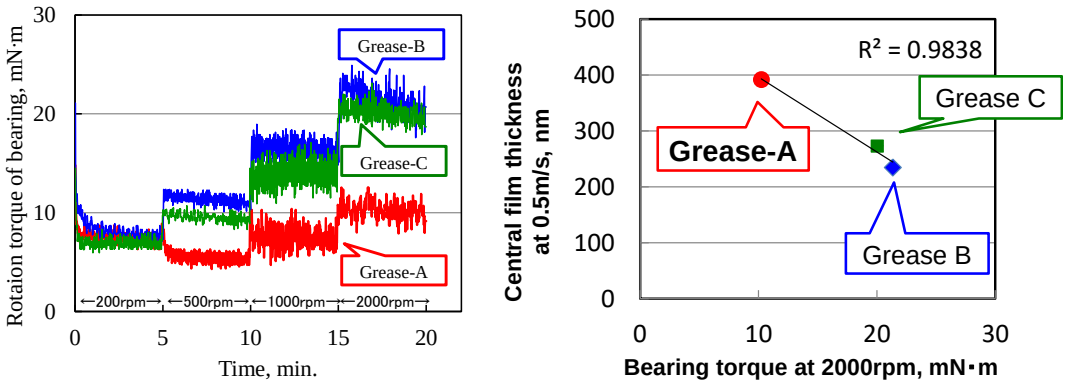

Fig. 8 (left) Friction torques of ball bearings using greases [12]
Fig. 8 (right) Relationship between the bearing torque and grease film thickness

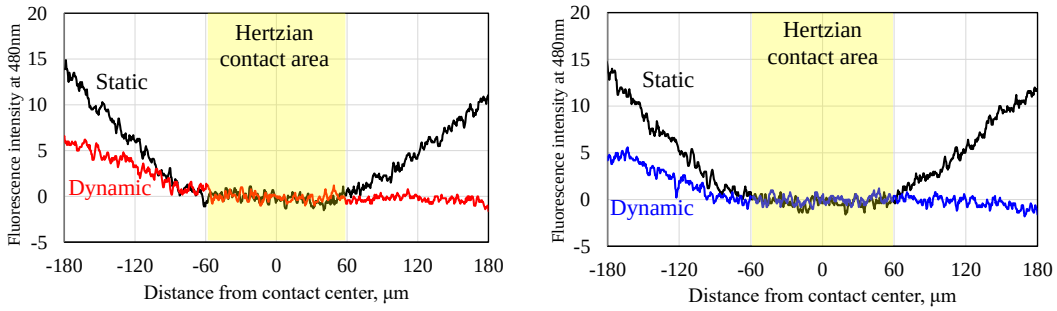

Fig. 9 (left) Line profile of fluorescence (Li-complex type grease) [12]
Fig. 9 (right) Line profile of fluorescence (single Li soap grease) [12]

Nitta et al. [25] referred that the cause of rolling element bearing torque can be roughly divided into the stirring resistance of lubricants, the friction resistance between the balls and the races, and the friction resistance between the balls and the cage. They focused on the stirring resistance and investigated the carbon chain length dependence of urea type greases on the bearing rotation torque and discussed the transition point of viscoelasticity (Tve) of greases. The grease thickened by diurea with the shortest carbon chain showed the lowest bearing torque as shown in Fig. 10.

The Tve values have correlations with the affinity between base oil and thickener as represented by SP (Solubility Parameter) values, and the surface areas of thickener particles as shown in Fig. 11 left and right, respectively. The lower the affinity is and the larger the surface area is, the higher the Tve value becomes and the grease provides lower rotation torque by reducing stirring resistance of the grease in a bearing.

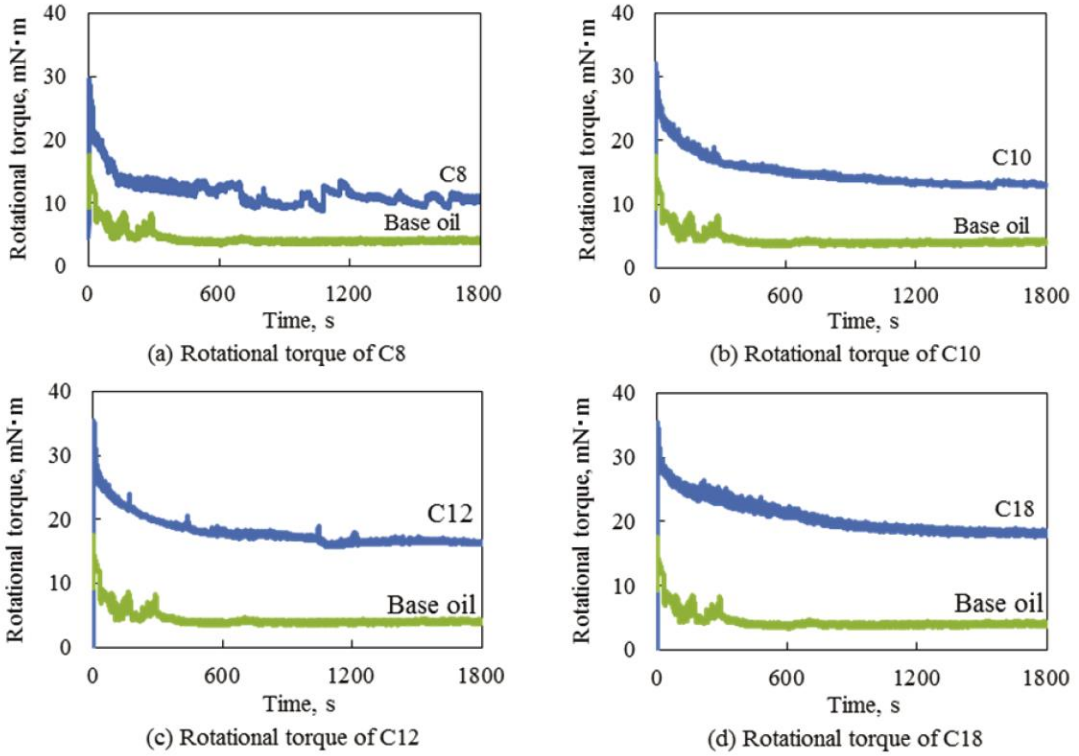

Fig. 10 Running torque of sample greases of (a) C8, (b) C10, (c) C12 and (d) C18 [25]

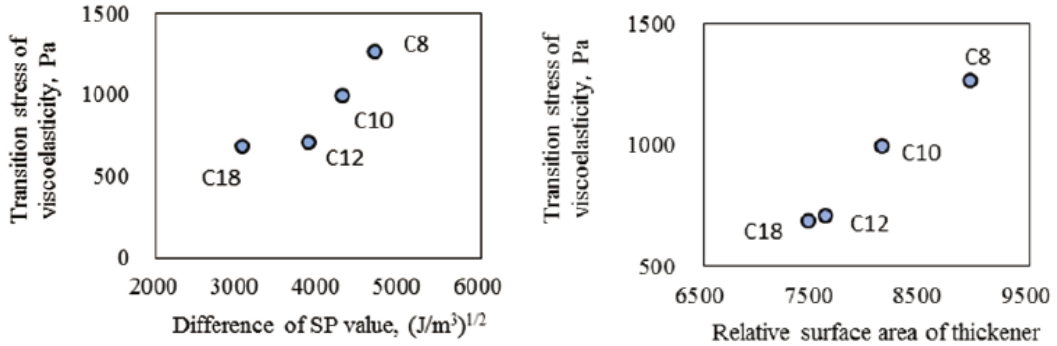

Fig. 11 (left) Correlation between difference of SP value and transition stress of viscoelasticity [25]

Fig. 11 (right) Correlation between relative surface area of thickener and transition stress of viscoelasticity [25]

2.2 Grease behaviors in bearings

In order to understand the grease influence on the bearing torque, grease behaviors in bearings are also important. As approaches of grease film thickness evaluation in bearings, numerical simulation and experimental measurement are introduced here. Venner et al. [13, 14] studied the film thickness decay related to the starvation phenomenon using a theoretical prediction model for bearings. Interferometric images of the full contact region are shown associated with the decay as shown in Fig. 12. The images show the characteristic butterfly shape of the flooded region characterizing a heavily starved contact. The analyses for a 22317 spherical roller bearing and a 209 deep grooved ball bearing were compered in Table 1 and the film thickness distribution is shown in Fig. 13. The decay time depended on the bearing speed; the higher the speed, the longer the decay time. The predicted decay time for the spherical bearing was larger than for the ball bearing. The influence of the bearing radial load was found to be small.

The model predicts that layer thickness decay periods are far shorter than the operation periods of bearings commonly found in practice. The results show that a bearing cannot sustain an adequate layer of base oil on the running track unless significant replenishment takes place. Therefore, not only fully flooded condition but also starved one should be considered in order to understand the bearing torque under grease lubrication.

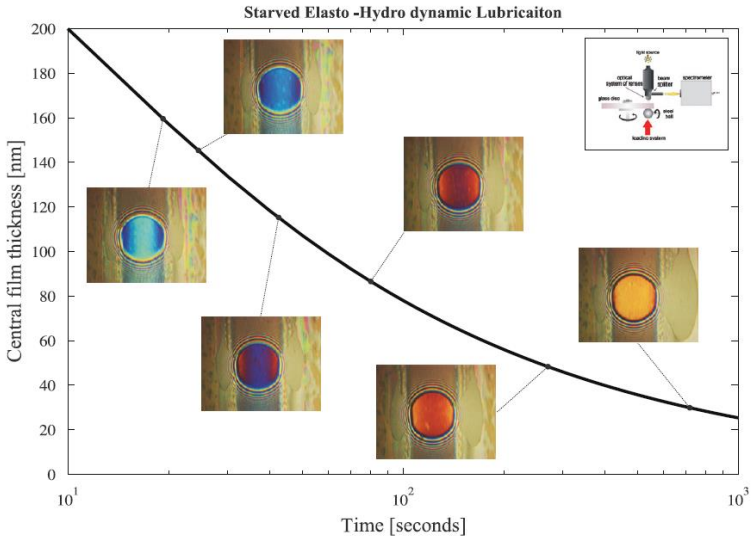

Fig. 12 Central film thickness decay in a starved circular EHL contact as a function of time [13].

Table 1 Parameters and central film thickness decay times for the deep groove ball bearing 209 and the spherical roller bearing 22317 [14]

		Spherical Roller Bearing 22317					Deep Groove Ball Bearing 209					
Case Number:		1	2	3	4	5	6	7	8	9	10	Unit
Radial load	F_r	10	10	10	5	2.5	10	10	10	5	2.5	kN
Rotational speed raceway	Ω_i	750	1,500	3,000	3,000	3,000	1,500	3,000	6,000	6,000	6,000	rpm
Contact speed	u_m	2.56	5.11	10.2	10.2	10.2	2.46	4.91	9.82	9.82	9.82	m/s
Centrifugal load	F_c	5.52	22.1	88.3	88.3	88.3	0.27	1.09	4.34	4.34	4.34	N
Maximum static load	F_{max}	4.98	4.98	4.98	2.82	1.62	5.07	5.07	5.07	2.59	1.34	kN
Load distribution factor	ε	0.16	0.16	0.16	0.12	0.09	0.44	0.44	0.44	0.41	0.38	—
Maximum Hertzian pressure, $F = F_{max}$	p_h	1.23	1.23	1.23	1.02	0.85	3.21	3.21	3.21	2.57	2.06	GPa
Max. half length inner raceway contact	a	0.220	0.220	0.220	0.182	0.151	0.285	0.285	0.285	0.228	0.183	mm
Max. half width inner raceway contact	b	8.80	8.80	8.80	7.29	6.06	2.64	2.64	2.64	2.12	1.70	mm
Fully flooded central film thickness inner raceway, $\psi = 0$	h_{cff}	122	194	309	321	333	92	147	234	245	256	nm
Decay time	t_{cr}	1.8	2.7	4.1	4.0	3.8	0.057	0.086	0.127	0.118	0.110	h

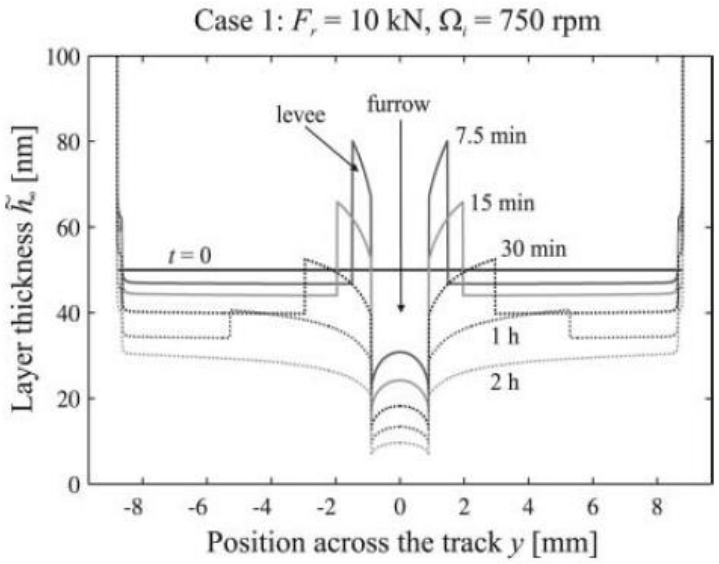

Fig. 13 Layer thickness distribution for spherical roller bearing 22317 [14].

Lugt et al. [22, 26] performed film thickness measurements in grease lubrication for different greases. They used not only the optical interferometry technique but also electrical capacitance method using rotating bearing (Fig. 14) under fully flooded condition. Grease film thickness results measured using optical interferometry technique showed substantially thicker film thickness respect to its base oil in fully flooded and low speed conditions. At higher speeds, the film thickness versus speed relation follows the conventional EHL behavior. Two greases were selected to be tested in a full bearing tester. By using dimensionless film thickness parameter, the film thickness behaviors corresponds in both the full bearing tester and the optical interferometry tester as shown in Fig. 15. The full bearing using greases results confirmed the V-shaped curve for the relationship between film thickness and speed. The grease film thickness at higher speeds can be predicted using base oil properties.

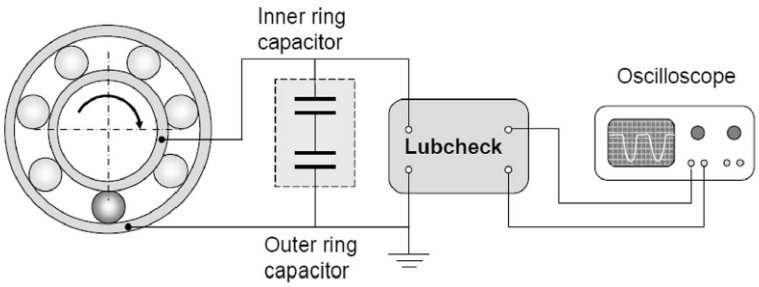

Fig. 14 Illustration of the full bearing tester [22]

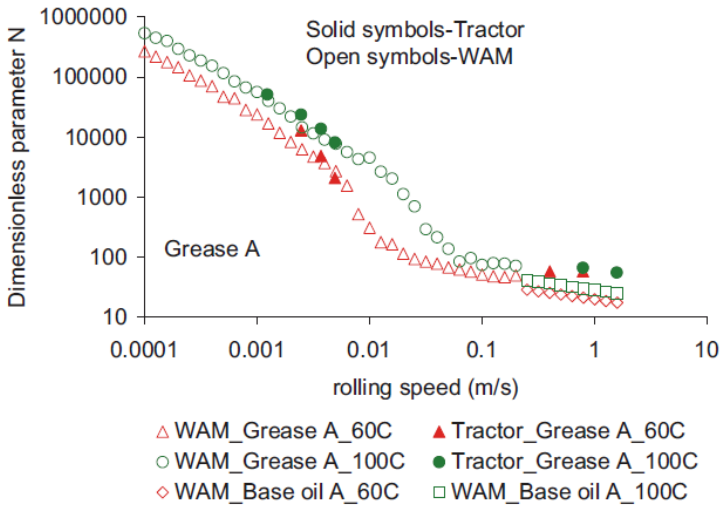

Fig. 15 Dimensionless film thickness parameter N comparison for Grease A [22]

2.3 EHL Film thickness under grease lubrication

Considering operating conditions of bearing, grease behaviors under EHL should be focused as shown above literatures. Observation of film thickness formed by greases have been reported as representative analyses of grease behaviors in bearings.

Cann et al. [15, 16] showed that a grease is pushed away with disk rotations in the ball-on disk contact, different from oil (Fig. 16 left). They used the greases composed of paraffinic mineral oils and lithium 12-hydroxystearate thickener. The dependence of base oil viscosity, thickener content, and operating conditions were evaluated. Film thickness was measured using optical interferometry technique. Under fully flooded condition and lower rolling speed, grease thickener lumps pass through the contacts distorting the EHL film and augment the film thickness compared with the base oil (Fig. 16 right). In this region, values in measurements fluctuate wildly. As speed increases, the behavior disappears and the thickness decreases and then climbed again. At higher speeds, the behavior is similar to conventional EHL film thickness of base oil. Film thickness increases with thickener content and base oil viscosity.

Under starved condition, the film thickness decay was observed through disk rotations. The degree of starvation increases with increasing base oil viscosity, thickener content, and rolling speed. The difference between fully flooded and starvation decreases with increasing temperature as shown in Fig. 17.

Hurley et al. [27] studied the thickener type influence on the lubricating film thickness in the starved regime as shown in Fig. 18. They showed the relationship with the yield stress (Fig. 19) and shear stability of the greases. Due to the shear degraded thickener structure, the yield stress decreases. As a result, the lubricant moves toward a predominantly viscous rheology.

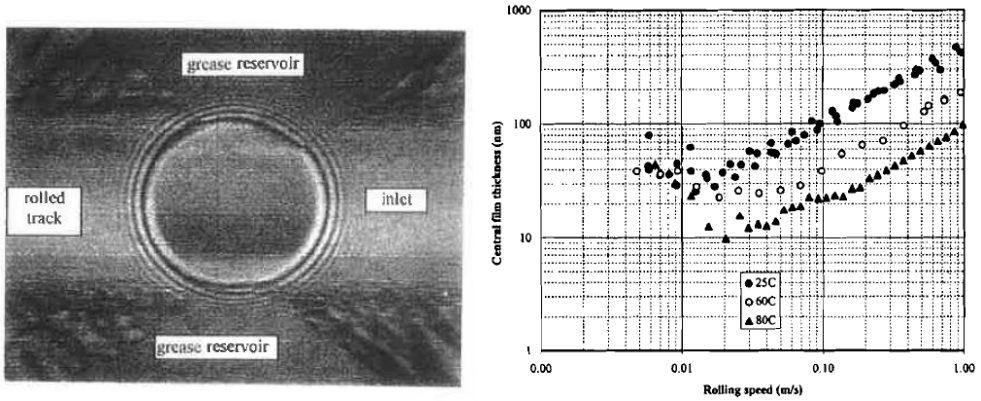

Fig. 16 (left) Photograph of a starved grease lubricated contact [15]
Fig. 16 (right) Comparison of fully flooded film thickness results at different temperatures for 5% 30 cSt greases [16]

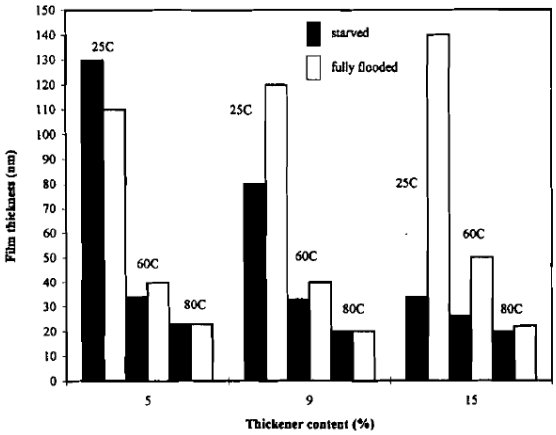

Fig. 17 Comparison of starved and fully flooded film thickness for a grease [16]

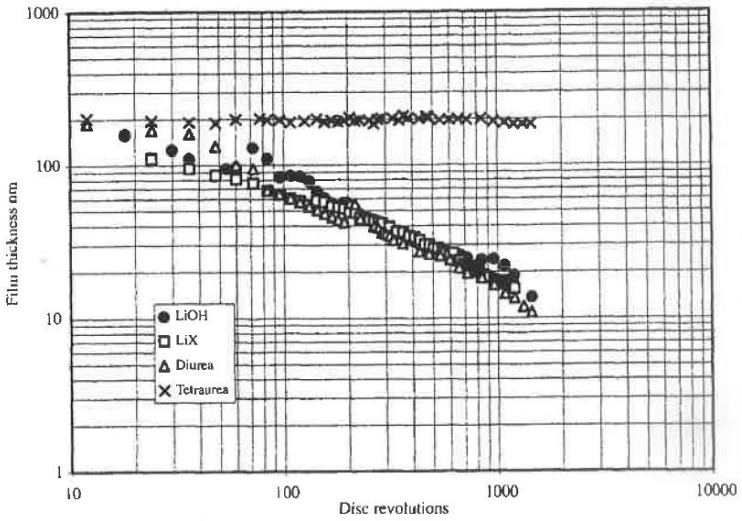

Fig. 18 Starved film results for the greases at 25°C [27]

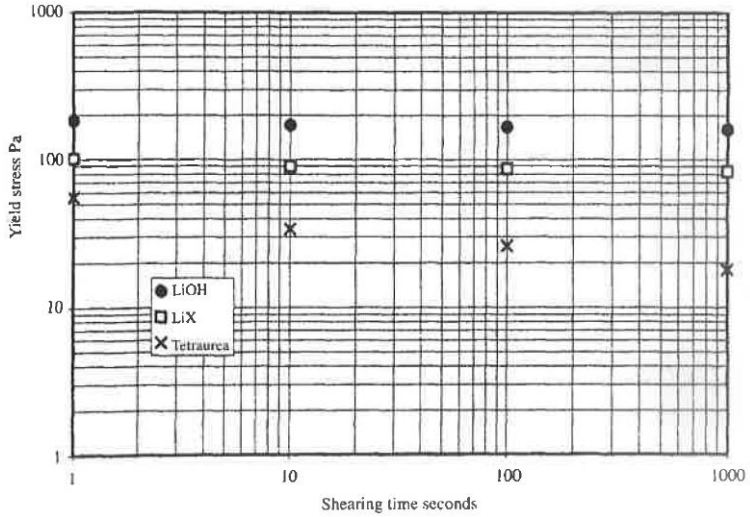

Fig. 19 Yield stress decay as a function of shearing time at $500s^{-1}$, 25°C [27]

The shear degradation effect was also studied by Kaneta et al. [21]. They investigated the film thicknesses for different types of urea greases. The thickness largely depends on thickener types and the thickener structures seem to influence on grease movements related to starvations. They showed the shear degradation suppresses starvation, but the film thicknesses of degraded greases were thinner than those of fresh greases especially at high temperature and speed. Cen et al. [28] stated that mechanically worked greases prepared in a roll stability tester (Fig. 20) showed lower film thickness than the fresh ones in slow speed as shown in Fig. 21. They also concluded that the thickener particles or fiber structure was degraded during mechanical aging and that led to smaller particles. They used at least 24 h for the degradation time in a roll stability tester.

Fig. 20 Roll stability tester and the cylinder/roller [28]

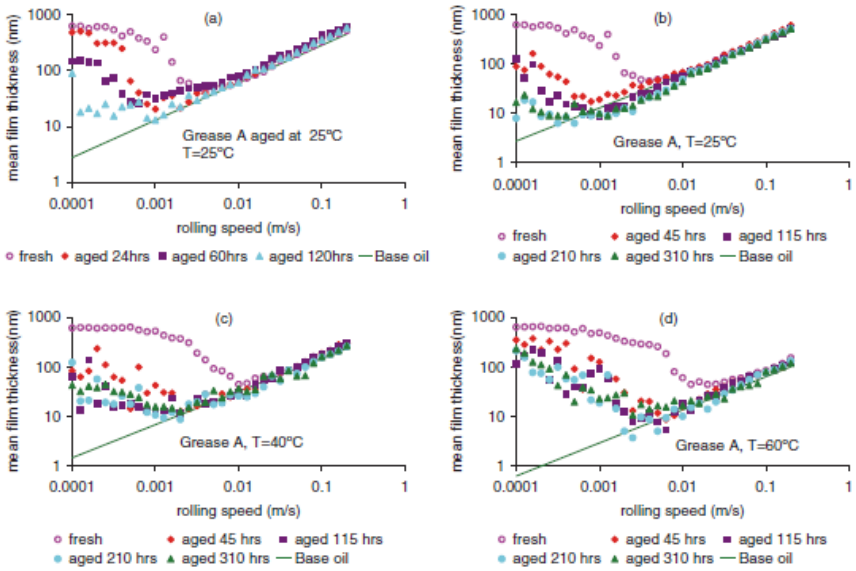

Fig. 21 Film thickness comparison for fresh and aged grease [28]

Cann [29] used a ball-on-disk traction (MTM) device for greases under fully flooded and starved conditions as shown in Fig. 22 left. She used also the lithium 12-hydroxystearate thickener greases. The fully flooded friction values were typically low over the entire test period. Friction coefficient increased under starved conditions as shown in Fig. 22 right, reflecting increase of starvation of the contact as the lubricant was pushed out the track due to repeated overolling.

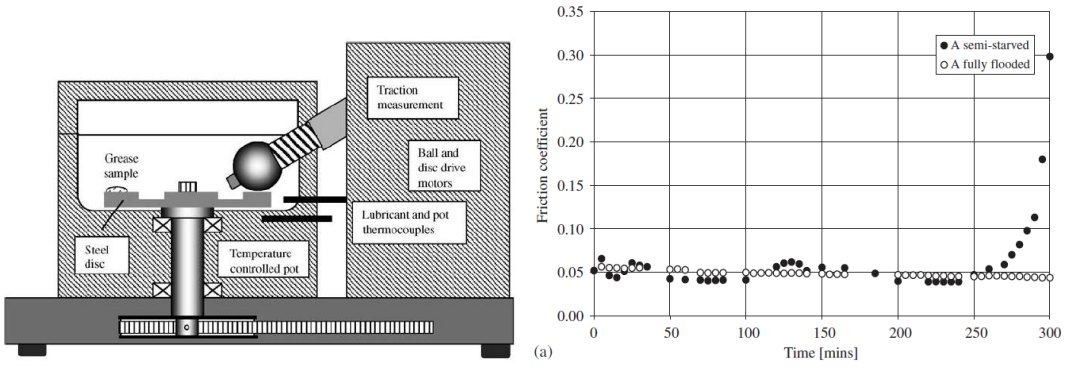

Fig. 22 (left) Schematic diagram of MTM test device [29]
Fig. 22 (right) Friction results-complete test. Friction value at end of 5-min load cycle plotted against time [29]

The film thickness of bled oil from grease was measured by Cousseau et al. [18]. Different type greases and their bled oils were compared in terms of film thickness in a ball-on-disk test rig through optical interferometry under fully flooded conditions. Three tested greases were composed of different base oils (mineral oil, ester, and PAO) and different thickeners (Li, Li/Ca, and polypropylene). Greases and their bleed oils showed higher film thickness compared with their base oils (Fig. 23). Most greases and the corresponding bleed oils generate similar film thickness values. However, the film thickness differences between base oils and bleed oils depended on their types, especially, PAO + polypropylene thickener grease showed large difference.

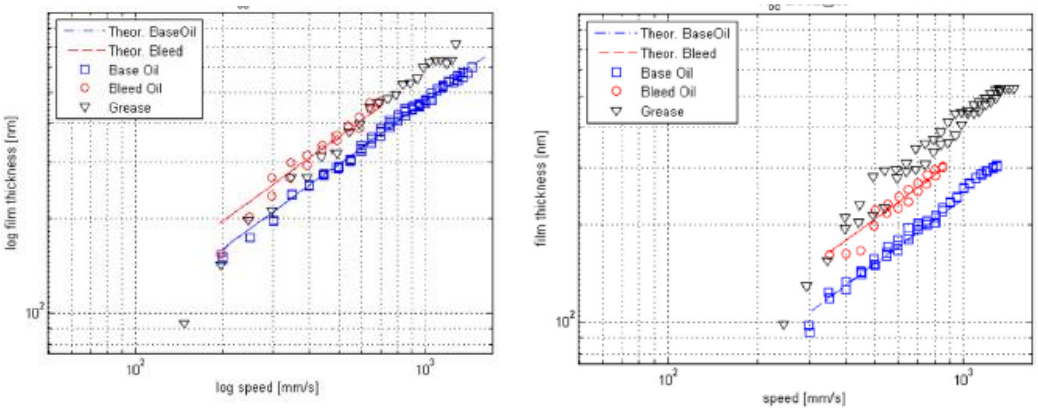

Fig. 23 (left) Film thickness for lithium thickner type grease at 60℃ [18]

Fig. 23 (right) Film thickness for lithium/calcium thickener type grease at 60℃ [18]

2.4 Chemical analysis of grease film thickness

The studies of EHL film analysis have been reported and the information could be important for bearing lubrications. The representative approach is the observation by microscopic FT-IR (Fourier Transform InfraRed spectroscopy) technique presented by Cann et al. [30, 31]. After the friction tests using MTM (Mini-Traction Machine) device, IR analysis of lubricant films in the rolled track on the MTM disk was performed. The greases tested for IR analysis were model LiXM grease (Mineral oil and Li complex thickener) and commercial CaSul grease (unknown base oil and calcium sulphonate thickener). Grease formed thick lubrication film at high temperature or low speeds and improved lubrication. The thickener influenced oil release indirectly and augmented the film thickness. Film related thickeners appeared to be a deposited solid layer, 40-100nm thickness (Fig.24). IR spectra shows that the film in track contains a much high thickener content as shown by the relative intensity of peaks at 1580 and 1560 cm^{-1} associated with the carboxylate asymmetric stretch vibration(Fig. 25).

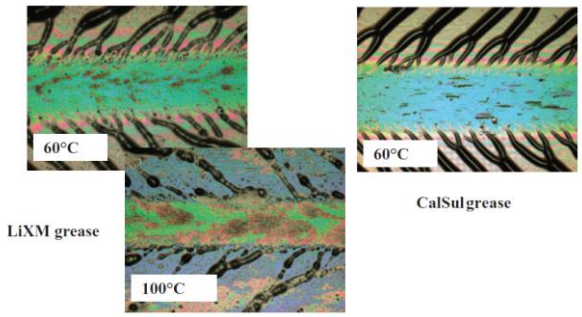

Fig. 24 Microphotographs taken from the rolled track on the glass disc for model (LiXM) and commercial (CaSul) greases [30].

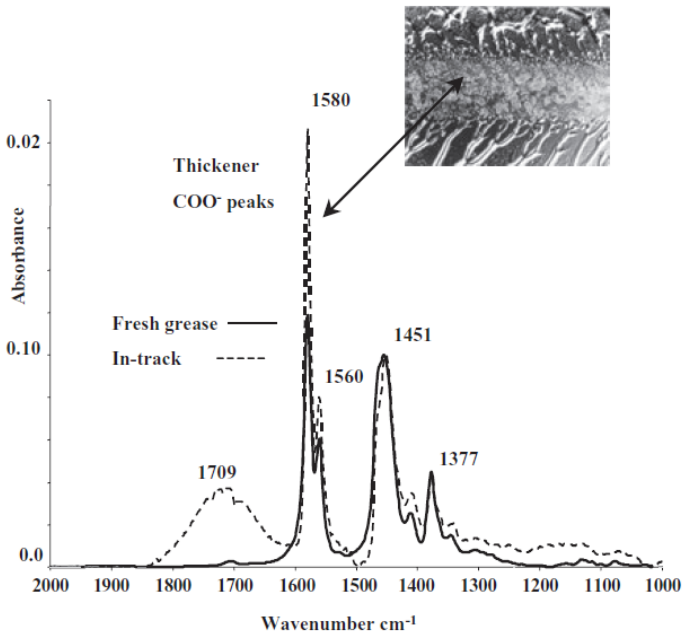

Fig. 25 Infrared spectra for fresh grease and from the film in the rolled track for LiXM grease [30].

Hoshi et al. [32] performed in situ observation of EHL film by micro IR analysis using a ball-on-disk tribometer. The ball was steel and the disk was single crystal silicon. In contrast, conventional sapphire disk absorbs the wavelength less than 2000cm^{-1}, therefore, only higher wavelength, such as C-H, N-H, and O-H vibrations can be observed. Silicon disk transmits wavelength less than 2000cm^{-1}, and enables to observe C=O vibration. Tested greases were Li grease (Li stearate thickener) and urea grease (Aromatic diurea thickener) using PAO base oil commonly. Figure 26 compares IR spectra of each grease from the inlet to the center of EHL contact area. C-H absorbance (base oil) decreases in the center of contact area. C=O absorbance (thickener) of Li grease decreases similarly, however that of urea grease remains. N-H absorbance (urea thickener) also keeps the intensity in the center of contact area. Therefore, in the EHL contact areas, thickener concentration of Li type grease decreased but that of urea type grease increased as illustrated in Fig. 27. It is indicated that how easily the thickener can enter the contact area depend on thickener types. The behaviors of thickeners under EHL could affect the bearing torque.

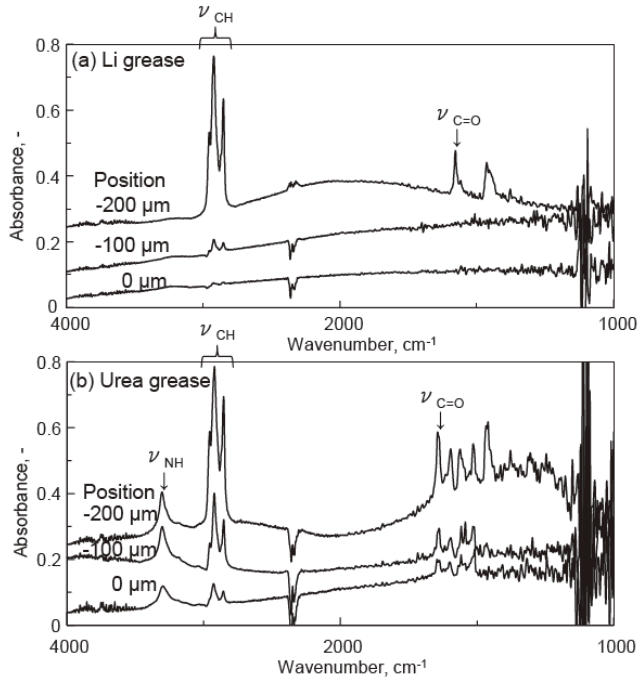

Fig. 26 Typical IR spectra of EHL film of Li grease and urea grease [32]

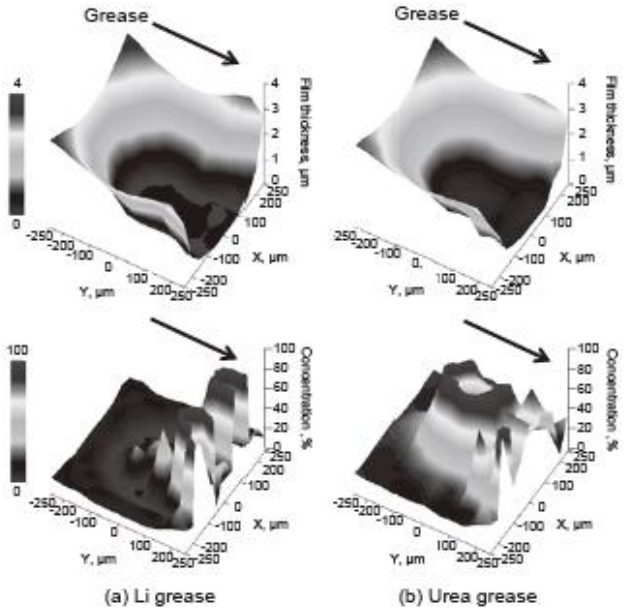

Fig. 27 3D images of film thickness and thickener concentration [32]

2.5 Observation of grease fluidity

Non-uniformity of grease thickeners seem to have influence on grease film thickness behaviors. Publications focused on grease movements are shown as follows. Astrom et al. [33] added a small amount of molybdenum disulfide to Li greases in order to investigate the grease replenishment of an EHL contact using a ball-on-disk apparatus. At the outlet zone, where the gap between the ball and the glass disk diverges, the lubricant cavitates. The cabitation pattern look like a tree stretching its branches to the rolling track as shown in Fig. 28. The thinner grease (lower Li soap contant) gave coarser cavitation branches due to the difference in consistency.

Chen et al. [34] also investigated the grease flow around the conjunction and the flow pattern on the track of the disk were observed with CCD camera. The sample greases were Li greases (Lithium 12-hydroxystearate thickener and PAO or POE base oils) and urea grease (diurea thickener and POE base oil). The features of grease track patterns changes with grease type and test conditions. Typical grease flow pattern is shown in Fig. 29. The finger interval λ is defined as the average interval measured perpendicular to the average tilt angle at a position 4 to 5 times the Herzian contact radius apart from the center of the track. The interval decreased with the increase of entrainment speed. The finger like patterns disappeared at high speeds in starved conditions. Starvation and finger-loss occur at higher entrainment speeds with all the tested greases. The starvation speeds are lower than the finger loss speeds.

Cann [35] also performed microscope examination of the rolled grease tracks after the tests. She stated that the pattern could be influenced by the non-wetted surface film as shown in Fig. 30. The thin lubricant film close to the track is unstable and has rutured, forming individual droplets. These results suggest that the patterns relate to the grease replenishment mechanism.

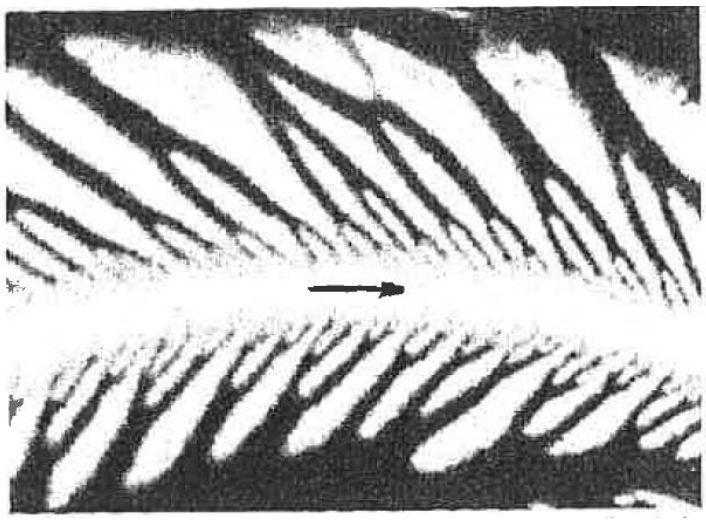

Fig. 28 Cavitation pattern created at the outlet of fully flooded grease-lubricated contact. Dark areas are grease and bright areas cavitation regions [33]

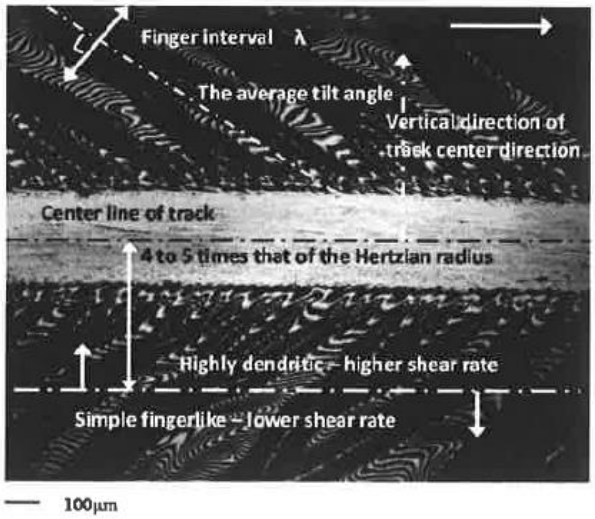

Fig. 29 Definition of finger interval in downstream image [34]

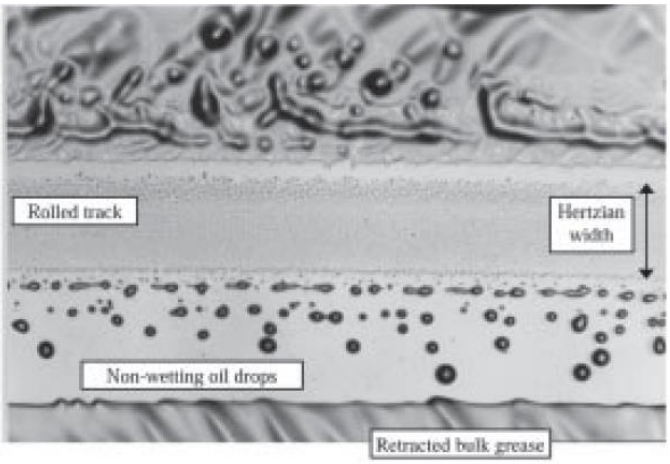

Fig. 30 Photograph of a rolled grease track showing a non-wetting surface film [35]

Yokouchi et al. [36] investigated the influence of fiber length of lithium-soap thickener greases on friction under boundary lubrication conditions using a ball-on-disk sliding tester. Two types of greases with different soap fiber lengths were used. One is with short fibers E03S (0.4μm) and the other is with longer fibers E03L (10μm) as shown in Fig. 31. The thickener was Li 12-hydroxystearate and the base oil was ester type (E03).

The friction coefficients for the greases were lower than that of E03 base oil. The E03L with longer fibers showed lower friction coefficients compared with E03S (Fig. 32). The friction tests under partially grease coated conditions also showed lower friction coefficient of E03L. That indicates the difference in the capability of the two greases to be entrained at the contact. From the rheological tests, E03L showed lower viscosity and yield stress, therefore, that suggests the better entrainment capability of longer fiber thickener. In addition to these study, Oikawa et al. [8] stated a grease channeling phenomenon correlates to the yield stress as referred. Such grease fluidity could relate to bearing torque behaviors.

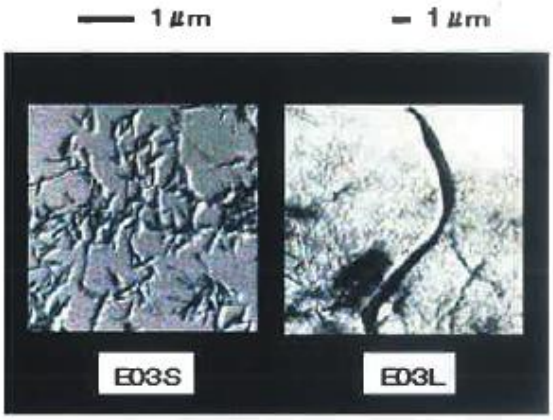

Fig. 31 Soap fibers of the greases [36]

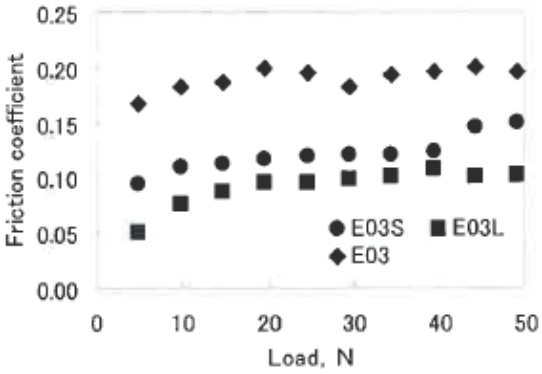

Fig. 32 Results of sliding tests [36]

2.6 Surface texturing for film thickness

Surface texturing effect for oil lubrication and non-conformal contacts is not basically beneficial. Due to the fluctuation of pressure and film thickness around the texture, even the lubrication film breakdown, it reduces the rolling contact fatigue life [37].

Wedeven [38] studied the influence of the dent debris on the EHL film in oil lubrication using an optical interferometry. The dent is deformed elastically associated to the central film thickness. As the central film thickness increases, the dent approaches its undeformed shape. A reduction in film thickness is confirmed at the leading edge and side of the dent.

Kaneta et al. [39] reported the influence of dents formed in the surfaces on the film thickness using optical interferometry technique, focused on the slide roll ratios. A dent was produced onto one part of the smooth ball surface (Ra: 5nm) with a spherical cemented carbide tool. The values of the dent depth were from 0.5μm to 3μm and those of the width were from 50μm to 100μm. A mineral bright stock was used for the lubricating oil. The film thickness were observed using the optical interferometry technique. The main valuable of the experimental conditions was slide roll ratios (Σ= -1, 0, and 1). The slide roll ratio dependence on the film thickness are shown in Fig. 33. When the dent passing through the EHL conjunction exists in the contact region under $\Sigma > 0$, a local reduction in film thickness occurs at downstream of the dent. Under pure rolling condition ($\Sigma = 0$), the film reduction occurs at the leading and trailing edge. Under the condition of $\Sigma < 0$, the film reduction occurs at the trailing edge. The oil within the dent is emitted to the downstream or upstream when the dent is slower or faster than moving surfaces, respectively. In cases of $\Sigma \neq 0$, the depth of the dent decreases as the dent enters the contact area.

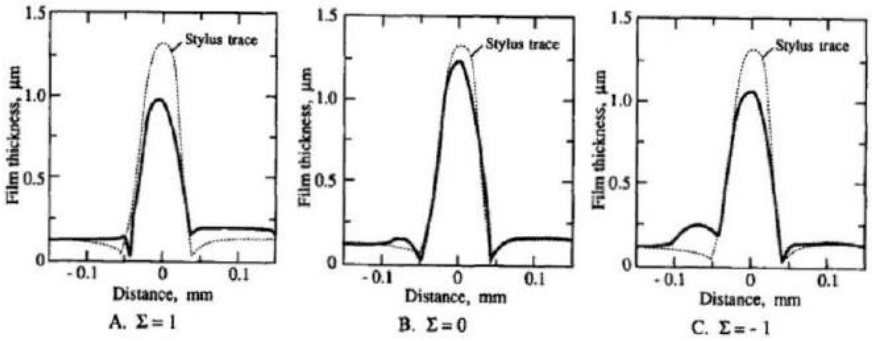

Fig. 33 Midplane film profile in the direction of motion [39]

Mourier et al. [40] analyzed the transient change of film thickness induced by circular micro-cavities passing through an EHL point contact. The experiments were conducted by actual observation and numerical simulation under rolling/sliding conditions. Micro-cavities were produced using LST (Laser Surface Texturing) method with ultra-short laser pulse. The micro-cavities with various diameters (20-120μm) and depths (0.2-100μm) were produced on steel balls. Film thickness was observed using the optical interferometry technique under rolling/sliding (Σ= -0.5) conditions. In the case of deep micro-cavity (0.7μm), film thickness reduced compared with the smooth surface case. In contrast, a shallower micro cavity (0.4μm) increased film thickness near the leading edge on the cavity as shown in Fig. 34 left. Under rolling/sliding conditions, deep cavity give a local decrease of the lubricant layer, and a significant increase in lubricant film thickness is induced by a shallow micro-cavity.

Krupka et al. [41, 42] investigated the effect of micro-dents of various depths on the film thickness considering slide roll ratio dependence. Micro-dents were produced by indentation of the ball surface with Rockwell indenter. The depth ranged from 0.23 to 1.02 μm. The deep micro dents on the ball decrease the film thickness but shallow micro dents increased the film thickness depending on the rolling/sliding conditions, especially negative slide roll ratio (Fig. 34 right). An increase in the lubricant film thickness has been observed upstream of the trailing edge of the micro-dent when the slide roll ratio is negative. For the positive slide roll ratio, the presence of the micro-dent reduce the film thickness located downstream of the leading edge.

Mourier and Krupka et al. found out the improvement of film thickness depending on the specific conditions in spite of the non-conformal contacts. Applications for grease lubrication has not been reported, and the behaviors could be different by the non-uniformity of greases.

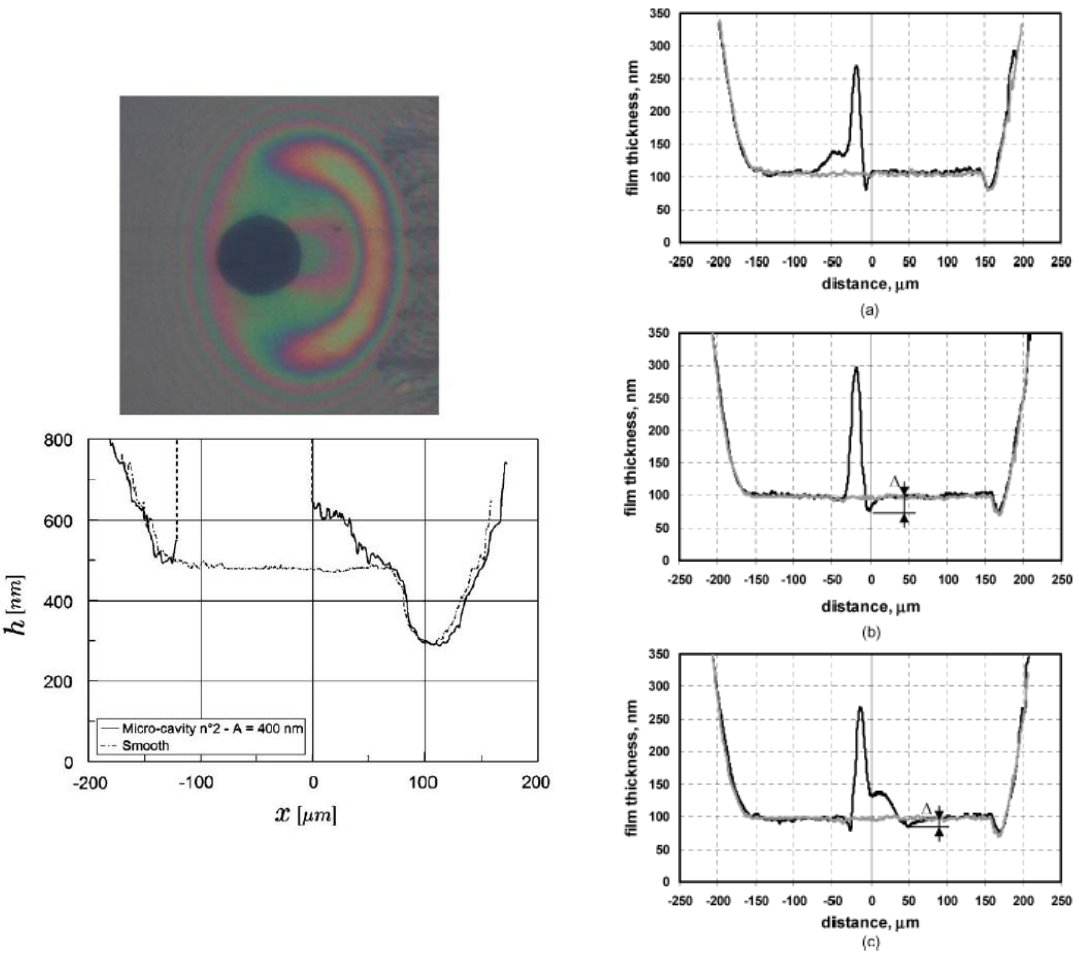

Fig. 34 (left) Transient increase of film thickness induced by a shallow micro-cavity under rolling-sliding [40]
Fig. 34 (right) Film thickness profiles depicting the effect of shallow micro-dent on lubrication film for Σ= -0.5(a), 0(b), and 0.5(c) [42]

3 ANALYSIS AND CONCLUSION OF LITERATURE REVIEW

As described above, there are some literatures about grease formulation and bearing torque and its lubrication, the relationship is illustrated on next page. However, each study includes unknown areas.

Cousseau et al. [3, 5] indicated their findings about greases and thrust bearing torque. It is not clear to be applicable to radial ball bearings. The sample greases are based on commercial ones, therefore the samples were composed of different base oil, thickener, and additives. In these samples, it could be difficult to evaluate the dependence of components. In addition, the results could contain the interaction among base oil, thickener, and additives.

Oikawa et al. [8] and Dong et al. [10] reported influence of Li greases on radial ball bearing torque. Their thickeners are limited to Li-12-hydroxy stearate, and the tendency for the different thickener type of greases are not necessarily similar. However, the influence of yield stress on the bearing torque is worth considering in terms of the grease channeling since Hatton [23] suggested the relationship of channeling and the bearing torque. Nitta et al. [25] also reported the similar relationship as transition stress of viscoelasticity in urea type greases.

Venner et al. [13-14] simulated grease behaviors in bearing, and Cann et al. [15-16, 27] reported grease film thickness under fully flooded and starved conditions, however, the relationship between those findings and bearing torque has not been clear. The effect of shear degradation on the grease film thickness has been reported by Kaneta et al. [21] and Cen et al. [28], therefore the influence on the bearing torque should be confirmed in this study. Since the shear degradation of the grease could occur in the bearing operation.

Chemical analysis of grease film [30-32] and grease flows [33, 34] could be significant factors determining bearing torque. In other words, grease rheological parameters, EHL films, and grease flows are necessary to understand the bearing torque under grease lubrications. In that meaning, recently the authors [12] proposed a lubrication mechanism about bearing torque by using of fluorescence observation of grease flows, but that was limited grease formulations.

In addition to these factors, surface influence to film thickness should be introduced in this research. The non-uniformity of greases due to mixture of oil and thickener could affect film thickness on non-smooth surfaces. In addition, the bearing surfaces of balls and races have the localized asperity of hundreds of nanometers depth, although the averaged roughness is less than 100 nm. Considering grease film thickness behaviors, especially the thickener entrainment to the contact, the asperity of hundreds of nanometers depth could have a significant meaning. The values of film thickness increase caused by the thickener entrainment are also hundreds of nanometers. However, a study of grease film thickness considering various surface conditions has not been reported. If the grease behaviors of film thickness are different from oil and there is some dependence for grease formulations, it will be a new subject to be discussed for considering the relationship between bearing torque and grease formulations. For instance, specific type of grease might form higher film thickness on dented surface.

Based on these literatures, grease formulation dependence or the important grease properties on the bearing torque have not been fully understood. In addition, the grease properties could correlate each other. The relationship should be verified in this PhD study.

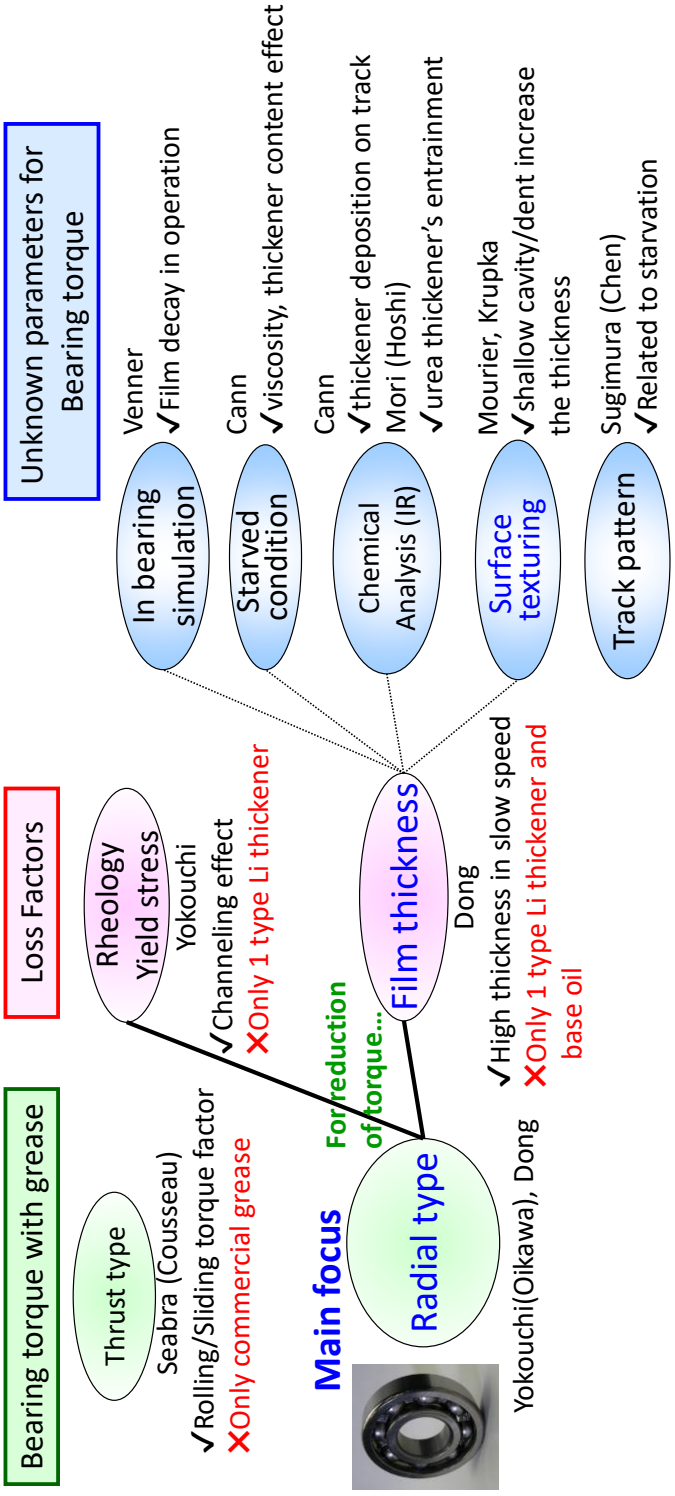
Bearing torque with grease
Loss Factors
Unknown parameters for Bearing torque
Thrust type
Seabra (Cousseau)
✓Rolling/Sliding torque factor
✗Only commercial grease
Rheology Yield stress
Yokouchi
✓Channeling effect
✗Only 1 type Li thickener
Main focus
For reduction of torque...
Radial type
Film thickness
Yokouchi(Oikawa), Dong
Dong
✓High thickness in slow speed
✗Only 1 type Li thickener and base oil
In bearing simulation
Venner
✓Film decay in operation
Starved condition
Cann
✓viscosity, thickener content effect
Chemical Analysis (IR)
Cann
✓thickener deposition on track
Mori (Hoshi)
✓urea thickener's entrainment
Surface texturing
Mourier, Krupka
✓shallow cavity/dent increase the thickness
Track pattern
Sugimura (Chen)
✓Related to starvation

4 AIM OF THESIS

The first objective of this research is to obtain the relationship between the radial ball bearing torque and grease formulations. The second objective is to understand the correlation of each grease parameter. The bearing torque in grease lubrication definitely correlates to several parameters as described above, and these parameters also interact each other. However, the detailed mechanism of how the components of greases simultaneously influence the bearing torque has not been fully understood.

In this research, radial ball bearing torque tendency was evaluated with Li type greases, considering base oil and thickener dependence. Analyses of the reason why each grease formulation provides the different bearing torque were conducted using comprehensive grease properties, such as rheological parameter and thickener structure, friction property, and behaviors including EHL films. Especially, EHL film thickness was measured by optical interferometry method with smooth and dented surfaces. Investigating grease behaviors on non-smooth surfaces and discussing the influence on the bearing torque were novel approaches in this field. The obtained findings could be significant knowledge for the development of advanced greases featuring energy-saving performance.

4.1 Scientific questions

- What properties of greases influence on the radial ball bearing torque?
- Are there relationship among the grease properties?

4.2 Working hypotheses

1. Rheological factor

As described in the literature [8], high yield stress of greases could have an influence on the reduction of bearing torque due to the grease channeling. The finding in the literature might be different depending on thickener types, therefore the tendency will be confirmed. Not only yield stress but also viscosity parameter will be evaluated for understanding correlations.

2. Thickener structure

Authors [12] indicated the thin and long thickener fiber structure lead to higher film thickness and superior grease fluidity in the inlet of contact area. Yokouchi [36] also suggested the fiber structure influence on how easily grease is entrained to the contact area. The best thickener structure providing lower torque will be judged if it exists.

3. Ability of film thickness and adaptability to surface conditions

Higher grease film thickness seems to have a relationship with the lower bearing torque according to Dong [10] and authors [12] study. It should be verified whether the tendency is applicable in the different thickener types.

A study on grease film thickness on non-smooth surface has not been reported. If a grease can form higher film thickness on dented surface, it could mean the higher adaptability to the surface conditions or higher fluidity as a grease. It should be confirmed whether the difference of the film forming properties of greases relate to the bearing torque properties.

4. Grease parameter correlation

Except for relationship with the bearing torque, observed grease parameters could have correlate each other. For instance, the grease with higher film thickness has specific thickener structure. Comparing the results of grease parameters, the relationship will be discussed.

5 MATERIALS AND METHODS

5.1 Material

5.1.1 Lubricants

Model grease formulations for samples were selected, considering actual grease formulations for bearing lubrications. As hydrocarbon type base oils, mineral oils (API Group-I) and poly-alfa-olefin (PAO, API Group-IV) were used and these viscosity grade was controlled to VG32. The relatively low viscosity grade is based on the recent grease development trend with energy-saving properties.

The mineral oil is composed of paraffinic, naphthenic, and aromatic hydrocarbons. On the contrary, PAO is composed of only paraffinic hydrocarbons.

Used thickeners were three types of Li soaps. Single Li soap is Li-stearate or Li-12-hydroxy stearate. Li complex soap is a mixture of Li-12-hydroxy stearate and Li-azelate. Therefore, grease samples can be the combination of two types of base oils and three types of thickeners. However, in this study, the thickener dependence was mainly focused, therefore, the comparison of three types of Li thickeners with the mineral oil was conducted usually. As necessary, grease penetration dependence was also evaluated by selecting the thickener content.

Table 2 Lubricants compositions

Samples	Li-complex grease	Single Li grease 1	Single Li grease 2	Base Oil
Base oil	Mineral oil(API G-I), PAO(G-IV)			
Thickener	12OH-stearic/ azelaic-Li	Stearic-Li	12OH-stearic-Li	-
Dropping point	250℃	200℃	200℃	-

5.1.2 Bearing

As the bearing for measurement of bearing torque, a conventional type of bearing, 6204 deep grooved radial ball bearing was used. The outer and inner diameters are 47 and 20 mm, respectively.

5.1.3 Balls and indentation for dents

Balls for film thickness measurements were AISI 52100 steel balls with the diameter of 25.4 mm and the surface roughness (RMS) of about 15 nm. The elastic modulus and the Poisson's ratio of the steel ball were 210 GPa and 0.3, respectively.

For the investigation of the influence of the dented surface ball on the film thickness, dents were produced on steel balls using a modified Rockwell indenter. Tungsten carbide (WC) balls with diameters of 2.5, 1.6, and 1.27 mm were used as a tip of the indenter. The dent producing program was decided so that only one dent would enter the contact center as closely as possible in film thickness measurements, considering the Herzian contact diameter (440μm). The program is shown in Table 3 and the dent array image is shown in Fig. 35. The depth profiles were obtained by 3D optical interferometry method as shown in Table 4. Dent size images for each indenter are shown in Fig. 36. The dent depth deviation was large, for instance, the

depth using 1.27 mm indenter ranged from 250 to 450 nm and the averaged value was about 360 nm. Therefore, the film thickness measurements on dents were conducted using averaged values for multiple dents as described in a following chapter. In order to evaluate the dent effect precisely, the depth profiles were identified for two particular dents created by the 1.27 mm indenter. Figure 37 shows the depth profiles of the targeted dents, referred as dent1 and dent2. The depths were 350 and 300 nm for dent1 and dent2, respectively.

Table 3 Dent producing program

Dent width, μm	1200
Number of dents (rotating direction)	60
Dent distance, μm	150
Dent offset, μm	400
Number of arrays	9
Total number of dents	540

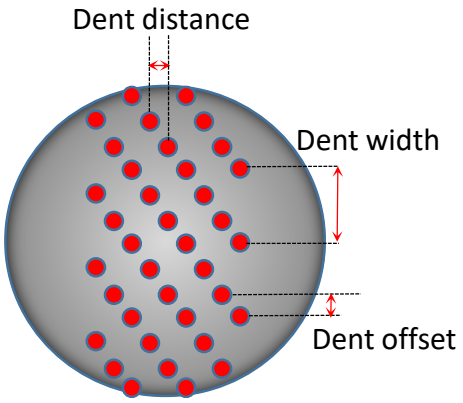

Fig. 35 Image of dent arrays

Table 4 Dent profiles

Diameter of indenter, mm	2.5	1.6	1.27
Width of dents (Averaged values), μm	120-160 (140)	110-130 (115)	100-110 (105)
Depth of dents (Averaged values), nm	130-360 (250)	250-400 (310)	250-450 (360)

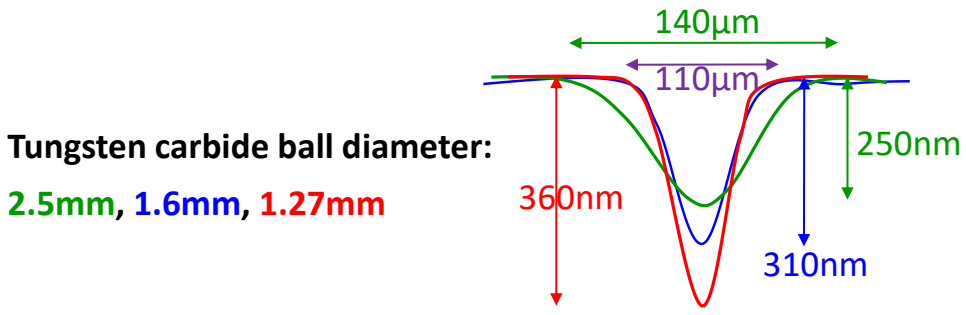

Fig. 36 Images of dents for different diameters of indenters

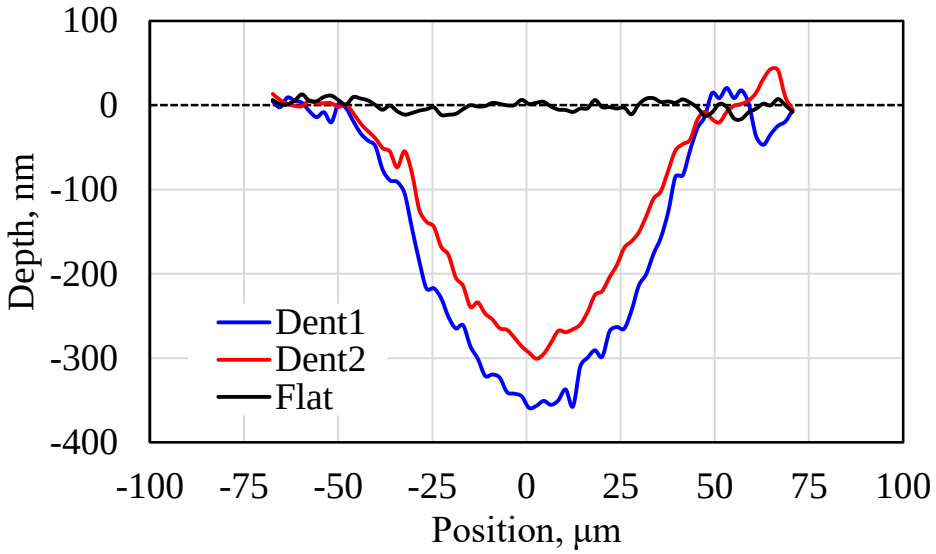

Fig. 37 Depth profiles of the dented steel ball for 1.27mm indenter

5.2 Bearing torque

In order to evaluate bearing friction torques caused by greases, bearing tests were conducted by using an original bearing friction torque testing machine as shown in Fig. 38. Radial and thrust loads can be applied to the bearing by weights and a coil spring, respectively, in the range of 10 N to 1000 N. Operating temperature can be controlled by air convection in the range of -50℃ to 200℃. Rotation speeds can vary from 200 rpm to 10000 rpm. Bearing torques are detected by a load cell through a wire fixed in the bearing housing in the range of 0 to 20 Nm.

For each measurement, a new 6204 bearing was used. The bearing was washed with white gasoline in order to remove the filled grease before a test grease was applied to the bearing. The bearing is filled with 2g of grease sample, approximately 35% of space volume of the bearing. Bearing seals were not used in this study in order to exclude the friction resistance of seals.

The inner race of bearing with the test grease was attached to a main shaft of the tester. After applying radial and thrust loads to the bearing in a housing, a wire was attached to the bearing housing in order to detect the bearing torque. The wire was also connected to a load cell. The temperature of bearing assembly was controlled in the chamber by air convection. After stabilizing the temperature in the chamber to 25℃, the main shaft was rotated at discrete speed in stepwise (200, 500, 1000, and 2000 rpm). The measurement time for each rotation speed was 10 minutes for screening the torque behaviors lubricated with each test grease. The tests were conducted 3 times since high deviations were observed depending on the grease thickener types. The bearing torque values at 2000 rpm were not stabilized in 10 minutes, therefore, the duration of 60 minutes was also tested only for 2000 rpm after stepwise speed increases from 200 to 1000 rpm. In addition, after finishing the 60 minutes measurement at 2000 rpm, the same test was proceeded in order to confirm the effect of grease channeling or grease distribution through the bearing operation. These test programs are shown in Table 5.

Table 5 Operating conditions of bearing torque tests

Condition	Screening	Long duration	Repetition
Axial load, N	50		
Thrust load, N	50		
Rotation speed, rpm (Duration)	200(10min.) -500(10min.) -1000(10min.) -2000(10min.)	200(10min.) -500(10min.) -1000(10min.) -2000(60min.)	After 'long duration' test, 200(10min.) -500(10min.) -1000(10min.) -2000(60min.)
Temperature, ℃	25		

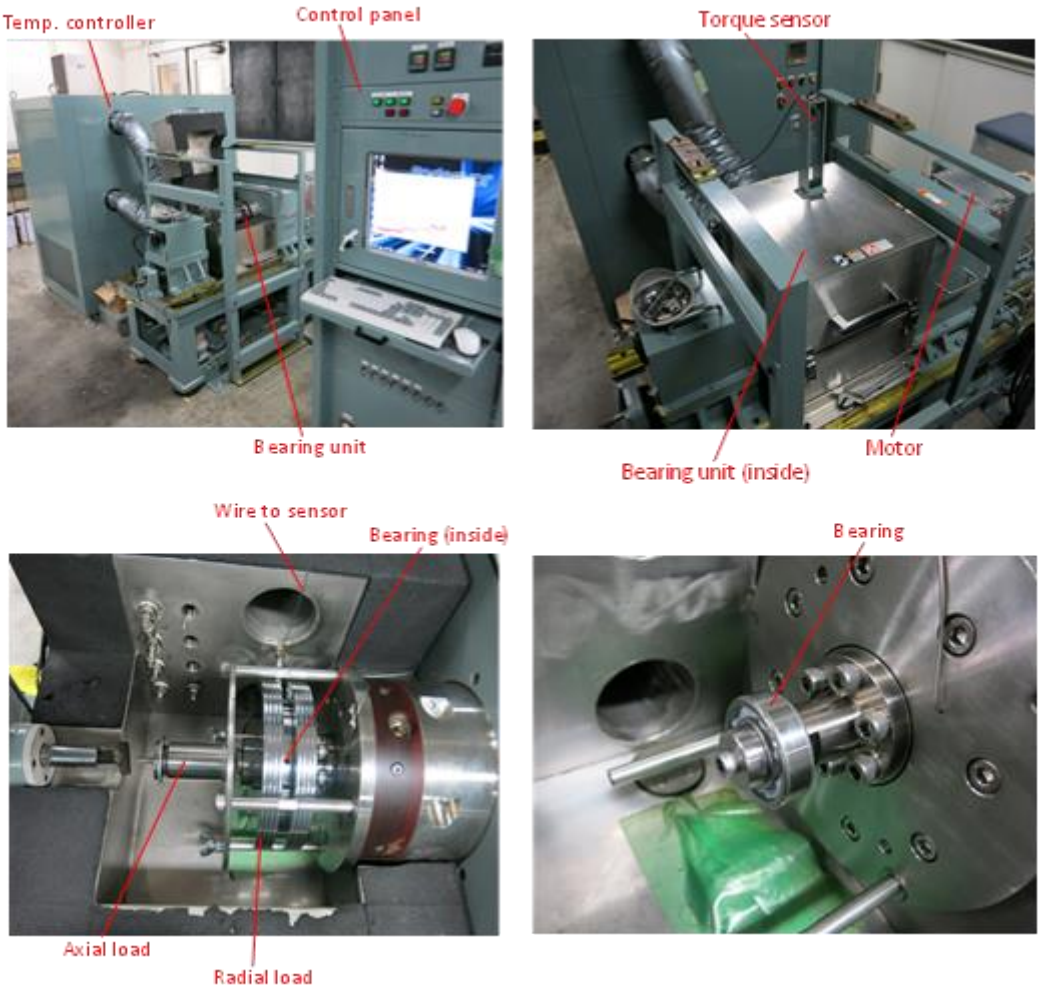

Fig. 38 Images of the bearing torque testing machine

5.3 Rheology

The apparent viscosity of each of the greases at a shear rate of 0.1-2000s^{-1} was determined by using a cone-plate type of rotational viscometer (HAAKE Viscometer 550). First, the viscosity was measured with acceleration of the shear rate and the measurement was continued with deceleration of the shear rates in order to understand the influence of the shear history. The cone is 20 mm in diameter and has an angle of 1 degree. Measurements of the yield stress of grease were conducted with parallel-plate type of rheometer (HAAKE MARS III), using viscoelastic parameters. Diameter of the two plates was 25mm and the frequency is 1Hz. The storage modulus (G'), the loss modulus (G''), and shear stress will be measured while the deformation is controlled from 0.01 to 100%. The yield stress is defined as the lowest shear stress when G'' is greater than G' (Fig. 39).

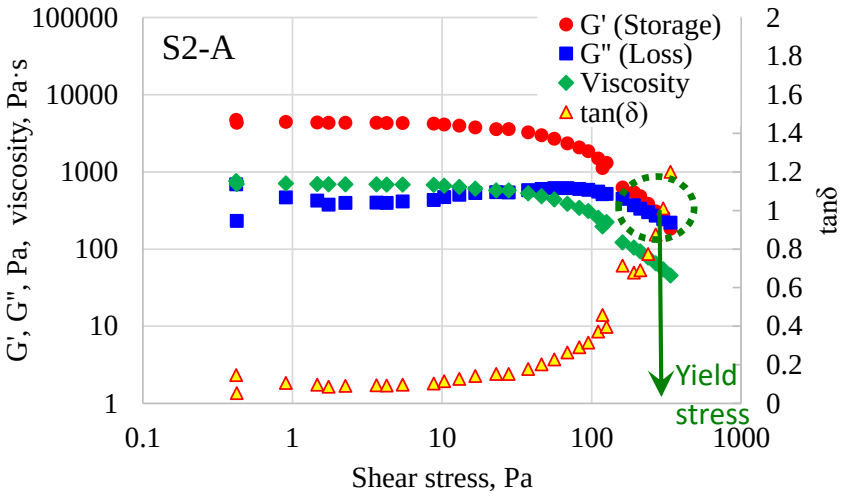

Fig. 39 Viscoelasticity of a grease

5.4 Grease structure

Grease thickener fiber structures were observed by TEM (Transmission Electron Microscope) in order to investigate influence of the structures on the bearing torque and other properties. Oil component was removed by n-hexane solvent, and the residual thickener components are observed by TEM (JEOL JEM-2010). Acceleration voltage was 200kV.

5.5 Traction property

Traction coefficients were measured using a ball-on-disk tribometer, PCS Instruments Mini Traction Machine (MTM). An AISI 52100 steel ball with the diameter of 3/4 in. and the same material disk were selected as the standard specimen. The RMS roughness values of ball and disk were about 6 and 10 nm, respectively. The maximum Hertzian pressure was 0.65 GPa. A scoop was used for maintaining fully flooded conditions during the friction tests. A condition without the scoop was also evaluated. Tests were conducted at ambient temperature.

Assuming the rotation speed of inner race of the bearing during the torque tests, the bearing rotation speeds from 200 to 2000 rpm correspond to from 0.2 to 2 m/s. As a velocity dependence test, the traction coefficient transition of samples were observed with stepwise increase of velocity from 0.1 to 3 m/s, every 0.1 m/s. Following to the measurement of 3 m/s, the velocity decreased to 0.1 m/s in stepwise, every 0.1 m/s, conversely. As the slide roll ratio (SRR), 3% was selected considering the typical SRR range, around 3-5%, found in rolling bearings [43].

The SRR dependence was also evaluated for each bearing operation speed, from 0.2 to 2 m/s. The SRR was controlled from 0.1 to 100% in stepwise. These test conditions are summarized in Table 6.

Table 6 Operating conditions of traction tests

Condition		Velocity dependence	Slide roll ratio dependence
Specimen	Ball	AISI52100, φ3/4in	
	Disk	AISI52100	
Maximum Hertzian pressure, GPa		0.65	
Velocity, m/s		0.1→3.0→0.1	0.2, 0.5, 1, 2 (constant)
Duration, sec.		15 each	15 each
Slide roll ratio, %		3	0→100
Temperature, ℃		25	

5.6 Film thickness

Grease and oil film thicknesses were measured by using the colorimetric interferometry technique [44]. The film thickness formed between a glass disk and a steel ball was observed as shown in Fig. 40 as a schematic image. The contact images were captured by a digital camera. The film thickness calculation from the interferograms is based on colorimetric analysis using color matching algorithm and CIELAB color film thickness calibration.

The detail of the steel ball was described in 5.1.3. BK7 glass disk with optically smooth surface was used. The elastic modulus and the Poisson's ratio of the glass disk were 81 GPa and 0.208, respectively. The bottom surface of the glass disk is

coated with a thin and reflective chromium layer, and the top of that is coated with antireflective layer. The used load for film thickness measurements were 27N and the maximum Hertzian pressure of the contact was 0.43GPa for the smooth ball-on-disk contact. The load was 54N and the maximum Hertzian pressure was 0.54GPa for the dented ball on the smooth glass disk contact. A v-shaped scoop was used for pushing the grease at the side trace back to the running track in order to maintain fully flooded conditions. The film thickness observations were conducted with the velocity from 0.01 to 1m/s under nominally pure rolling conditions and 22˚C. The disk was driven and the ball was followed for the smooth ball-on-disk contact. The ball was driven and the disk was followed for the dented ball on the smooth glass disk contact. The observed film thickness using greases was fluctuated due to the entrainment of thickener particles, therefore the averaged thickness values of central circle areas with a diameter of 100 μm were selected for central film thickness. In addition, the central film thickness values were averaged from the results of 5 captured images for the smooth surface contact. Following to the measurement from 0.01 to 1 m/s (acceleration), the film observation was continued from 1 to 0.01m/s (deceleration). For the dented surface, the central film thickness was also measured on smooth areas, not dented areas for comparison. Focused on the dent1 and dent2 as shown in Fig. 37, the highest thickness values observed on the dents were selected for the film thickness on dents.

In order to observe the grease film thickness decay under starved conditions, film thickness measurements without the scoop were conducted for the smooth surface contact. The contact images were captured with the velocity increase by 0.024 m/s every 30 seconds.

.

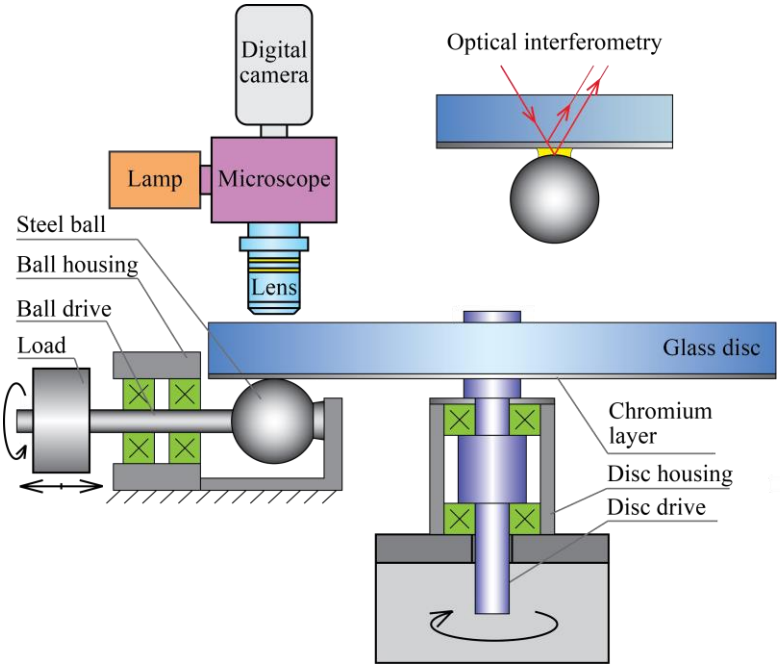

Fig. 40 Schematic image of film thickness measurement

5.6 Track pattern

After the film thickness measurements at each velocity under fully flooded conditions between the smooth surfaces, the grease flow patterns created at the downstream of the contact on the disk were observed. As well as the film thickness measurements, observation was conducted from 0.01 to 1 m/s (acceleration), subsequently from 1 m/s to 0.01m/s (deceleration).

5.7 Interpretation of obtained results

The dependence of thickener and base oil types on the bearing torque were obtained through the process described in 5.1 and 5.2. The causes of the difference are also analyzed through 5.3 to 5.6. Based on the hypotheses described in 4.2, the correlation between bearing torque values and each parameter was discussed. In addition, the relationship among grease properties except for the bearing torque property was also evaluated. The lubrication mechanisms were proposed based on the discussion.

6 RESULTS

6.1 Bearing torque

Bearing torque behaviors were investigated for the six model greases as shown in Table 7. The greases are the combination of two types of base oil and three types of Li thickeners. Table 8 describes the base oil property.

Table 7 Sample greases

Grease	L-A	S1-A	S2-A	OilA	L-B	S1-B	S2-B	OilB
Mineral oil (G-I), %	88	92	92	100	-	-	-	-
Poly-α-olefin (PAO), %	-	-	-	-	88	92	92	100
Li complex thickener, %	12	-	-	-	12	-	-	-
Li stearate, %	-	8	-	-	-	8	-	-
Li-12OH-stearate, %	-	-	8	-	-	-	8	-
Penetration (60W)	265	293	359	-	311	305	341	-

Table 8 Base oil property

Base oil		Mineral oil	PAO
Kinetic viscosity, mm^2/s	40℃	33.2	30.6
	100℃	5.6	5.8
Viscosity index		107	135
Hydrocarbon group, % (n-d-M method)	Paraffinic	67	100
	Naphthenic	28	0
	Aromatic	5	0

First, the bearing torque was examined by using ‘Screening’ condition as described in Table 5. Figures 41 and 42 show the speed dependence of bearing friction torques for greases with mineral oil and PAO, respectively. The velocity value of the inner race of the bearing for each bearing rotation speed was indicated in brackets, such as 200 rpm (0.21 m/s). The bearing torque values at 200, 500, and 1000 rpm seem almost constant during the 10 minutes test duration shown in Fig. 41. On the contrary, the bearing torque values at 2000 rpm were not stabilized within 10 minutes. In order to confirm the reproducibility, three tests with the same condition were conducted for the mineral oil based greases. Figure 43 shows the averaged torque values including deviations for each rotation speed. Each torque value was the averaged torque value during 30 seconds at the end of each duration of each rotation speed. There can be found some deviations, but the rank showing lower torque values did not change.

Returning to the results of Figs. 41 and 42, the torque values for all the samples increased with increment of the bearing rotation speed. L-A (mineral oil + Li-complex) indicated the minimal torque increase with the rotation speed increase. In contrast, those torque increase of S2-A and S2-B with Li-OHSt thickener were remarkably large. In the low rotation speed range of 200 rpm, S1-A provided the lowest torque, while L-A showed the lowest value in the high speed range. This inversion of the grease providing lower torque depending on bearing rotation speed suggests the lubricating condition change due to the rotation speed.

Comparing the result of the previous work [12], the lower torque for Grease A with a combination of mineral oil and Li-complex in the high rotation speed range (2000rpm) was similar, even if the test rigs for the measurement of bearing torque were not identical. Regarding the base oil type dependence, the difference between S1-A and S1-B with Li-St was small, that can be applicable to S2-A and S2-B with Li-OHSt. According to the results of Wikstrom et al. [7], PAO base oil provided the lower running torque compared with the mineral (Naphthenic) oil for Li-OHSt greases and cylindrical roller bearings at 100rpm. In the present study, the comparison between S2-A and S2-B at the rotation speed of 200rpm seems relatively close to the past result, and actually S2-B with PAO base oil showed lower bearing torque than S2-A with mineral (paraffinic) oil. However, the relationship appears to change depending on the rotation speeds. On the contrary, the difference between L-A and L-B with Li-complex was quite large, especially in the high speed range. The influence of the affinity between base oil and thickener could be significant in Li-complex greases, therefore the base oil dependence on the bearing torque was larger in Li-complex greases.

These results of 'Screening' conditions show the clear thickener type dependence especially in mineral base oil greases. Therefore, this study focuses on these three type greases (L-A, S1-A, S2-A) mainly.

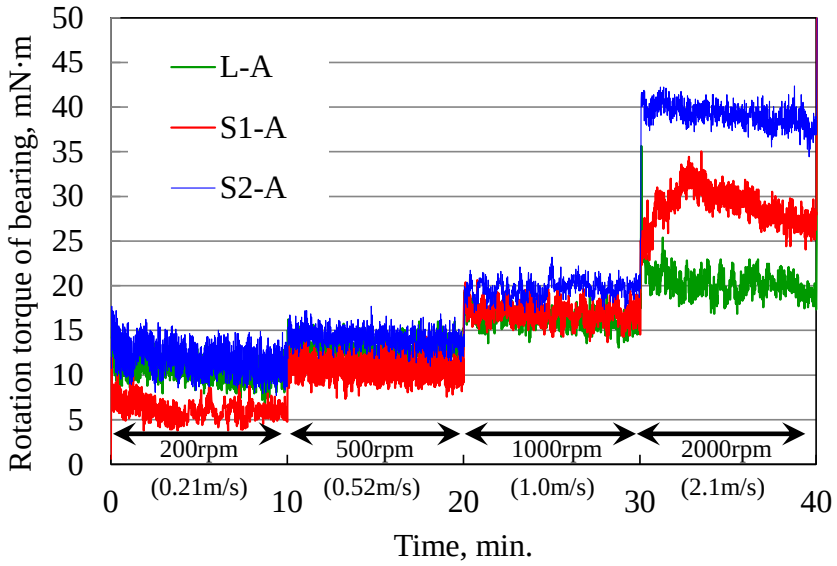

Fig. 41 Speed dependence of bearing torque with mineral oil based greases under the 'Screening' condition

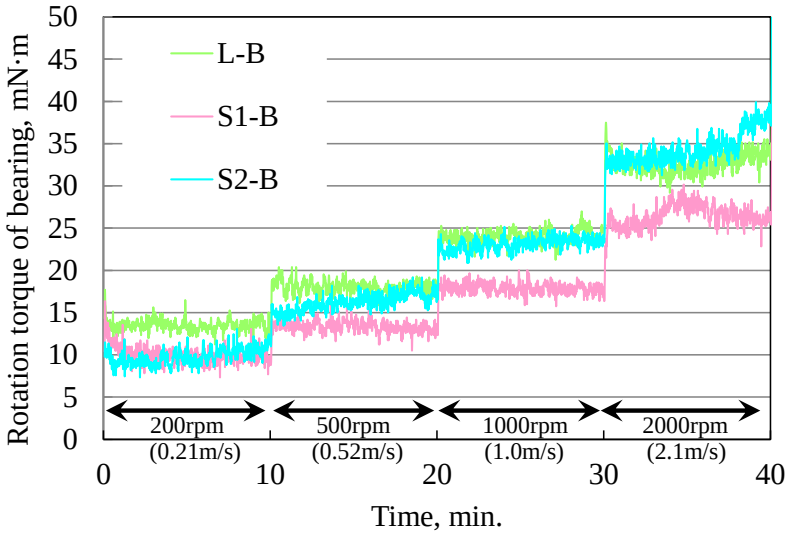

Fig. 42 Speed dependence of bearing torque with PAO based greases under the 'Screening' condition

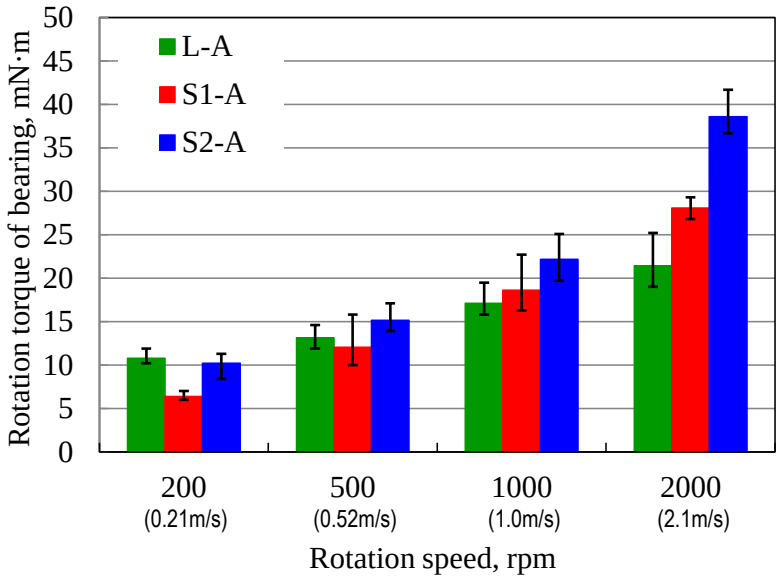

Fig. 43 Averaged values of bearing torque with mineral oil based greases for each rotation speed under the 'Screening' condition.

Although the screening tests of 10 minutes showed the reproducibility at 2000 rpm, the long duration tests of 60 minutes were conducted for 2000 rpm in order to confirm the thickener dependence in detail. Figure 44 shows the thickener dependence focused on the long duration at 2000 rpm. During first 10 minutes at 2000rpm, S2-A showed the highest bearing torque as similar to the Fig. 41. As the time passes, the torque difference between S2-A and S1-A shrank. At the end of the test, the torque values of them reached almost the same. In contrast, L-A kept the lower torque values through the 60 minutes test of 2000 rpm. In addition, the torque values stabilized until 60 minutes duration of 2000 rpm. The torque transition during

this 60 minutes especially in S1-A and S2-A indicates the grease re-distribution in the bearing or the change of the grease property due to the shearing through the test.

In order to investigate the effect of the long duration test, the same test program was continued after finishing the ‘Long duration’ test. Figure 45 shows the bearing torque behaviors under the ‘Repetition’ condition. The bearing torque values in Fig. 45 were more stabilized compared with Fig. 44, especially at 2000rpm. The most of fluctuations about S1-A and S2-A disappeared. In contrast, L-A still showed lower bearing torque, similar to long duration condition in Fig. 44. In the ‘Repetition’ test, the tendency showing lower torque at high rotation speed unchanged. Considering the slow rotation speed of 200 rpm, the tendency was not the same. Figure 46 shows the averaged torque values for each rotation speed. The values were selected during 30 seconds at the end of each duration of each rotation speed. The grease rank showing the lower torque were unchanged between the ‘Long duration’ and ’Repetition’ tests, except for the condition of 200 rpm. Although the difference is small, S1-A showed the lowest bearing torque in Figs. 41 and 43. However, the predominance of S1-A diminished in the ‘Repetition’ condition. The bearing torque values at 200 rpm in the ‘Repetition’ condition were almost the same among the three greases.

For the understanding the cause of the difference of bearing torque behaviors for greases, greases properties were measured as follows.

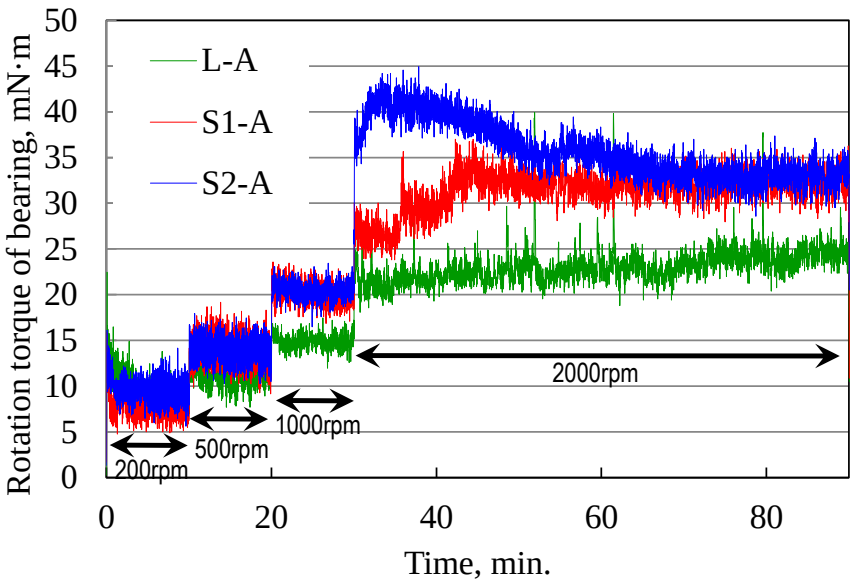

Fig. 44 Speed dependence of bearing torque with mineral oil based greases under the ‘Long duration’ condition.

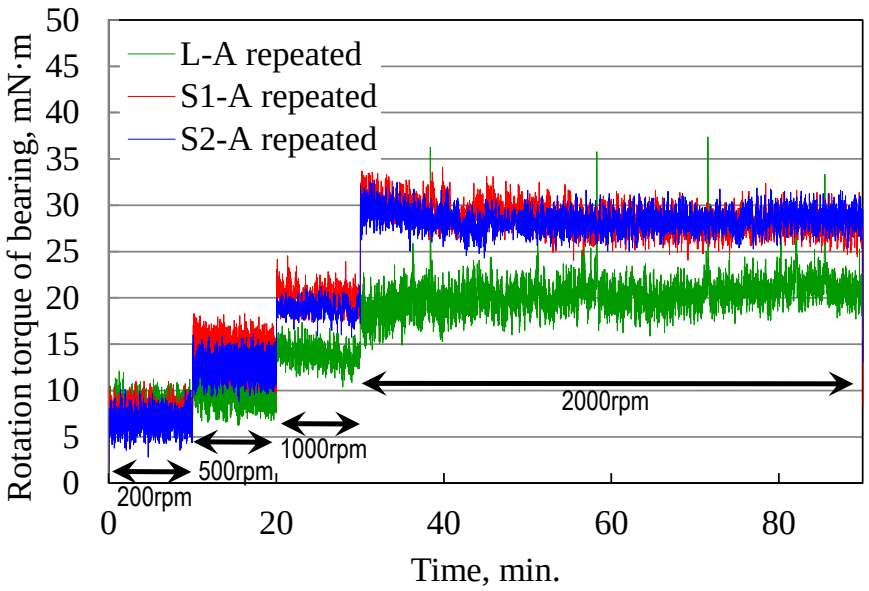

Fig. 45 Speed dependence of bearing torque with mineral oil based greases under the 'Repetition' condition.

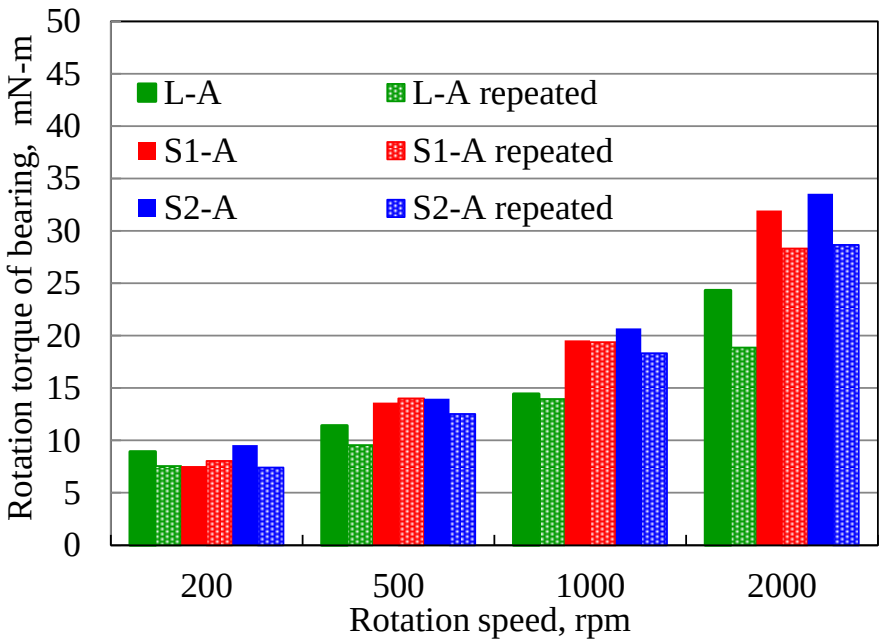

Fig. 46 Influence of repetition tests on the bearing torque values for each rotation speed.

6.2 Rheological parameters

The shear rate dependence of apparent viscosity for grease samples with mineral oil were measured. Figs. 47 and 48 show the results in acceleration and deceleration conditions, respectively. The viscosities of S2-A with Li-OHSt thickener were relatively lower than those of other thickener type greases. In addition, L-A with Li-complex thickener showed higher viscosities in all speed range. Figures 49-51 show each grease viscosity in order to focus on the shear history influence. Viscosities with increase of the shear rate were higher than those in decrease of the shear rate for all the greases. The gap between acceleration and deceleration differed by the thickener type, for instance, S1-A with Li-St showed larger gap.

As mentioned in 5.3, Figure 39 shows the viscoelasticity of S2-A. The yield stress is defined as the lowest shear stress when tanδ (= G''/G') is greater than one, and the yield stresses of greases are summarized in Fig. 52. S1-A showed the highest yield stress. This tendency could relate to the viscosity result. The large viscosity gap could be because the grease was pushed away from the cone of the viscometer. On the contrary, Oikawa et al. [8] reported the grease with higher yield stress causes channeling easily. Considering these grease movement, viscosity gap and yield stress could correlate each other.

In addition, Oikawa et al. also reported that the grease with higher yield stress causes torque reduction high speed rotation speed (1800rpm, 6305 deep grooved radial ball bearing). However, such behavior of S1-A was not observed in this study as referred in 6.1. One of the reasons can be the different thickener types. In Oikawa's study, the greases with the same Li-OHSt thickener were used. Regarding the same type thickener, L-A (Li-complex) type greases with the different thickener content were also investigated as listed in Table 9. The penetration (hardness) of greases depends on the thickener content. Figure 53 compares the yield stress of different thickener contents. The harder grease showed the higher yield stress. Considering channeling effect of greases, it is easy to imagine that harder grease can cause channeling more easily. Therefore, the result is reasonable, however, for grease with different thickener types, the interpretation becomes more complicated.

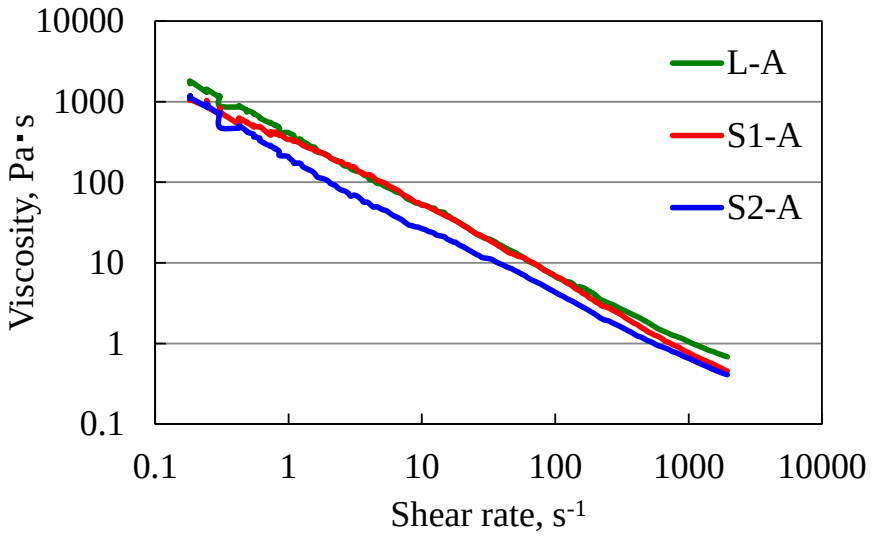

Fig. 47 Apparent viscosity of mineral oil based greases (Acceleration)

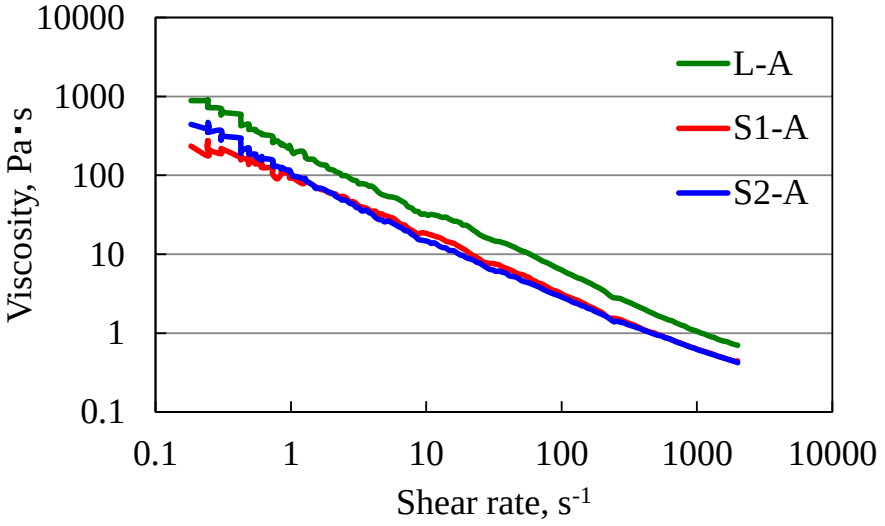

Fig. 48 Apparent viscosity of mineral oil based greases (Deceleration)

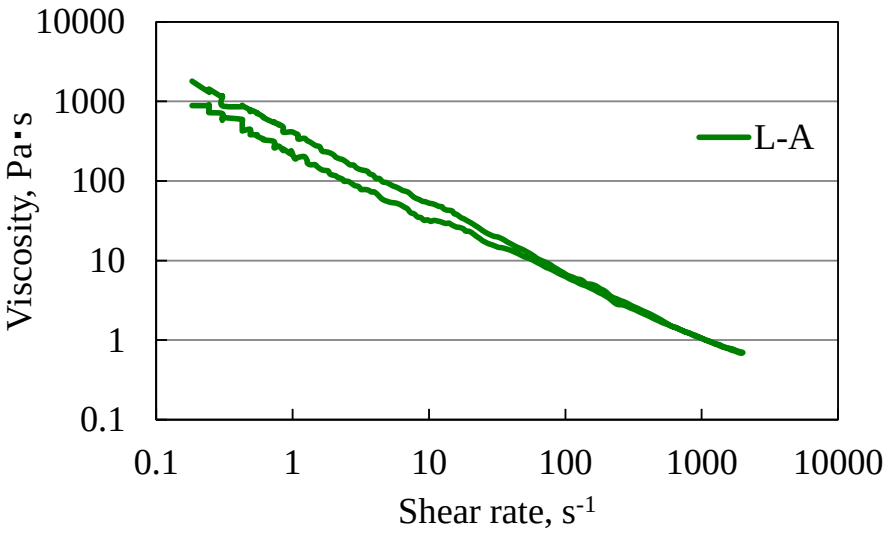

Fig. 49 Apparent viscosity of L-A including high shear history

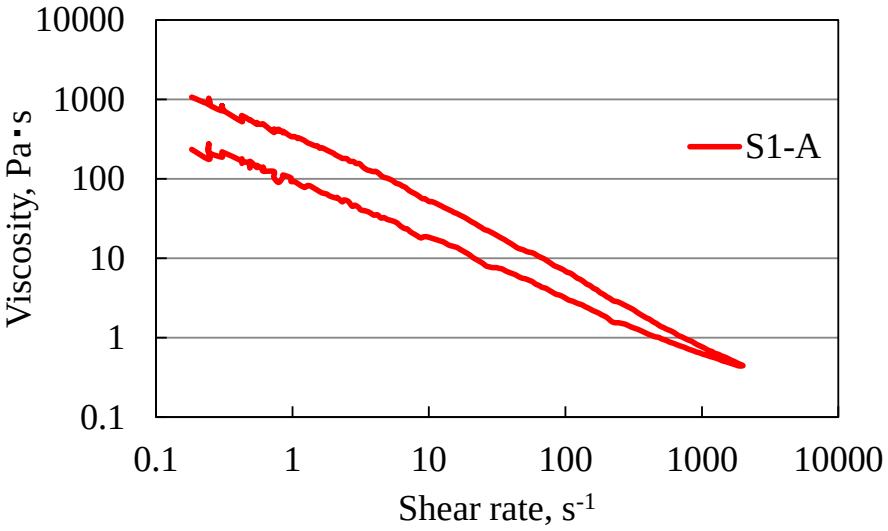

Fig. 50 Apparent viscosity of S1-A including high shear history

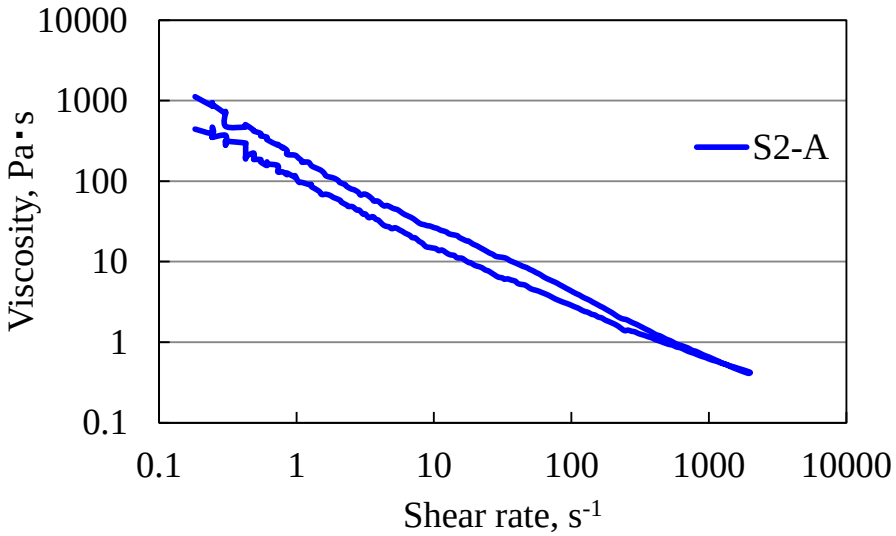

Fig. 51 Apparent viscosity of S2-A including high shear history

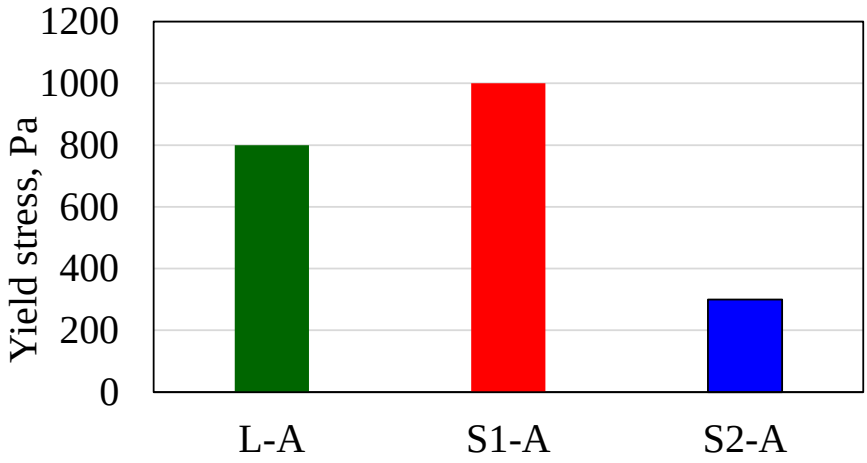

Fig. 52 Yield stress of greases (thickener type dependence)

Table 9 Sample greases

Grease	L-A	L-A(M)	L-A(S)
Mineral oil (G-I), %	88	90	92
Li complex thickener, %	12	10	8
Penetration (60W)	265	289	360

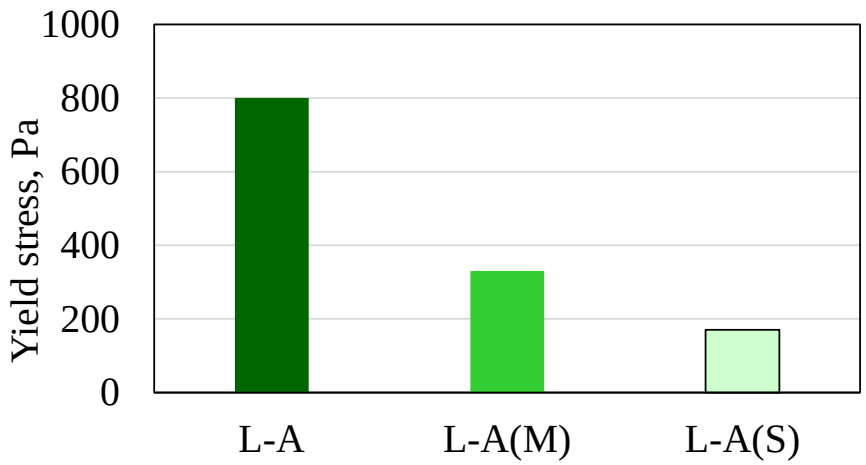

Fig. 53 Yield stress of greases (thickener content dependence)

6.3 Thickener structure

The thickener structures of greases were examined by TEM observation. Figures 54-56 compare the thickener structure of sample greases with different thickeners. All the thickeners formed fiber structures. The fiber shape of Li-complex (L-A) appears thinner and longer structure. On the contrary, the fibers of Li-St (S1-A) and Li-OHSt (S2-A) seem similar and these shapes are thick and short. This difference of structures could be attributed to mainly the thickener types, complex or single soap. This thickener shapes might influence on the grease properties, however, S1-A and S2-A showed completely different behaviors in spite of the similar thickener structures. The effect of the fiber structure does not seem significant in this study.

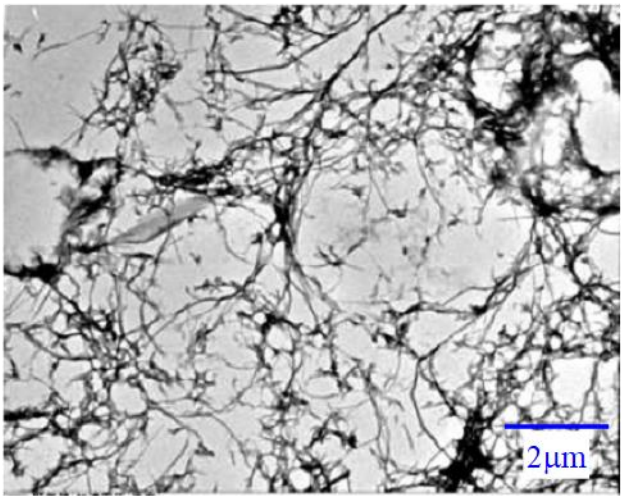

Fig. 54 TEM images of Li-complex thickener (Grease L-A)

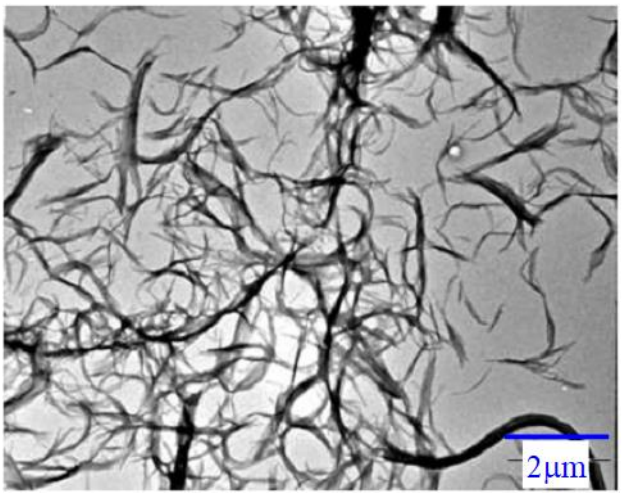

Fig. 55 TEM images of Li-St thickener (Grease S1-A)

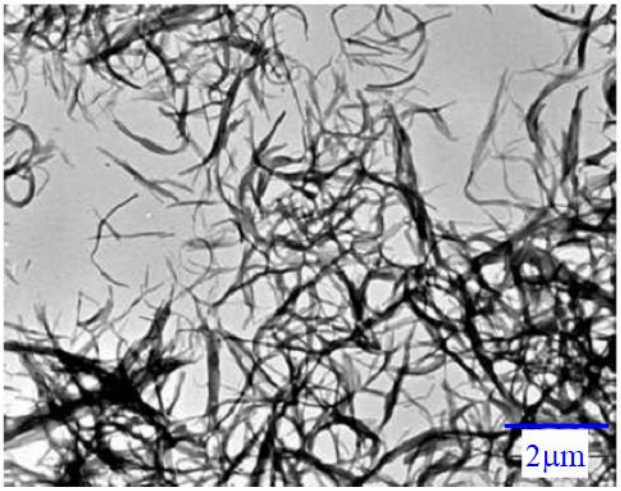

Fig. 56 TEM images of Li-OHSt thickener (Grease S2-A)

6.4 Traction property

The traction property was investigated using a MTM device. Figure 57 compares the velocity dependence of the traction coefficients of the greases and their base oil with 3% of SRR under acceleration conditions. Without a scoop for maintaining fully flooded conditions, three greases showed the temporary traction increase and with increasing the velocity. The traction increased again at high velocity for only L-A. S1-A and S2-A kept the lower constant traction values at the high velocity region. The base oil used for the greases (OilA) showed the almost constant traction values through the all velocity. The values were close to the traction values of S1-A and S2-A at the high velocity region. In addition, the effect of the scoop was also confirmed for L-A. L-A with the scoop showed the stable traction coefficients close to the base oil. This result suggests that the traction properties of the grease depends on the base oil at least under fully flooded conditions. The increase of the traction values compared with the base oil could be related to the lack

of the lubricant at the contact area. Berthe et al. [45] studied the lubricant starvation using a MTM device and reported that the increase of traction coefficients is caused by the lack of lubricants due to the high velocity or the long duration of tests under limited volume of lubricants. In this study, the temporary traction increase for all the greases at low velocity region could be the running-in process of the greases because all the samples showed the behavior commonly. After that, S1-A and S2-A can supply the lubricant (only oil or grease itself) to the contact, therefore the traction values approach those of the base oil. On the contrary, L-A is not able to provide the lubricant to the contact at high velocity region, therefore the traction increases. This phenomenon could be related to the channeling in the bearing operation at high rotation speed. After the measurement shown in Fig. 57, the traction measurements were continued under deceleration conditions as shown in Fig. 58. The traction behavior of L-A with scoop was similar to that in acceleration condition. In contrast, the other greases and base oil showed higher traction coefficients compared with Fig. 57. These traction increase could be the lack of the lubricant to the contact because the lubricant was pushed away at the high velocity conditions in former experiments. This result of the higher traction coefficients of L-A also indicates that L-A is easy to be pushed away from the contact.

The tests of the velocity dependence of the traction property without the scoop conditions seems to reflect the grease movement at the contact. SRR dependence was also investigated in order to confirm the grease movements. Considering the velocity of the inner race of the bearing at the bearing torque tests, the velocity was selected as 0.2, 0.5, 1, and 2 m/s, corresponding to the 200, 500, 1000, and 2000 rpm, respectively. Figures 59-62 compare the SRR dependence of the greases and the base oil at 0.2, 0.5, 1, 2 m/s, respectively. OilA showed the typical traction curve for each velocity condition. The temporary traction increase was observed for the greases occasionally, similar to the velocity dependence as shown in Fig. 57. As the overall tendency, with increasing SRR, L-A showed the traction increase at high SRR conditions following to the temporary traction increase at low SRR and the decrease of the traction (only for low velocity conditions). The traction increase was significant at higher velocity conditions. Conversely, S1-A and S2-A showed the lower traction coefficients which are close to those of the OilA at high SRR conditions. These findings are similar to the velocity dependence results, therefore, it is suggested that L-A is easy to be pushed away from the contact at high SRR condition, compared with S1-A and S2-A. These phenomenon could be related to the bearing torque results at high rotation speed. That will be discussed in the discussion section.

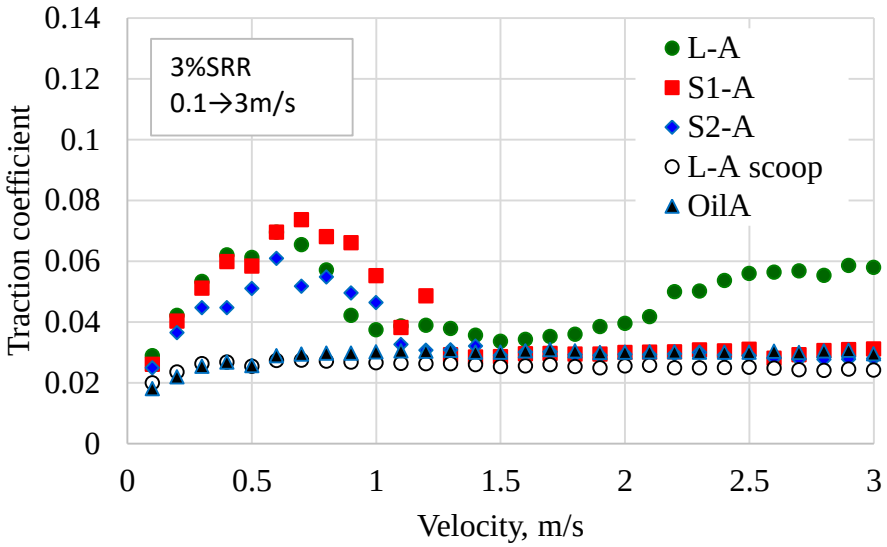

Fig. 57 Velocity dependence on traction property (acceleration)

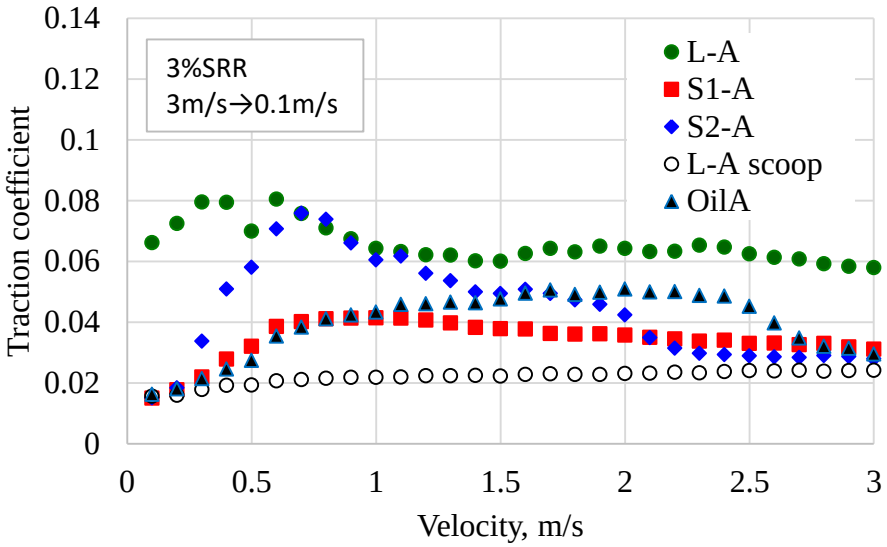

Fig. 58 Velocity dependence on traction property (deceleration)

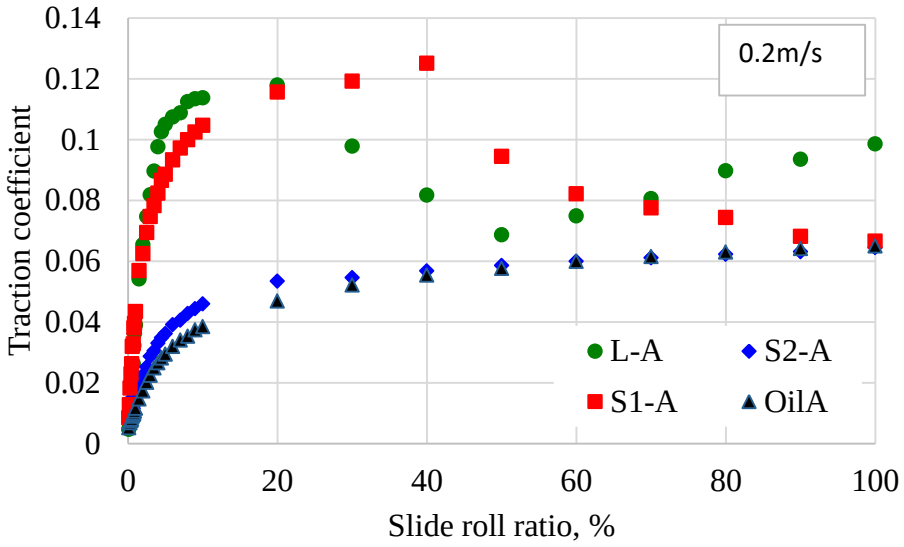

Fig. 59 Slide roll ratio dependence on traction property (0.2m/s)

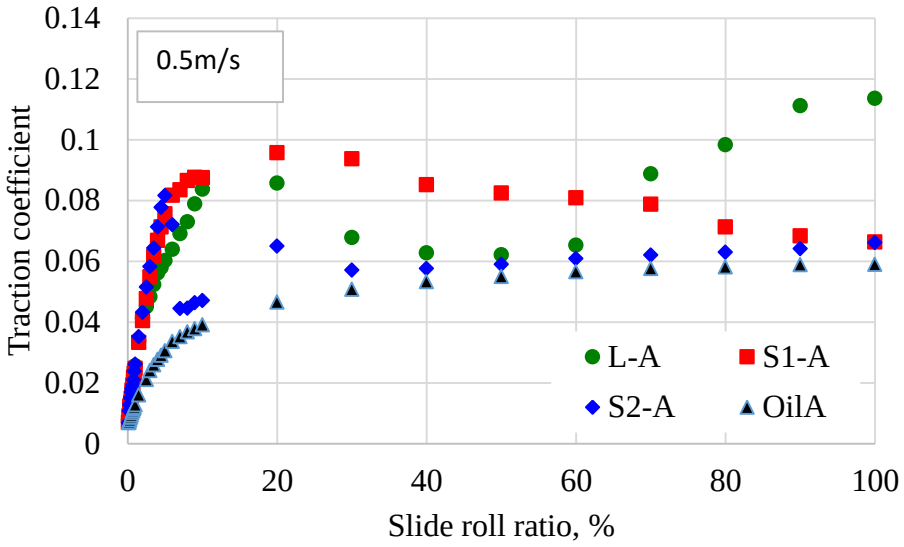

Fig. 60 Slide roll ratio dependence on traction property (0.5m/s)

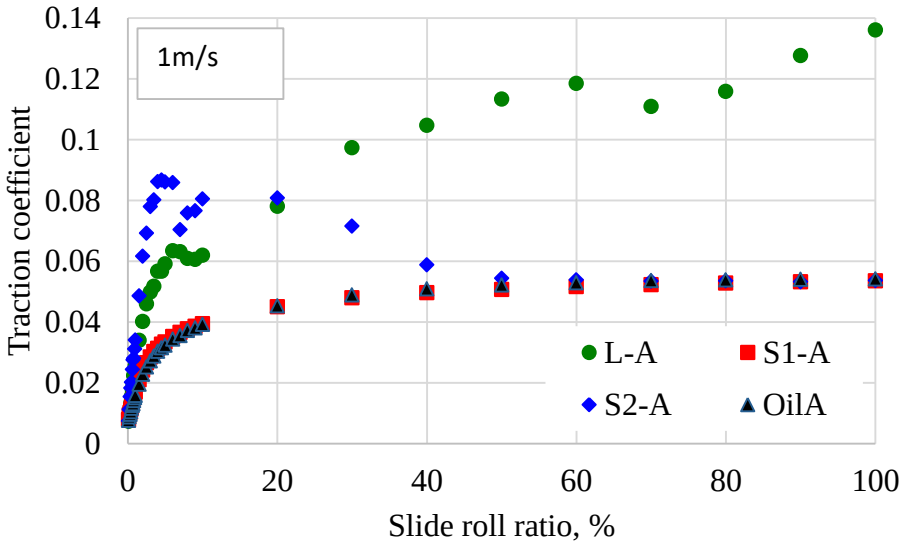

Fig. 61 Slide roll ratio dependence on traction property (1m/s)

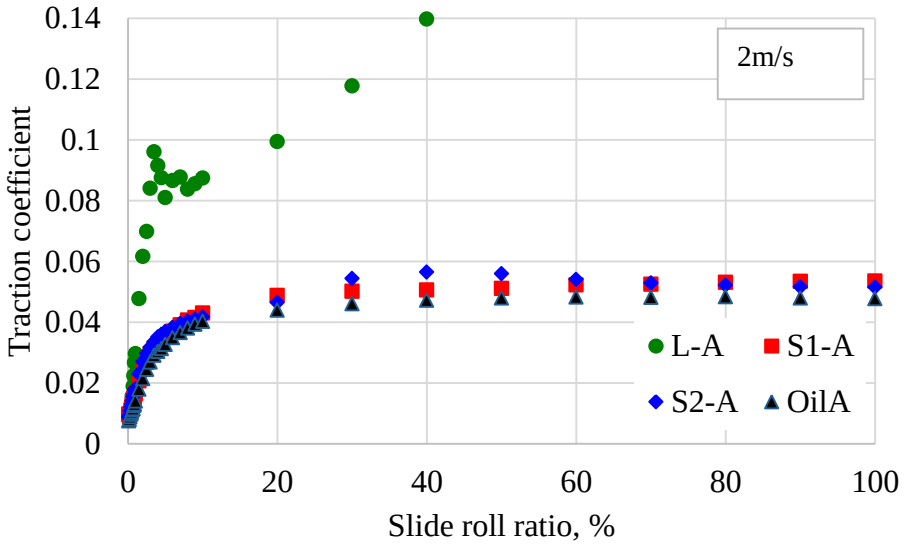

Fig. 62 Slide roll ratio dependence on traction property (2m/s)

6.5 Film thickness for smooth surfaces

6.5.1 Film thickness under fully flooded conditions

Figure 63 compares the central film thicknesses for greases and base oil under fully flooded conditions with 'acceleration' velocity. Regarding the low velocity region, greases with Li-complex (L-A) and Li-OHSt (S2-A) formed thick film thicknesses compared with those formed by the base oil itself since the thickener particle entrainment to the contacts occurred as shown in Fig. 64, observed interferometry images at 0.025 m/s. The thickness values between L-A and S2-A were similar. In contrast, film thickness values formed by Li-St thickened grease (S1-A) were close to those of the base oil. At high velocity region, the dependence of

thickener types on the film thicknesses turned to be less significant, although all the greases formed thicker films than the base oil to some extent.

The central film thicknesses with the velocity condition of 'deceleration' are plotted in Fig. 65. At higher speed range of more than 0.3 m/s, all the greases gave almost the same thicknesses compared with the condition of 'acceleration'. However, the thicknesses for the two greases, L-A and S2-A, apparently decreased in low speed range. Figure 66 also illustrates the interferometry images at 0.025 m/s with the velocity condition of 'deceleration'. The thickener entrainments dramatically diminished about L-A and S2-A. This entrainment changes influenced on the film thickness values especially at low speed. In contrast, OilA and S1-A showed no difference of film thicknesses between the 2 conditions.

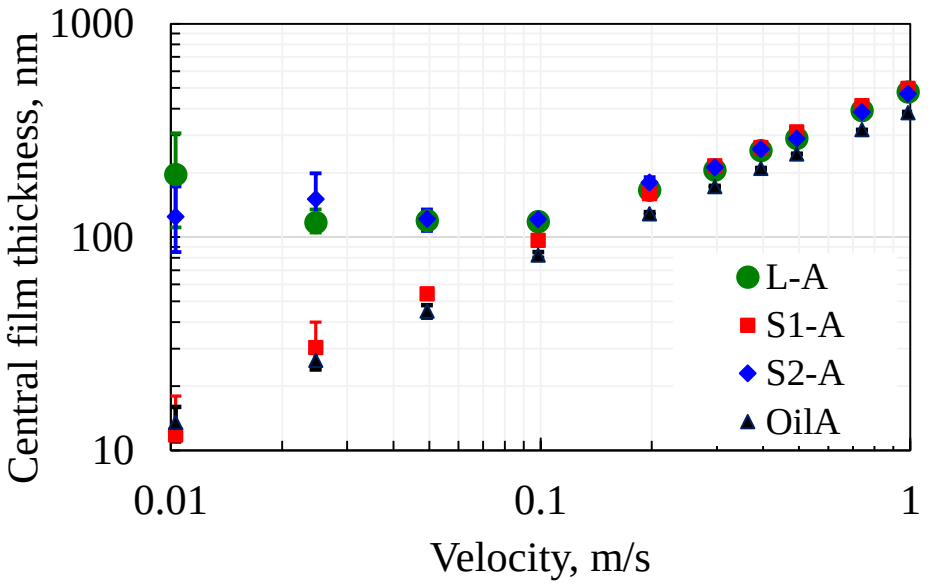

Fig. 63 Central film thickness of greases and base oil under fully flooded condition (acceleration)

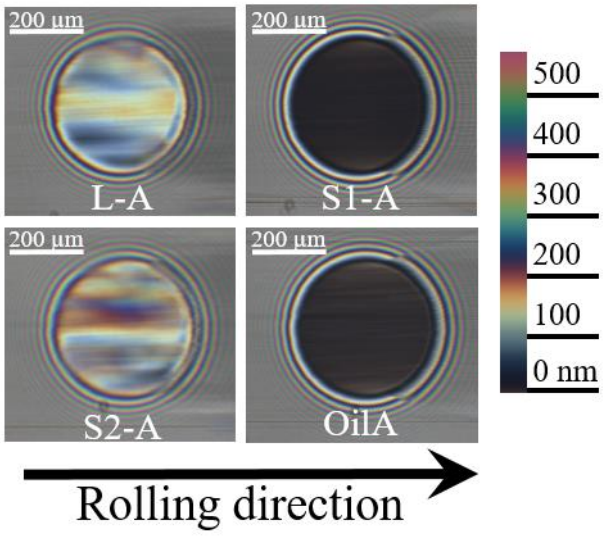

Fig. 64 Interferometry images at 0.025m/s (acceleration)

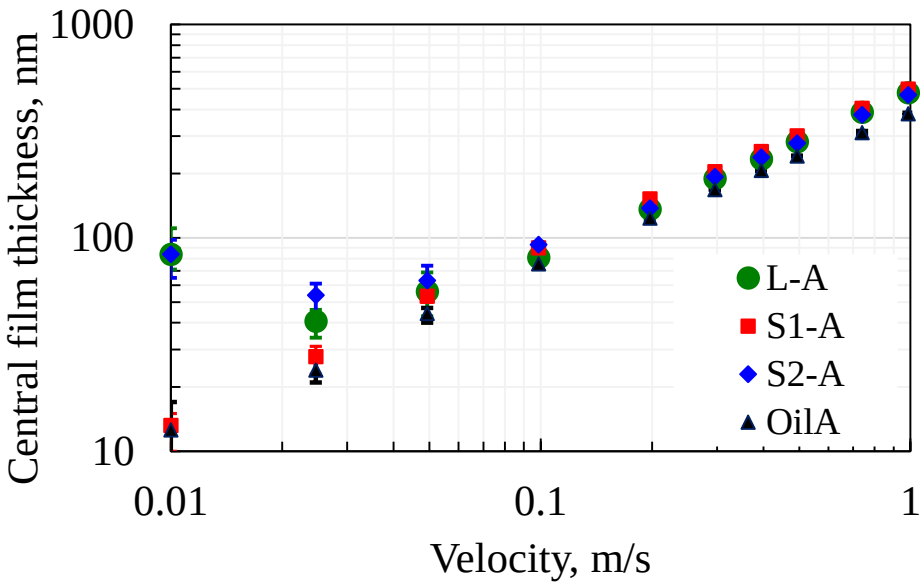

Fig. 65 Central film thickness of greases and base oil under fully flooded condition (deceleration)

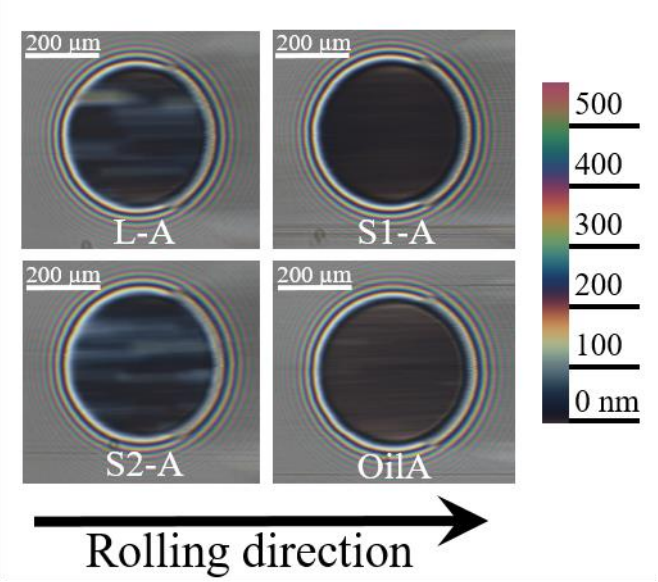

Fig. 66 Interferometry images at 0.025m/s (deceleration)

6.5.2 Track pattern

Flow patterns created on the disk during film thickness measurements under fully flooded conditions were also investigated. Figure 67 compares the patterns at the low velocity of 0.025m/s without high speed history (‘acceleration’ condition). These images show the contact track in the center and the flow patterns on both sides of the track. It was reported that the finger-like patterns are formed by the outlet cavity [33, 34], and the patterns were dependent on the thickener types in this study. Both L-A and S2-A showed flow patterns stretching to the track. In contrast, the pattern formed by S1-A did not reach to the track. This difference can be recognized more clearly in the magnified images of L-A and S1-A. The color of the images is relevant to the thickness of the grease to some extent, like Figs. 64 and 66. However, it should be noted that the value of the thickness is not precise, because the interference is not related between the steel ball and the glass disk but between the air and the disk. Although the interference colors do not show adequate quantitative values, it can be stated that brown and dark blue show thinner film (shown in black arrows) and green and purple show thicker film (shown in blue arrows), and no colors (or grey) show much thicker film (shown in red arrows). For instance, in the flow pattern of the side track of L-A, there can be found that thick area without colors and thin area with some colors repeat alternately. The thick area without colors distributed to the near side of the track. In the case of the S1-A, the edge of the track was surrounded by the thin area such as brown color. These difference could relate to the film thickness behaviors.

Flow patterns observed in the high speed of 0.4 m/s are illustrated in Fig. 68. In the case of L-A and S2-A, the intervals of the finger-like patterns on both side of the track were shorter compared with the images in Fig. 67. This tendency corresponds to the Chen’s study [34], which indicates the interval depends on the entrainment speed. On the contrary, the flow pattern about S1-A was vague. At least, the brown color shows some thickness on the track. However, the edge of the track was also surrounded by thin area, different from the images of L-A and S2-A.

As well as the film thickness measurements in order to understand the influence of the high speed history, the flow patterns were compared in the speed of 0.025 m/s with the velocity condition of ‘deceleration’ as show in Fig. 69. The flow pattern on the side track formed by S1-A was almost the same to the one observed under the ‘acceleration’ condition as shown in Fig. 67. In the cases of L-A and S2-A, the flow patterns after high speed condition became more distinct compared with those in Fig. 67. These pattern changes indicate the correlation with the film thickness changes observed in Fig. 65. Figure 70 also compares the flow patterns at 0.4 m/s with the velocity condition of ‘deceleration’, however, the clear difference was not found compared with Fig. 68.

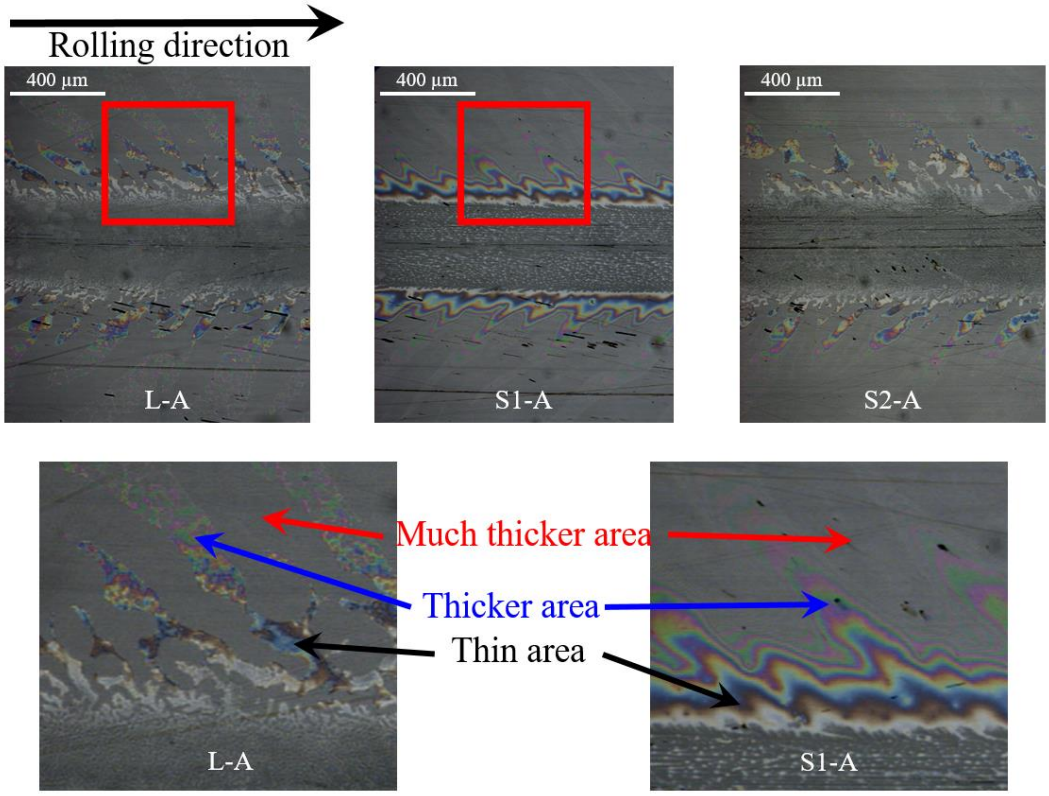

Fig. 67 Grease flow patterns at the downstream of the contact at 0.025m/s (acceleration) and magnified images of the zone shown in red rectangles

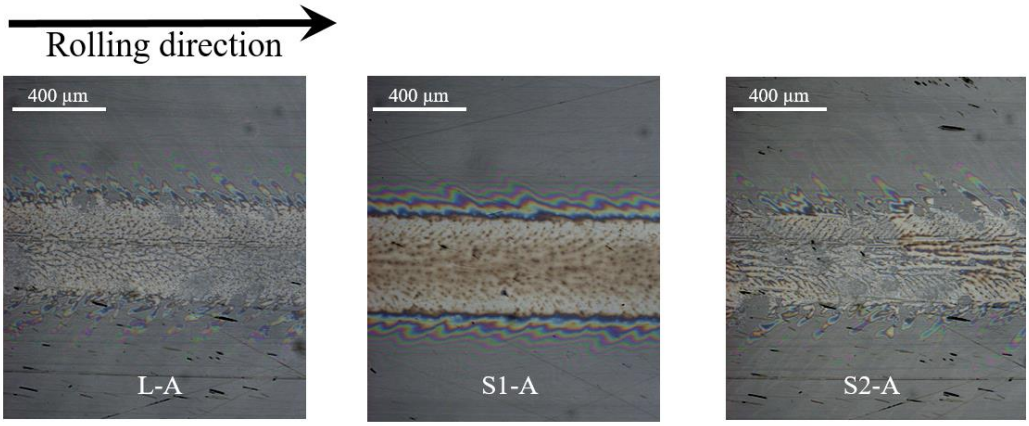

Fig. 68 Grease flow patterns at the downstream of the contact at 0.4m/s (acceleration)

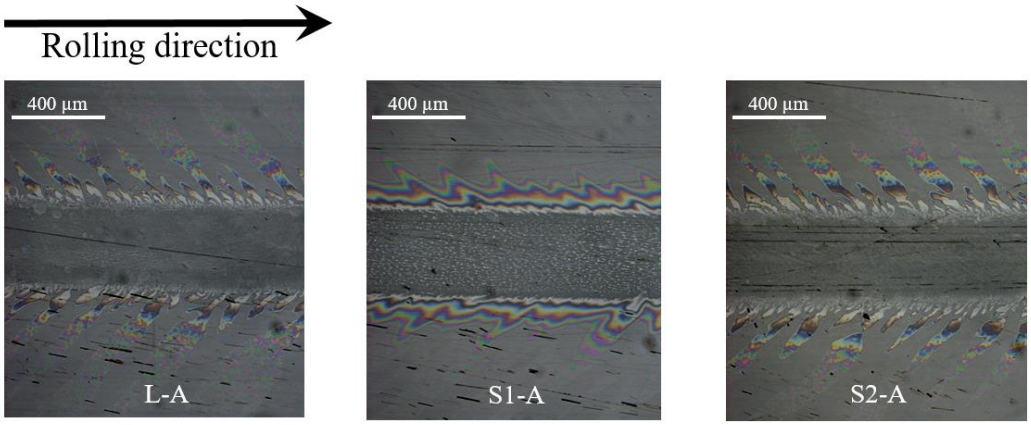

Fig. 69 Grease flow patterns at the downstream of the contact at 0.025m/s (deceleration)

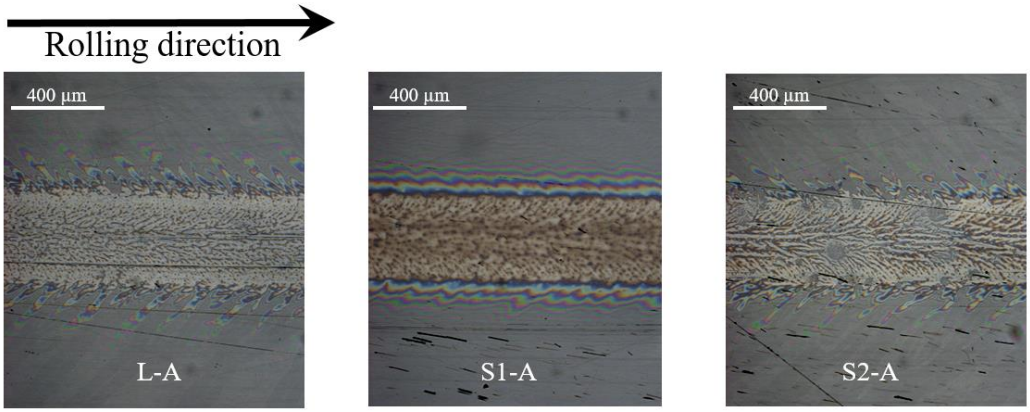

Fig. 70 Grease flow patterns at the downstream of the contact at 0.4m/s (deceleration)

6.5.3 Film thickness under starved conditions

Figure 71 shows the grease film thickness transition with the velocity increase without a scoop under starved conditions. The film thickness values for all the greases showed the transition to starvation between 0.2 and 0.5 m/s. In the low speed range just before the film thickness drops, the film thickness values were similar to those under fully flooded conditions as shown in Fig. 63. The grease film thickness transition related to the starvation corresponded to the former research [17]. The film decay of S1-A occurred early in 0.2 m/s, and that of S2-A did latest in more than 0.3 m/s. The interferograms of the contacts for each grease were illustrated in Fig. 72 at 0.25 m/s. S1-A shows the typical starvation image with the visible meniscus. Conversely, L-A and S2-A did not reach the starvation and kept substantial film thicknesses in spite of the approach of the meniscus to the contacts. Comparing L-A and L-A(S) (with the higher worked penetration), the film decay

occurred relatively late in L-A(S), therefore, it suggests that the softer grease can contribute to the higher lubricant replenishment.

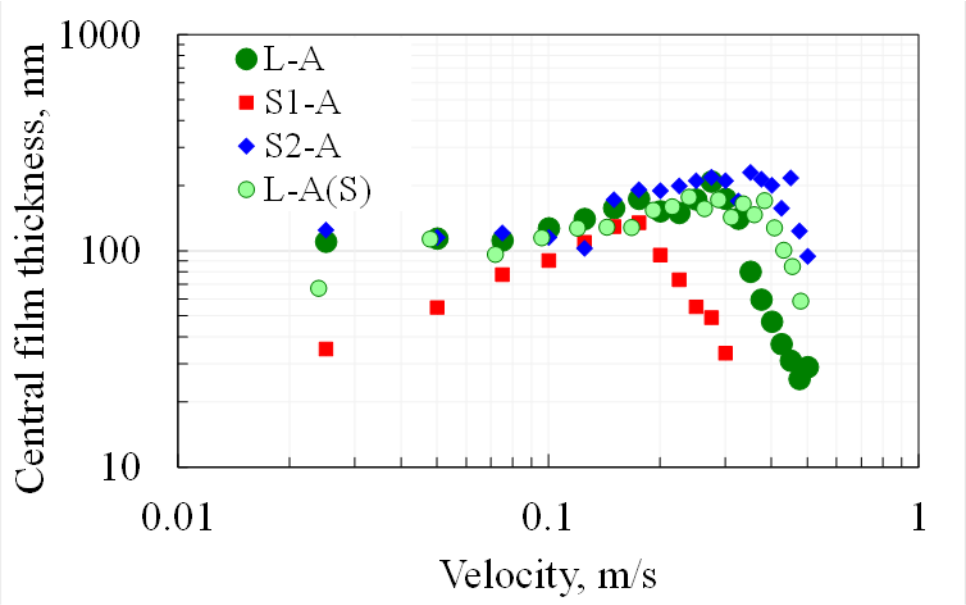

Fig. 71 Central film thickness of greases under starved condition

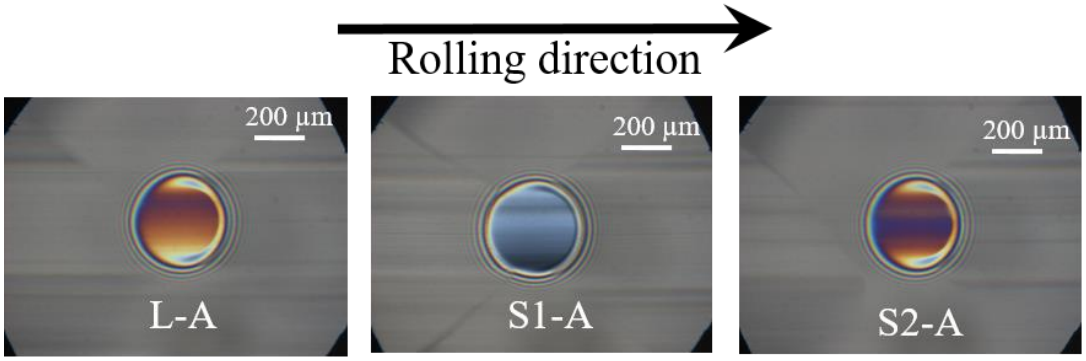

Fig. 72 Interferometry images at 0.25m/s (starved conditions)

6.6 Film thickness for dented surfaces

6.6.1 Surface profiles of bearing

Surface profiles of the bearing used in the bearing torque tests were determined by 3D optical interferometry in order to compare the real asperity of the bearing surfaces and the dented surfaces produced in this study. A 6204 bearing was cut for the observation of the surfaces of each bearing part as shown in Fig. 73. Figures 74, 75, and 76 illustrate the surface profiles of the bearing ball, inner race, and outer race, respectively. The RMS roughness values of 6204 bearing ball, outer race, and inner race were about 25, 20, and 27 nm, respectively. However, from the profiles the asperities of hundreds of nanometers were observed on all the bearing surfaces from Figs. 74-76. Therefore, it is valuable to consider the influence of dents

of a few hundreds of nanometer depth (see Table 4) on the film thickness in this study although the aspect ratios of the asperity of the real bearing and the dents produced in this study are not the same.

Fig. 73 6204 bearing

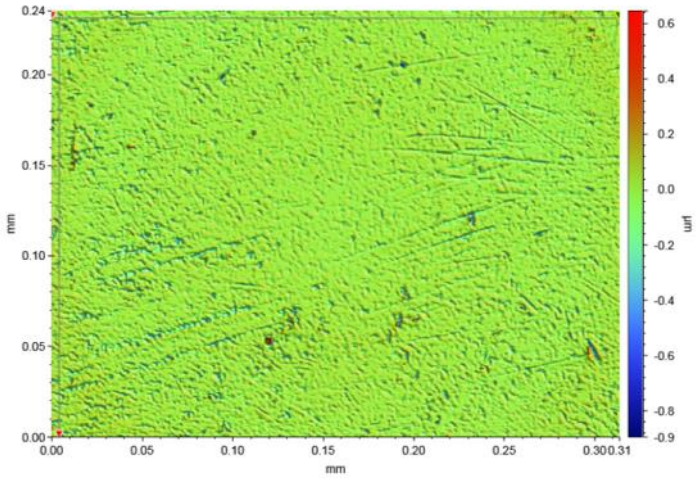

Fig. 74 Surface profile of a ball of 6204 bearing

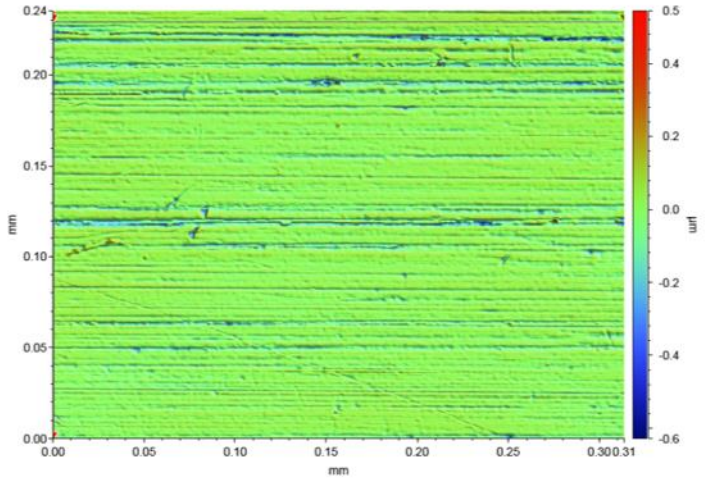

Fig. 75 Surface profile of the inner race of 6204 bearing

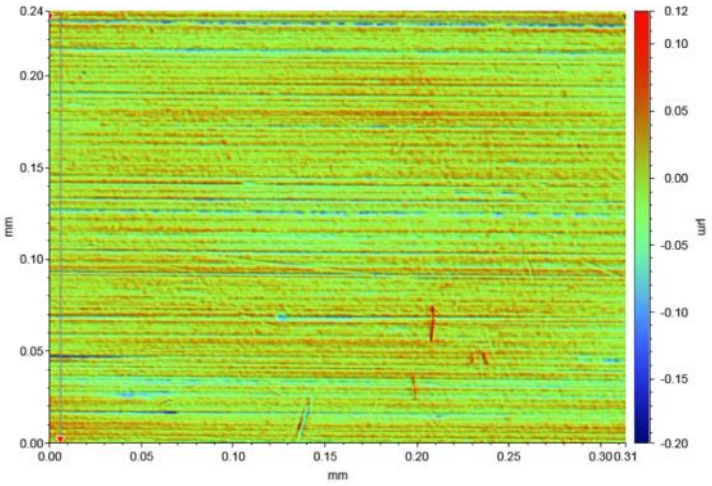

Fig. 76 Surface profile of the outer race of 6204 bearing

6.6.2 Film thickness under fully flooded conditions

The effect of the dent size on the film thickness was investigated for the greases and the base oil. Figure 77 shows the representative interferometry images when the dented ball produced by the WC indenter with a diameter of 2.5 mm was used. These dents were the shallowest and widest sized in this study as shown in Table 4. The images were captured when the dents of the ball approached the center of the contact.

The film thicknesses on the dents were higher than those on the smooth area. The film decrease at the downstream of the dents was also observed, corresponding to the previous study in oil lubrication [38, 41, 42]. In this study, the thickener entrainments to the contact were found in the case of L-A and S2-A, not only in smooth areas but also in dented areas. The entrainment was rarely observed for S1-A. Comparing the interferometry images from L-A and S2-A, the difference of particle entrainments was not large. For the thickener entrainment, the film decrease at the

downstream of the particles was not observed in these interferometry images. The values of the central film thickness on smooth areas and the thickness on dents were shown in Fig. 78. ‘Accel’ and ‘decel’ mean the conditions of ‘acceleration’ and ‘deceleration’, respectively. The values of the film thickness were the averaged values calculated from 5 captured images since the values fluctuated especially at low speeds. Under the ‘acceleration’ conditions, L-A and S2-A showed much higher film thickness on dents occasionally, not always. That increase depends on the random entrainments of the thickener to the dents. However, the most of film increases on the dents in L-A and S2-A disappeared under the ‘deceleration’ condition. The tendency is similar to the results for smooth surfaces contacts as shown in Figs. 63 and 65. S1-A and the base oil did not show such ‘inconsistency’ on the film thickness for dented surfaces, because the thickener entrainments to the dents did not occur. The differences between smooth and dented areas were almost the same in S1-A and the base oil. The difference values are also close to the case of L-A and S2-A under the ‘deceleration’ condition. That suggests that grease film behavior on dents is similar to oil behavior if the thickener does not enter the dent.

For the investigation of the influence of different size of dents, Figure 79 shows the interferometry images when the medium sized WC (1.6mm in diameter) indenter was used for the production of the dents. The values of the film thickness on smooth and the dented areas were shown in Fig. 80. In general, the tendency is similar to the results of the shallowest and widest indenter shown in Figs. 77 and 78. However, there can be found the tendency that the thickener particles of S2-A were dragged into the dents more frequently than those of L-A. In another words, the particle entrainment could be influenced by the dent shape, therefore, the detailed investigation was performed for the sharpest dent size produced by the indenter with the diameter of 1.27 mm. For the evaluation of the influence of the dent produced by the smallest WC indenter, the depth profiles of the targeted dents were identified as shown in Fig. 37. Figures 81 and 82 show the interferometry images including the high speed history (‘deceleration’ condition) for dent1. The results for dent2 are shown in Figs. 83 and 84. In order to compare the smooth surfaces, the images on the smooth contacts are shown in Figs. 85 and 86. Figure 87 shows the averaged film thickness values, and Figures 88 and 89 show the thickness values on targeted dent for dent1 and dent2, respectively. The tendency of the thickener types under these sharp dent conditions was similar to that under the dents produced by the WC with the diameter of 1.6mm (medium size). Thickener particles of S2-A were entrained to the contact more frequently than those of L-A in ‘acceleration’ condition. These difference was not clear under the shallow dent condition (WC with 2.5mm in diameter), therefore it is suggested that the feature of the thickener types become remarkable under the sharp dent conditions.

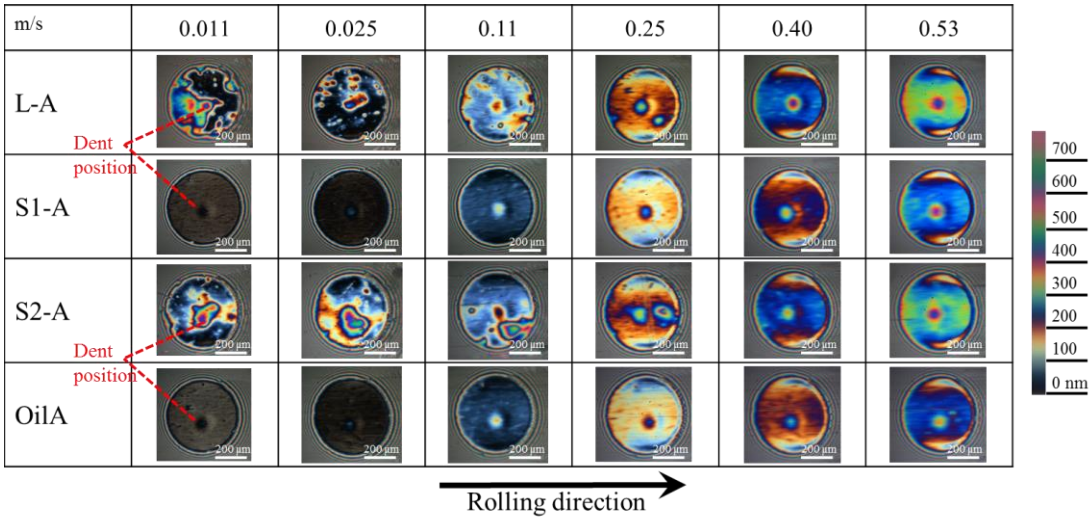

Fig. 77 Interferometry images on dented surfaces produced by the indenter with a diameter of 2.5mm (acceleration)

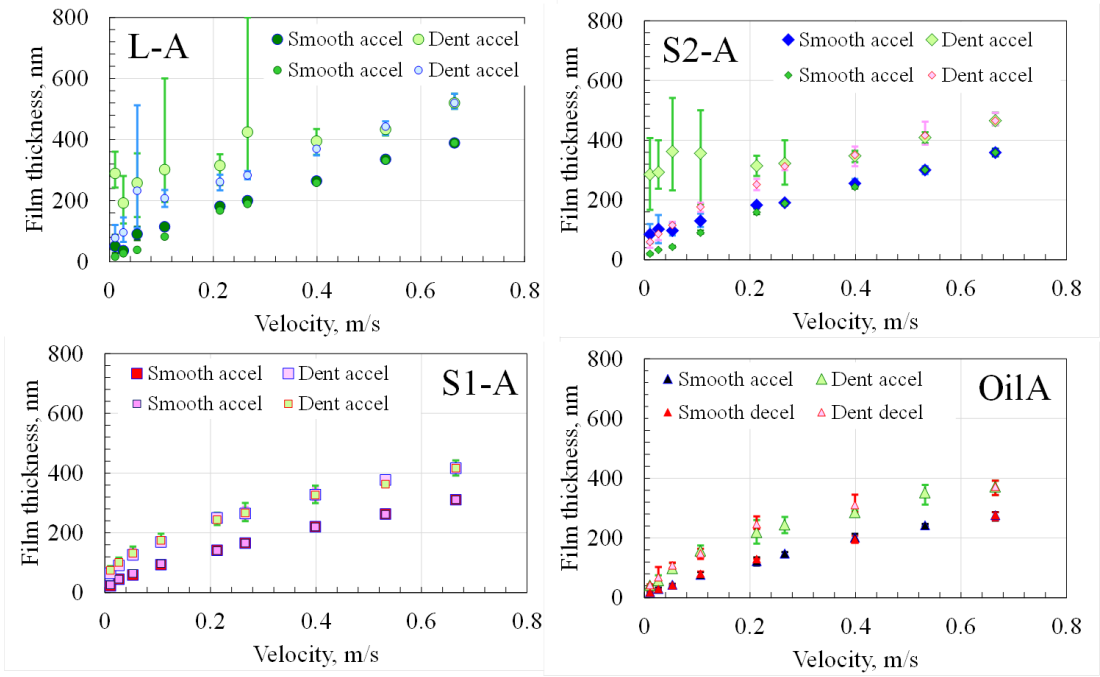

Fig. 78 Film thickness of central smooth and dented areas under fully flooded conditions (indenter with a diameter of 2.5mm)

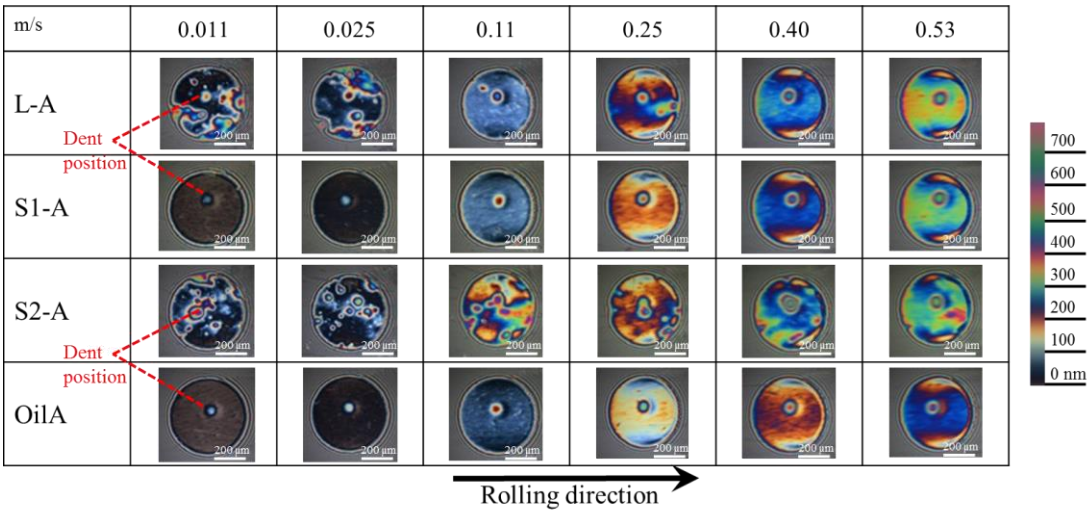

Fig. 79 Interferometry images on dented surfaces produced by the indenter with a diameter of 1.6mm (acceleration)

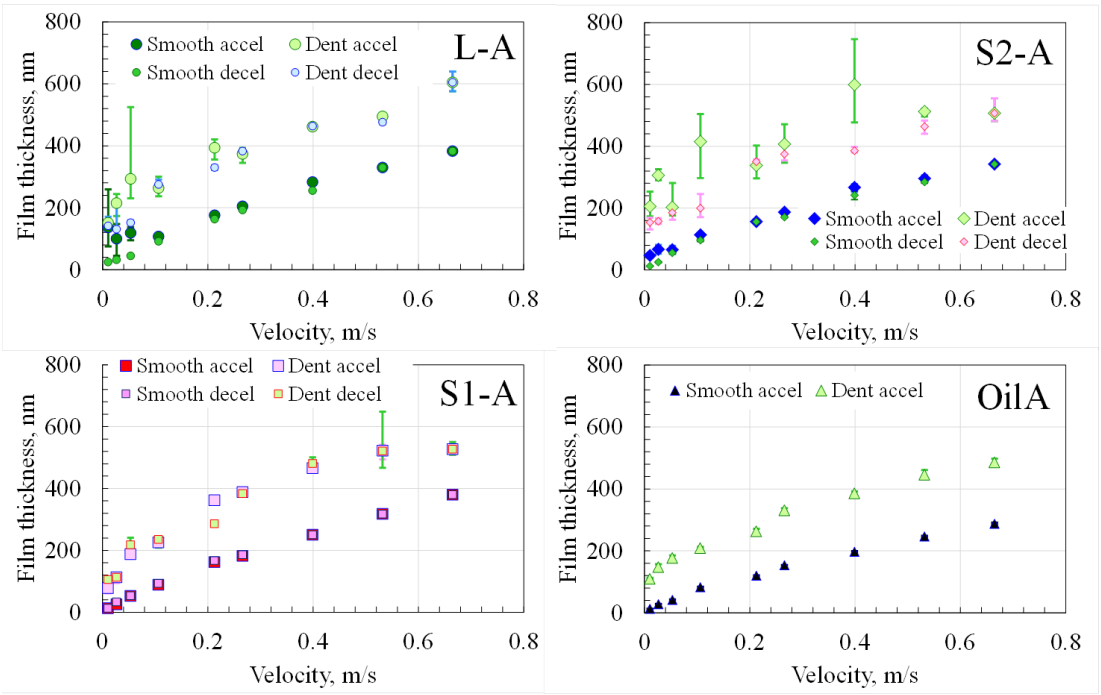

Fig. 80 Film thickness of central smooth and dented areas under fully flooded conditions (indenter with a diameter of 1.6mm)

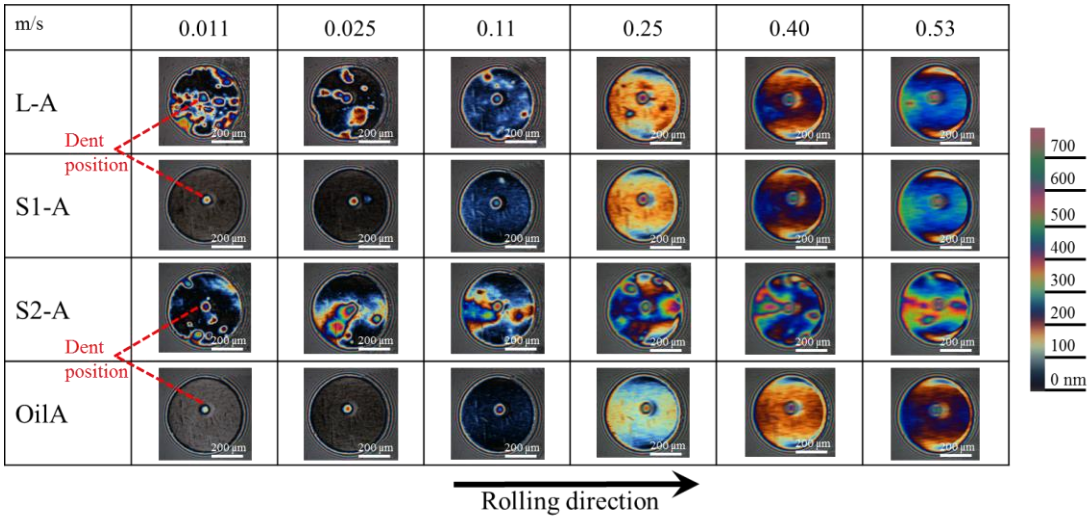

Fig. 81 Interferometry images on the dented surface produced by the indenter with a diameter of 1.27mm (dent1, acceleration)

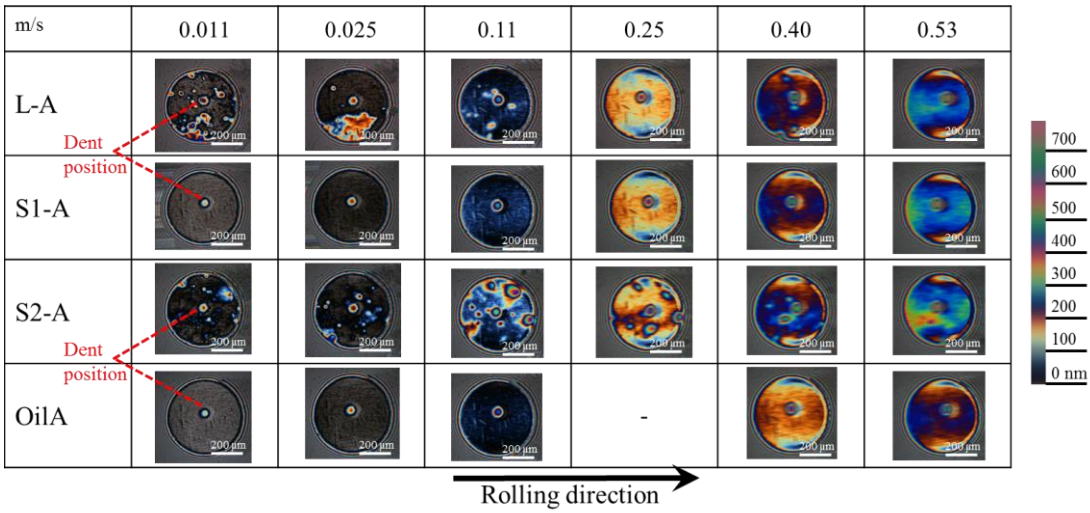

Fig. 82 Interferometry images on the dented surface produced by the indenter with a diameter of 1.27mm (dent1, deceleration)

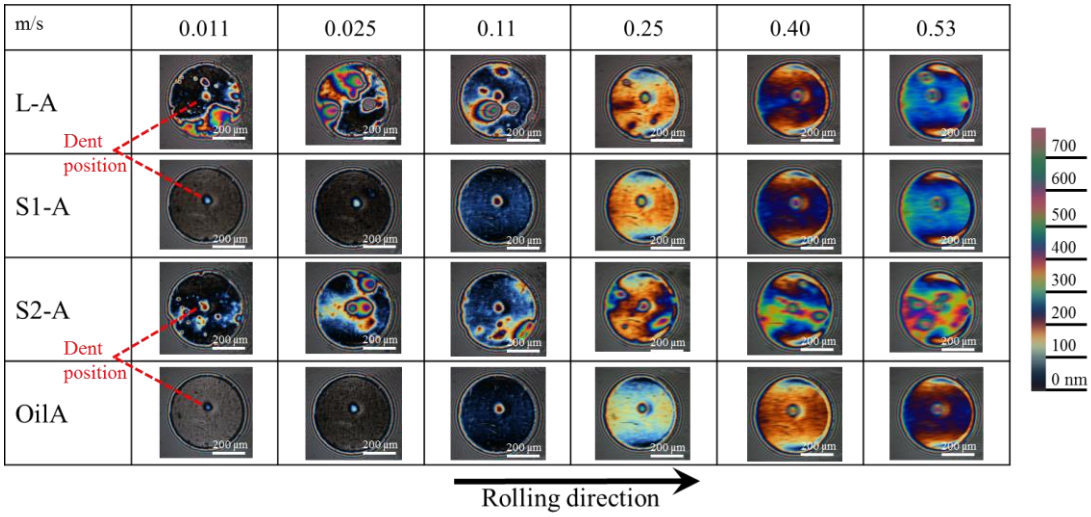

Fig. 83 Interferometry images on the dented surface produced by the indenter with a diameter of 1.27mm (dent2, acceleration)

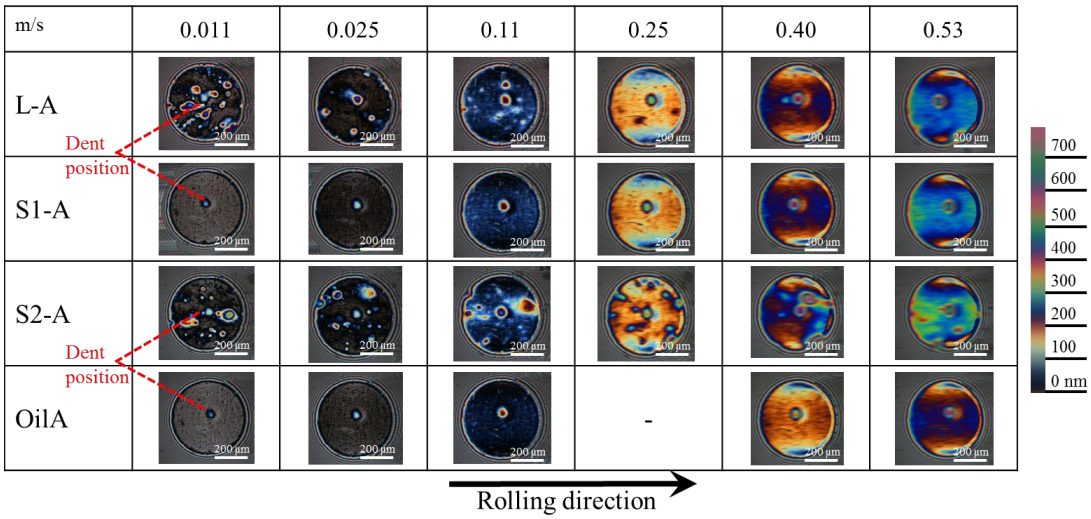

Fig. 84 Interferometry images on the dented surface produced by the indenter with a diameter of 1.27mm (dent2, deceleration)

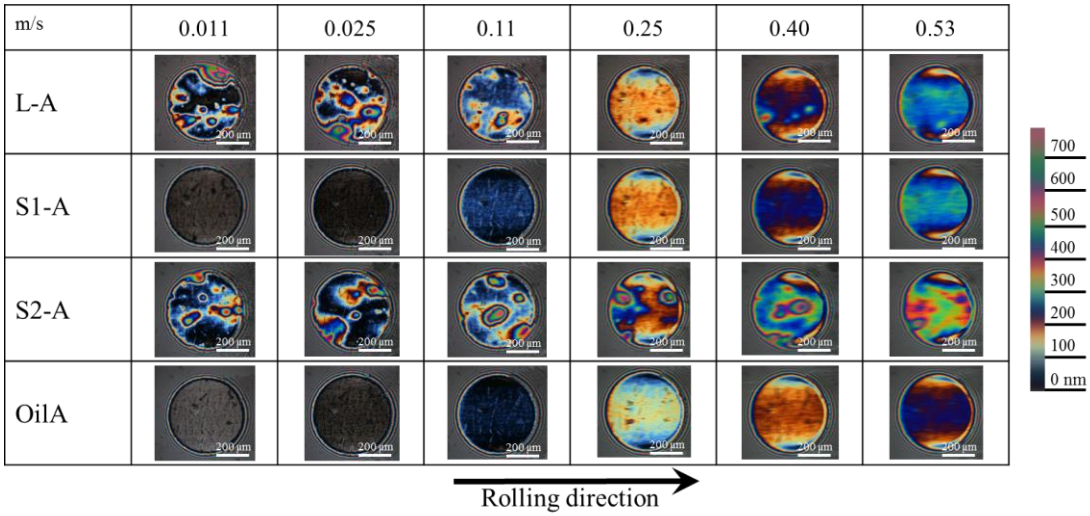

Fig. 85 Interferometry images on smooth surfaces (acceleration)

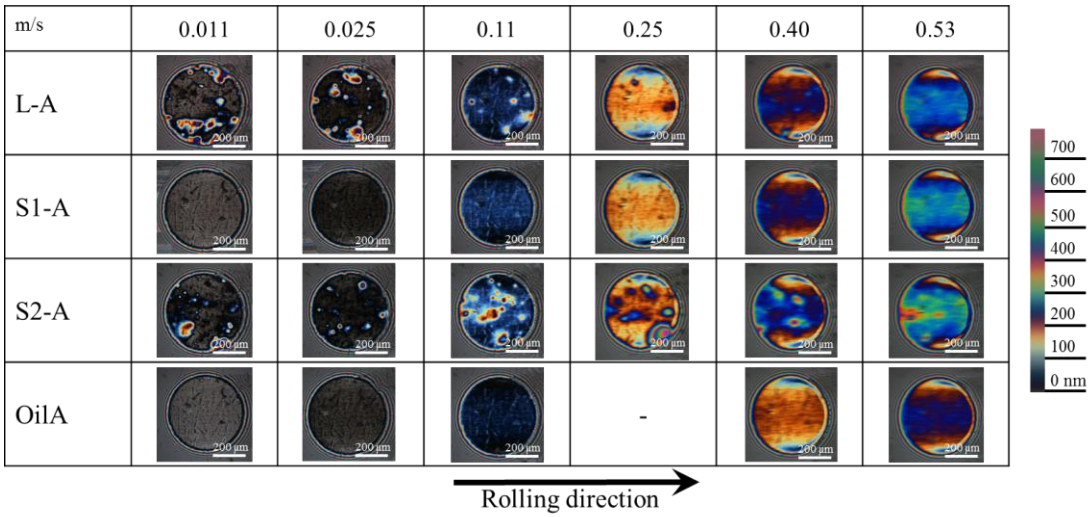

Fig. 86 Interferometry images on smooth surfaces (deceleration)

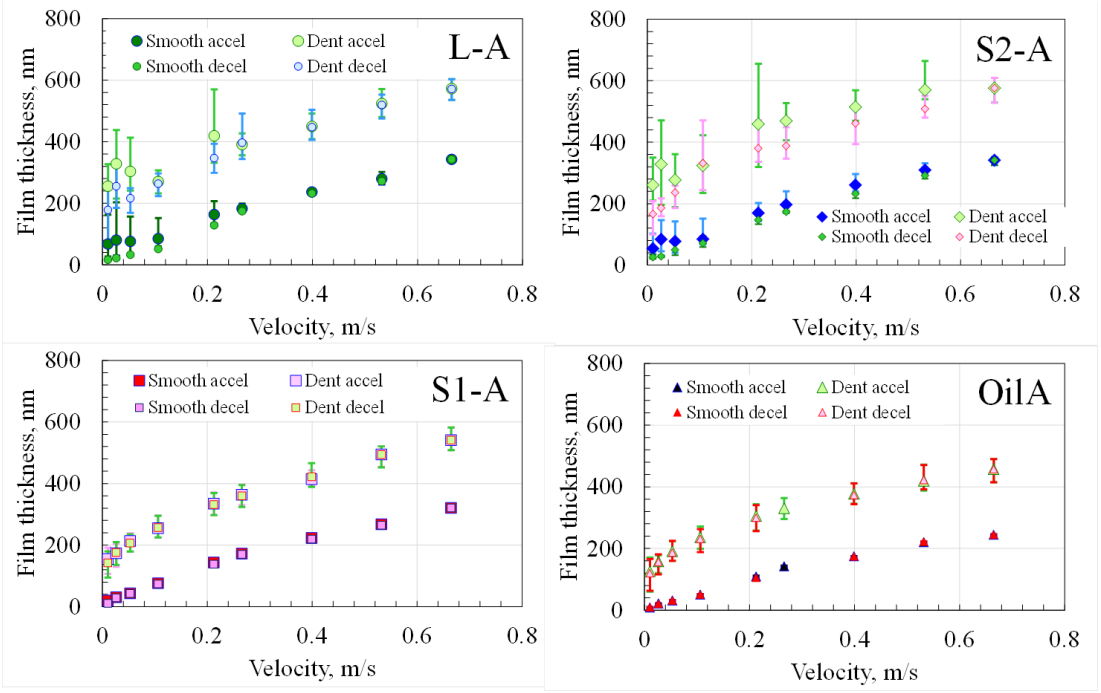

Fig. 87 Film thickness of central smooth and dented areas under fully flooded conditions (indenter with a diameter of 1.27mm)

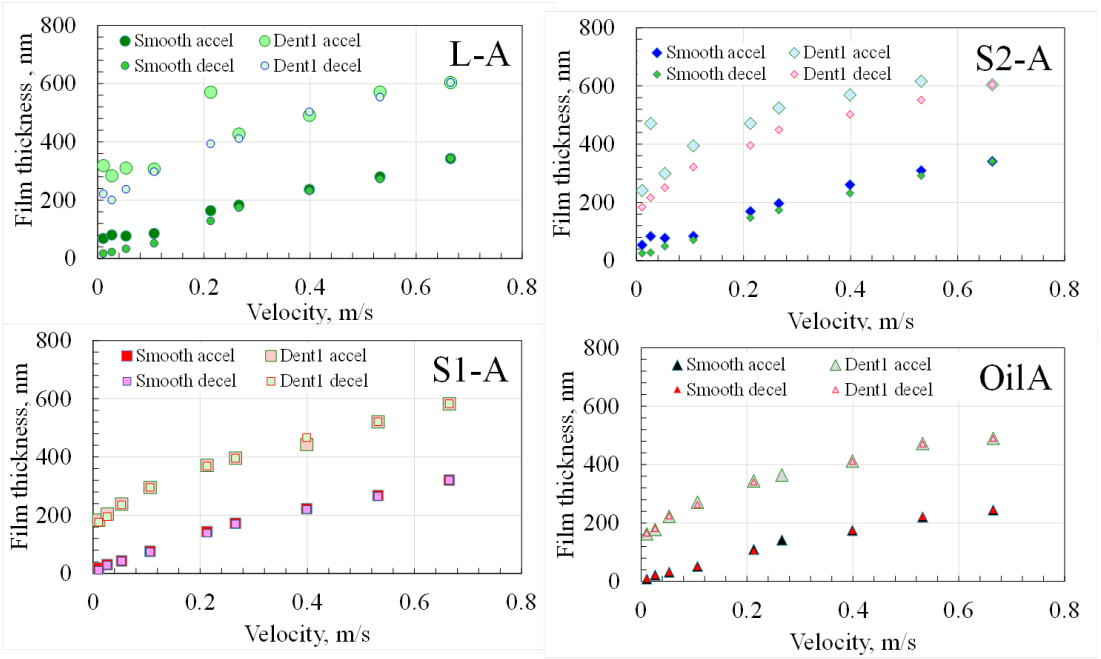

Fig. 88 Film thickness of central smooth and dented areas under fully flooded conditions (dent1)

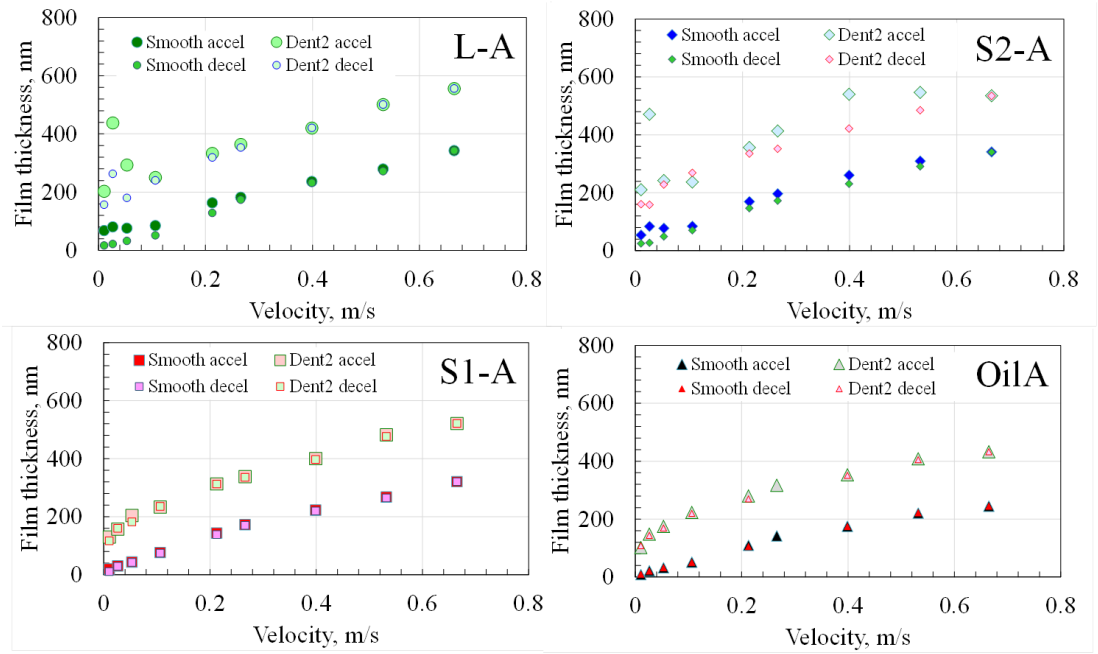

Fig. 89 Film thickness of central smooth and dented areas under fully flooded conditions (dent2)

7 DISCUSSION

The results obtained in 6.1 indicate that the rank showing the lower bearing torque be influenced by the bearing rotation conditions. In this discussion, the correlation with the grease properties is verified for each rotation speed condition. In addition, the grease behaviors which seem to have no relationship with the bearing torque are discussed considering the relationship among grease properties.

7.1 Correlation with bearing torque under low speed conditions

As described in 6.1, the bearing torque behaviors were screened in Figs. 41 and 43. In the low rotation speed region of 200 rpm, S1-A with Li-St showed the lower bearing torque comparing other type thickeners (Li-complex and Li-OHSt). This tendency could correlate to the film thickness behaviors at low speeds. Figures 63 and 64 suggest that Li-St thickened grease forms thinner film thickness similar to the base oil and that Li-complex and Li-OHSt thickened greases form thicker film thickness at low speed. This difference is attributed to the thickener particle entrainment to the contact. The particle entrainment is also confirmed on the dented surfaces, such as in Figs. 77, 79, and 81. However, the frequency of the entrainment to the dent areas does not seem to relate to the bearing torque comparing L-A and S2-A. This particle entrainment could disturb the smooth rotation in bearings and cause the higher bearing torque at low rotation speed conditions.

The thickener chemical structures could be one of the reasons of thickener entrainment to the contact. For instance, high polar 12-hydroxyl groups of aliphatic chains in Li-complex and Li-OHSt could have higher affinity for the metal surface, since the surfaces should be in metal oxide state and have polarity, and promote the entrainment of greases into the contact area. Hoshi et al. [32] observed grease EHL film thickness by using micro infrared spectroscopy and reported the concentrations of the thickeners in the contact area decreased in Li thickener (Li-St) and increased in urea type thickener. The chemical structure of the urea thickener was aromatic diurea, high polarity thickener due to the urea groups and the aromatic hydrocarbons. In other words, it can be considered that higher polarity thickener is easy to be entrained to the contact area. In addition, their result that Li-St was difficult to be entrained to the contact area corresponds to the present study.

As another possibility, the fiber structure can be raised as shown in Figs. 54-56. The fiber structures of Li-St and Li-OHSt seem similar, however, the bearing torque behaviors and the film thicknesses for the greases containing each thickener under lower velocity were largely different. Therefore, it can be stated that the increase of film thickness due to the thickener depends on the thickener polarity rather than the thickener fiber structure for the comparison of Li type greases.

As another finding on the bearing torque in low speed conditions, the effect of the ‘repetition’ is shown in Fig. 46. The bearing torque of each grease at 200 rpm under the ‘repetition’ condition was almost the same. In another words, the higher bearing torque from L-A and S2-A at the first operation decreased at the ‘Repetition’ condition. These phenomena seem to correspond to the film thickness behaviors at low speeds under ‘deceleration’ conditions. Figures 65 and 66 suggest that the film augmenting effects of L-A and S2-A diminish after high speed conditions. The film thickness decrease at low speed after high speed condition can relate to the torque decrease of L-A and S2-A at 200 rpm after long duration tests.

That could be due to shearing effect on the thickeners. The high pressure and speed in the contact can break the thickener particles into small fragments. Therefore, the film thickness is not fully built up even if the small particles are dragged into the contact. Cann [29, 46] reported the grease film thickness decay during rotation and Kaneta et al. [21] studied the shear degradation effect on the grease film thickness decay, however, these film thickness measurements were focused on starvation behaviors (without a scoop). Cann showed the film thickness decay depends on the rotation speed and the disk revolution. Kaneta et al. showed the degraded grease film thickness is similar to that of the fresh grease at 22℃ but thinner at 75℃. Cen et al. [28] stated that mechanically worked greases prepared in a roll stability tester show lower film thickness than the fresh ones in slow speed. They also concluded that the thickener particles or fiber structure is degraded during mechanical aging and that lead to smaller particles. They used at least 24 h for the degradation time in a roll stability tester. In this study, the degradation could occur in shorter time in ball on disk contact, since the measurement of the film thickness in this study was conducted within 1 h. Hurley et al. [47] discussed the thickener lumps effect on the film thickness. The film thickness increase of the speed "increasing" curve at low speed is attributed to the passage of thickener lumps or agglomerations through the contact. However, the speed "decreasing" curve showed a smaller film thickness. This phenomenon is significant in the lumpy thickener, whose bundles are 50-300 μm in diameter. They argued that the lumps either break down in the inlet or pass around contact zone, which relates to the "noisy" behavior, and that the film thickness can actually drop with increasing speed. Such difference of the film thickness is very small for "low noise" grease with even size distribution.

In order to confirm the particles effect on the film thickness in this study, L-A prepared with different manufacturing process was examined. L-AR is highly milled L-A with the same components, therefore, the thickener particles of L-AR are finer than those of L-A. Figure 90 compares the film thickness behaviors under fully flooded condition. The interferometry images at 0.025 m/s are shown in Fig. 91. The film thickness behavior of L-AR is similar to L-A under 'deceleration' condition. In another words, the film augmenting effect at low speed conditions is negligible for L-AR. This result suggests the thickener particles of L-A changes to small particles after high speed condition. In addition, this tendency is close to Hurley's findings [47].

Considering the above discussion, it is probable that the grease thickener particles are also broken into small fragments during the bearing operation. The change of the particle can reduce the film thickness and the bearing torque at slow speeds without preventing the smooth rotations of the balls in the bearing.

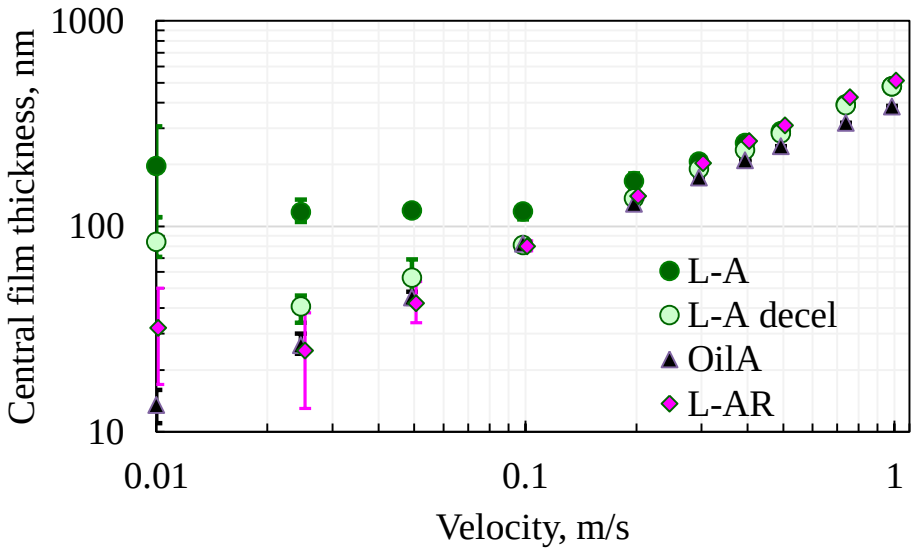

Fig. 90 Central film thickness of greases and base oil under fully flooded condition

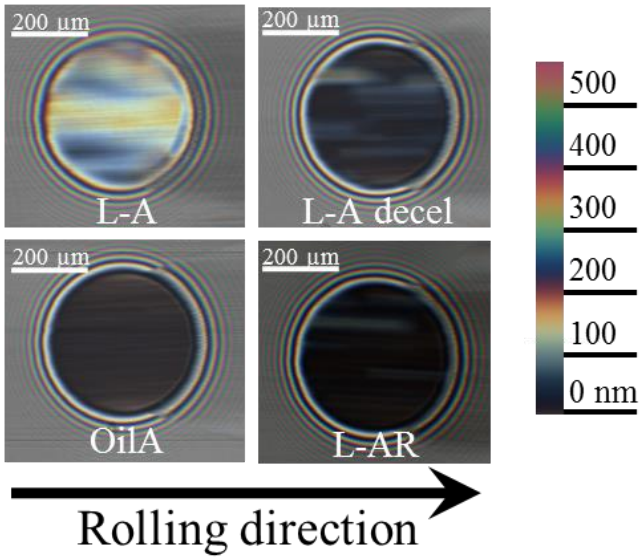

Fig. 91 Interferometry images at 0.025 m/s

7.2 Correlation with bearing torque under high speed conditions

In the high speed condition of 2000 rpm in the bearing operation, the grease movement in the bearing could occur. Therefore, the grease channeling should play an important role in reducing the bearing torque. The results described in 6.1 indicate the consistent lower bearing torques with L-A at 2000 rpm. The yield stresses of greases are shown in Fig. 52, which indicates the highest yield stress of S1-A. The viscosity gap shown in Figs. 49-51 also suggests the higher yield stress of S1-A. Since the grease could be pushed away from the cone detector during the measurement of the high shear rate, therefore, the observed viscosity became small in deceleration conditions. Oikawa et al. [8] and Nitta et al. [25] reported the correlation of the grease channeling and the bearing torque. The grease with high yield stress needs high force to start to move. Therefore, once the grease with high yield stress is excluded from the contacts in the bearing, the grease does not easily flow back to the contact area. In other words, the grease with high yield stress tends to cause the channeling, which reduces the stirring resistance of the grease in the bearing. However, this tendency may not necessarily true in all the grease types.

One of the reasons could be the thickener type. The past studies dealt with the same type grease thickener, however, this study has used three different type of Li thickeners. In this case the relationship between the yield stress and the bearing torque might become weak. Figure 53 shows the yield stresses of greases with the same Li-complex type and different thickener contents (see Table 9). Figure 92 compares the bearing torque behaviors for the Li-complex greases and indicates the lower torque with L-A at 2000 rpm. On the contrary, the torques with softer greases such as L-A(M) and L-A(S) were higher than those of harder grease (L-A) at 2000rpm. Comparing Figs. 53 and 92, there is the correlation between yield stress and the bearing torque at high rotation speed. Therefore, these results and past reports suggest that the relationship between the yield stress and the bearing torque can be recognized with the same type grease thickener.

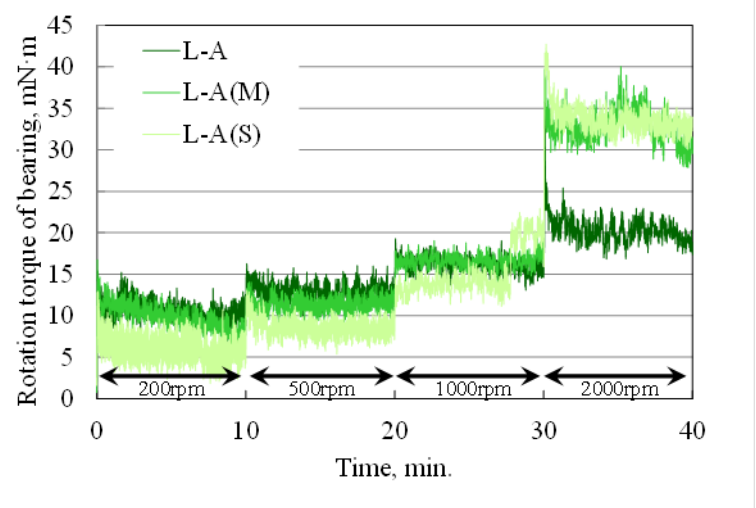

Fig. 92 Speed dependence of bearing torque with Li-complex greases with different thickener content under the ‘Screening’ condition

As another correlation factor of the bearing torque in high speed conditions, the traction coefficients behavior of greases without the scoop can be raised. As described in 6.4, L-A showed the tendency of traction coefficient increase at high velocity or SRR conditions compared with S1-A and S2-A. This increase could be due to the lack of the lubricant to the contact because the lubricant was pushed away during the disk rotation. This traction behavior of L-A without the scoop could be an indicator of the channeling of greases. Figure 93 compares traction behaviors of Li-complex greases with different thickener contents. In the high speed range, there is a tendency that the harder grease causes the higher traction coefficient. Considering the correlation of the yield stress of the Li-complex greases, these traction behaviors could relate to the bearing torque at high speed conditions.

Meanwhile, comparing bearing torque values at 2000 rpm and these traction coefficients without the scoop, torque values with L-A were low but traction coefficients of L-A were high. According to the cause of the bearing torque referred by Nitta et al. [25], the stirring resistance of lubricants should relate to channeling and the friction resistance should relate to traction coefficients. Even though the traction coefficients of L-A were high, the fact that the bearing torque values of L-A at 2000 rpm were low indicates the stirring resistance is the major cause of the bearing torque in this bearing condition. Nitta et al. [25] also discussed the significance of the stirring resistance effect on the bearing torque, therefore, this tendency in this study can be reasonable.

Based on the discussion, the bearing torque behaviors in high speed range could relate to the grease channeling. The yield stress of greases could reflect how easily the grease causes the channeling to some extent with the same type thickener. In addition, there is a possibility that the traction behaviors without a grease scoop can indicate the degree of the grease channeling.

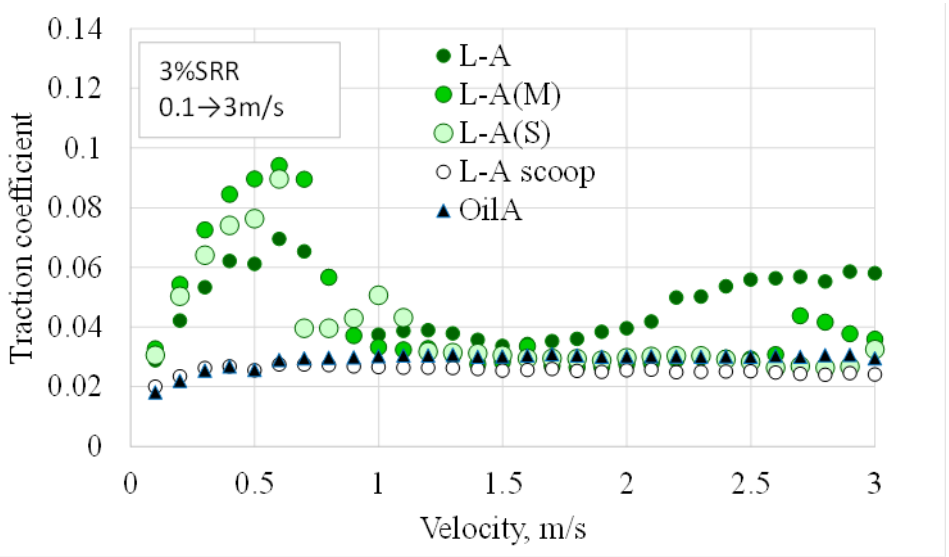

Fig. 93 Velocity dependence of Li-complex greases on traction property

7.3 Relationship among grease properties

The obtained results in this study are summarized in Table 10 regardless of the relationship with the bearing torque.

The typical grease like behaviors about the film thickness of Li-complex and Li-OHSt on smooth contacts under fully flooded conditions were explained in 7.1. The main reason could exist on the thickener particle entrainment to the contact area. On the contrary, for the Li-St thickened grease, the thickener entrainment to the contact does not occur, therefore the change of film thickness buildup effect through the high speed history is not observed.

The thickener entrainment influences not only the film thickness but also the flow patterns. Li-complex and Li-OHSt thickened greases showed flow patterns at the side track of downstream of the contact under both slow and high speed conditions. The images that thick area without colors distributes to the near side of the track as shown in Fig. 67 could be attributed to the thickener entrainments to the contacts. In contrast, Li-St thickener is not dragged into the contact, therefore the edge of the track was also surrounded by thin area. In addition, the flow patterns disappear in high speed. The high speed history has also influence the flow pattern formations. The flow patterns in slow speeds formed by L-A and S2-A became clear after high speed condition comparing Figs. 67 and 69. In Fig. 69, the large sized thickener particles pass through the contact to the side track, therefore the patterns are not so homogenized. After high speed condition, the thickener particles turn to be small and the flow pattern formed by particles passing through the contact to the side track becomes clear as shown in Fig. 69. In high speed condition, such effect on the film thickness is negligible, consequently, the flow patterns are almost the same as shown in Figs. 68 and 70. Chen et al. [34] argued that the “finger-loss” is observed after the starvation occurs with increase of the velocity. In this study, the “finger-loss,” of S1-A at high speed could relate to the starvation behavior as following discussion.

Table 10 Summary of the results

<table>
<tr><th>Supply</th><th>Surface</th><th>Property</th><th>Li-complex</th><th>Li-OHSt</th><th>Li-St</th></tr>
<tr><td rowspan="2">Flooded</td><td rowspan="3">Smooth</td><td>Thickness</td><td colspan="2">Thick in slow speed
Influenced by high speed history</td><td>Close to base oil
No change after high speed</td></tr>
<tr><td>Flow pattern</td><td colspan="2">Finger patterns on side track
Sharpened by high speed history</td><td>No fingers in high speed</td></tr>
<tr><td>Starved</td><td>Film decay</td><td colspan="2">Late starvation</td><td>Quick starvation</td></tr>
<tr><td>Flooded</td><td>Dented</td><td>Particle entrainment</td><td>Occurred</td><td>Frequently occurred</td><td>Not occurred</td></tr>
</table>

For the film thickness measurement under starved conditions without using a scoop, the Li-St thickened grease caused the quick starvation as shown in Fig. 71. One of the reasons could be that the Li-St thickener is not dragged into the contact. Without thickener entrainments, the lubricant replenishment to the contact reduces. As previously described, S1-A did not show the clear flow pattern in high speed condition at 0.4 m/s as shown in Fig. 68. Although this image was obtained under the

fully flooded condition, that indicates that S1-A is likely to cause the starvation considering the relationship between the “finger-loss” and the starvation proposed by Chen et al [34]. Comparing L-A and L-A(S) for Li-complex greases, the softer L-A(S) caused late starvation. That tendency corresponds to the Cann’s study [16], which shows the degree of starvation increases with increasing thickener content. In addition, the Li-OHSt thickened S2-A caused later starvation. Worked penetrations of S2-A and L-A(S) are almost the same, therefore the cause of difference should be the thickener type. L-A and S2-A with different thickeners have shown almost the same behaviors such as thick film thickness in slow speeds, similar flow patterns at the side of the track, and the influence of the high speed conditions on the film thickness and the flow patterns. The difference between the two greases can be observed in the film thickness formed between a dented ball and a glass disk.

The thickener entrainment to the contact area between a dented ball and a glass disk was observed in L-A and S2-A as well as between the smooth surfaces in order to understand thickener dependence on the particle entrainment to the dent. The thickener particles of the two greases sometimes existed on the dent positions, however the tendency of the greases was different. The thickener particles of L-A entered both smooth and dented areas independently. It was often observed that the thickener particles of S2-A existed near the dent areas. As a result, it was frequently observed that the thicknesses on the dents were higher in S2-A rather than in L-A, especially for sharper dents such as shown in Figs. 80 and 87. In addition, considering the result of the film thickness decay as shown in Fig. 71, the easier entrainment of S2-A to the contact and dents could bring the higher replenishment effect and postpone the starvation.

Although there is not complete evidence, it is possible that one of the causes of the difference is the chemical structure of the thickeners. Li-complex consists of Li-12-hydroxy stearate and Li-azelate, on the contrary Li-OHSt is composed of only Li-12-hydroxy stearate. High polar 12-hydroxyl groups of aliphatic chains in Li-12-hydroxy stearate could have higher affinity for the metal surface and promote the entrainment of greases into the contact area since the surfaces should be in metal oxide state and have polarity. In addition, the ratio of the 12-hydroxyl groups of aliphatic chain is higher in S2-A compared with L-A, and that difference could influence the thickener entrainment to the dented area. The higher polarity of S2-A thickener could be effective in introduction to the dented area. In other words, it can be considered that higher polarity thickener is easy to be entrained to the contact area.

This study also suggests that grease film thickness could be influenced by the surface asperity conditions depending on the thickener types. In addition, the thickener type tendency for dented surfaces could influence the film thickness of real bearings locally, since the surface of the bearing has the asperity whose depth size is similar to the dent size used in this study. However, the influence could be limited to the beginning of the bearing operation, since the effect of thickener entrainment to the contact related to the film thickness diminishes after high speed condition in the ball on disk contact.

7.4 Lubrication mechanisms

The lubrication mechanism images of bearing torque measurements in this study are illustrated in Fig. 94. First, S1-A (Li-St) showed the lowest bearing torque at low rotation speed as shown in Fig. 41. In this condition, it is considered that the grease is difficult to be pushed away, therefore, the bearing is operated under fully flooded condition, and that the channeling effect could be negligible. Based on this situation, the film thickness measurement under fully flooded conditions and at low velocity range should be focused. In the bearing, balls pass through grease lumps. If thickener particles are dragged into the contacts (L-A and S2-A), they provide the film augmenting effect but can cause resistance and increase the torque in the bearing, for instance, the thickener fibers or particles might prevent smooth rotations of bearing balls. In contrast, S1-A showed thin film thickness similar to base oil under low velocity condition, such as shown in Fig. 63. In addition, the thickener particles were not observed on the contact area. This oil-like behavior of S1-A could bring about the lower torque at low bearing rotation speed. This particle entrainment depends on the thickener type, and the structure of Li-St without 12-hydroxy group could be the reason of the difference from the other two greases. Thickener structure influence seemed weak from the TEM observation result as illustrated in Figs. 54-56. Second, at the high rotation speed of the bearing tests, L-A provided the lowest torque from Fig. 41. In this condition, the grease pathway in the bearing can be formed, therefore, the grease channeling effect could be significant. As Oikawa pointed out the correlation of the yield stress and channeling [8], the relationship with the yield stress within the same type thickener greases was confirmed as shown in Figs. 53 and 92. In addition, grease traction measurements using a MTM device without a scoop could indicate the channeling of L-A. The traction increases of L-A were observed under the high speed condition as shown in Fig. 57 and the high SRR condition as shown in Fig. 62. It can be considered that these increases were observed because the grease was pushed away from the contact area. It is worth noting that the result was observed at 2 m/s which is close to the velocity of the inner race of the bearing at high speed condition (2000 rpm), indicating the significance of the channeling effect of L-A for this condition. In addition, it is suggested that the stirring resistance should be the major cause of the bearing torque in this bearing condition rather than the friction resistance between the contacts.

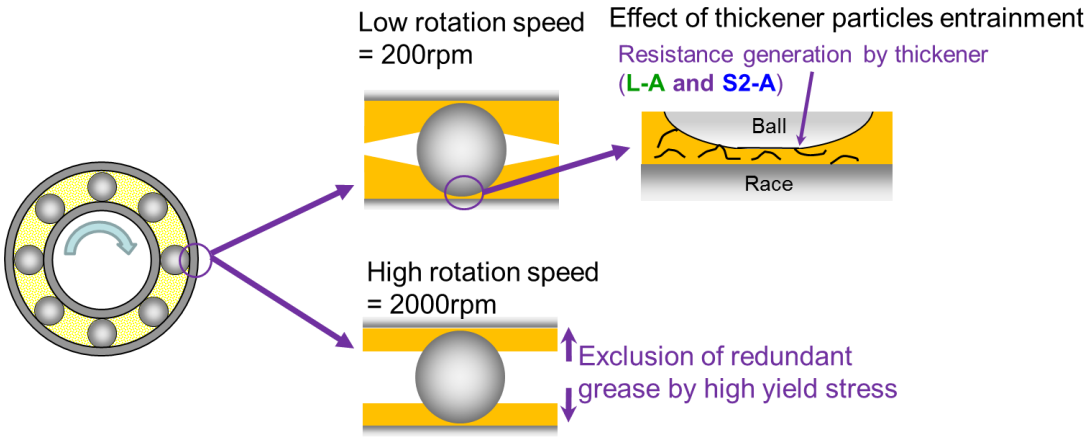

Fig. 94 Lubrication images in bearing operation

Apart from the bearing torque behaviors with greases, lubrication mechanisms for ball-on-disk contacts are proposed as illustrated in Fig. 95. The thickener of Li greases forms as fibers usually, however particle images were used as the agglomeration of thickener fibers in this discussion in accordance with the images obtained in film thickness measurements. The thickeners of L-A (Li-complex) and S2-A (Li-OHSt) can easily enter the contact surfaces due to the chemical structure with high polarity and form the thick film especially in slow speeds. In addition, the thickener of S2-A tends to be dragged into the dents with the higher polarity. However, the effect of thickness building up decreases after high speed conditions since the thickener particles are broken into small fragments by high pressure and speed condition. On the contrary, the thickeners of S1-A (Li-St) are not entrained to the contact due to lower polarity, therefore the thickness building up effect is limited and the behavior is similar to the base oil. As a result, the influence of high speed is not observed in S1-A.
The thickener entrainment to the contact reflects on the formation of the flow patterns at the downstream of the contact as shown in Fig. 96. L-A and S2-A with thickener entrainments form finger-like flow patterns and the patterns become clear after high speed condition because the size of thickeners particles diminish through the ball-on-disk contact. The thickeners of S1-A are not dragged to the contact so the flow pattern is not formed. Without the particle entrainment, the starvation could occur for S1-A quickly.

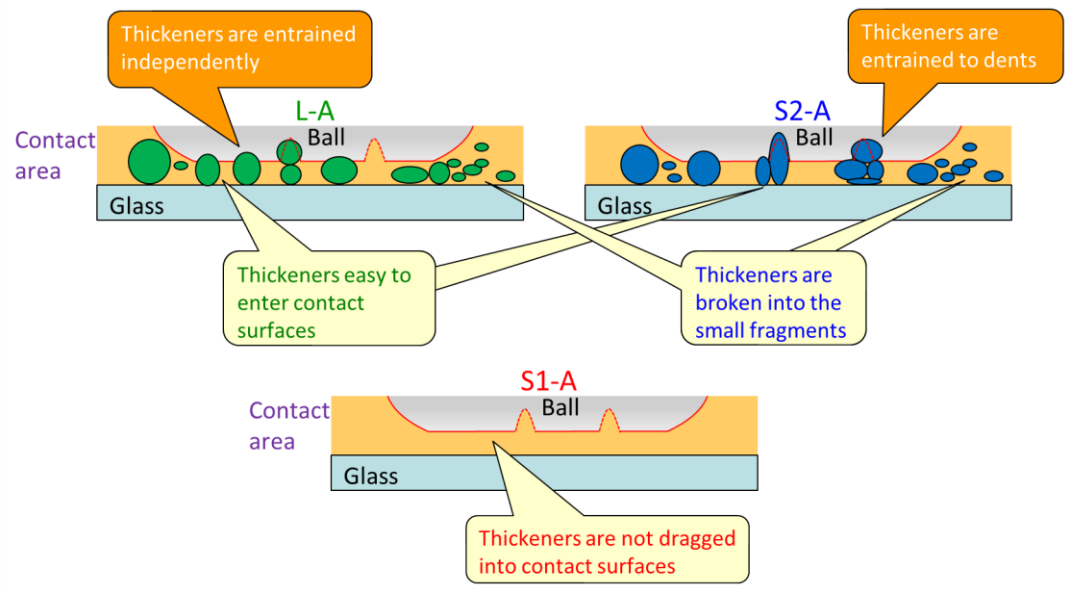

Fig. 95 Lubrication images on the contact including thickener behavior for each grease

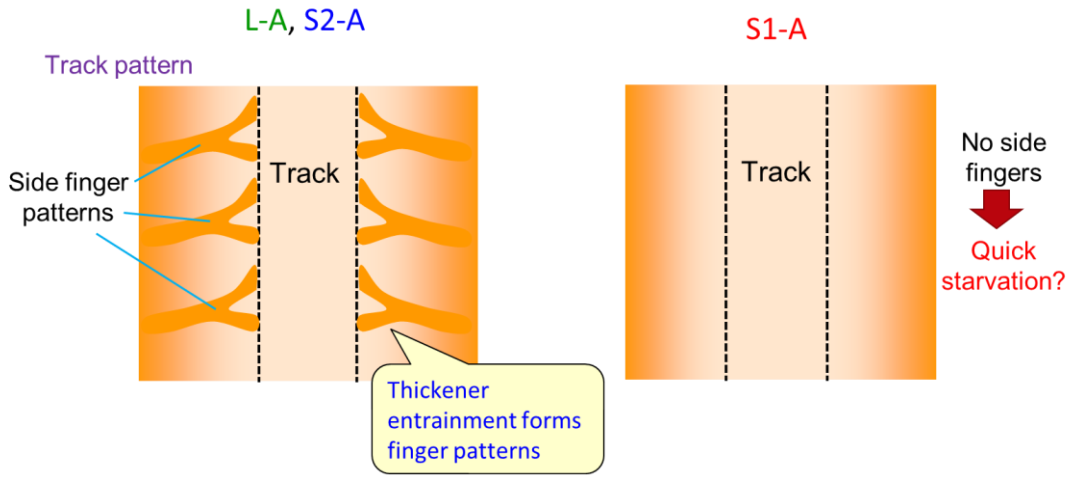

Fig. 96 The relationship between the track patterns and thickener entrainments to the contact

8 CONCLUSIONS

Most rolling element bearings are lubricated with greases. Not only the improvement of energy-saving properties by means of lowering bearing torque with appropriate grease formulations but also the clarification of the mechanism of grease lubrications is also essential for the future development of greases.

The present thesis deals with the dependence of the base oil and the Li thickener types of model greases on the bearing torque behaviors. Grease parameters such as rheology and thickener fiber structure and film thickness including surface texturing and track patterns were investigated in order to understand the relationship with the bearing torque behaviors. Especially, the effect of surface texturing on the grease film thickness had not been investigated yet.

According to the bearing torque results, the grease rank showing lower bearing torques differed by depending on the bearing operating conditions. S1-A (mineral oil and Li-St thickener) provided the lowest bearing torque at low speed condition, and L-A (mineral oil and Li-complex thickener) reduced the bearing torque at high speed condition. Grease parameters were investigated focused on the thickener dependence.

For the low speed conditions of the bearing, the film thickness behaviors seem to correlate to the bearing torque behaviors. Grease thickener entrainments to the contacts (Li-complex and Li-OHSt) build up the film thickness at low speed conditions, however, that could cause the increase of the torque in the bearing since the thickener fibers or particles might prevent smooth rotations of bearing balls. This idea is also supported by the bearing tests under ‘repetition’ conditions. After operations at high speed conditions, the bearing torques with Li-complex and Li-OHSt thickened greases at low speed condition reduced compared with the first operations and the torque values were almost the same to the Li-St thickened grease. In addition, the film augmenting effect of Li-complex and Li-OHSt diminished in the film thickness measurements with ‘deceleration’ conditions. The reason should be that grease thickener particles are broken into small fragments during the high speed conditions. The film thickness and bearing torque behaviors at low speed conditions seem correlate each other.

At high speed conditions for the bearing operation, the grease channeling could be the important factor for the bearing torque. As far as the greases with the same thickener type, the yield stress of the greases can show how easily the grease causes the channeling to some extent. For instance, the harder grease with the higher thickener content shows the higher yield stress and the lower bearing torque at high speeds. However, the tendency cannot be recognized for the different thickener greases. Instead of the yield stress, the traction coefficient behaviors of greases without grease supply could be a standard showing the grease channeling. Li-complex thickened grease (L-A) showed the obvious traction increase at high velocity or SRR conditions compared with other Li type thickeners. This traction increase could be the lack of the lubricant to the contact because the lubricant was pushed away at the high velocity or SRR conditions. This traction behavior of L-A without the grease supply could be an indicator of the channeling of greases. This tendency was confirmed in the same type Li-complex greases with different thickener contents.

Except for the bearing torque relationship, there can be found some correlations among the grease properties. The grease thickener entrainments to the contact influence on not only film thickness but also the flow patterns created at the downstream of the contact. The definite track patterns were observed for Li-complex and Li-OHSt thickened greases with particle entrainments. The patterns are also influenced by the speed history. At low speed conditions, the large sized thickener particles pass through the contact to the side track, therefore the patterns are not so homogenized. In the high speed condition, the thickener particles are broken into small particles. After that, the flow pattern formed by finer particles passing through the contact to the side track becomes clear. In contrast, track patterns were not observed clearly for Li-St thickened grease without thickener entrainment to the contact. This phenomenon could correlate to the starvation behaviors. The Li-St thickened grease caused the quick starvation. Not thickener entrainments to the contact could reduce the lubricant replenishment to the contact.

Between the Li-complex and Li-OHSt thickened greases, the difference can be confirmed on the film thickness behaviors on dented surfaces. The thickener particles of the two greases sometimes existed on the dent positions, however, it was often observed that the thickener particles of S2-A existed near the dent areas compared with L-A. The tendency was remarkable especially for sharper dents. The easier entrainment of S2-A to the contact and dents could bring the higher replenishment effect and postpone the starvation. It is possible that one of the causes of the difference is the chemical structure of the thickeners. Li-complex consists of Li-12-hydroxy stearate and Li-azelate, on the contrary Li-OHSt is composed of only Li-12-hydroxy stearate. High polar 12-hydroxyl groups of aliphatic chains could have higher affinity for the metal surface, since the surfaces should have some polarity, and promote the entrainment of greases into the contact area. The higher polarity of S2-A thickener could be effective in introduction to the dented area. On the contrary, the Li-St thickener is not entrained to the contact due to lower polarity, therefore the thickness building up effect is limited and the film thickness behavior is similar to the base oil.

In association with the scientific questions and the working hypotheses, the findings from this thesis can be concluded as follows.

1. Rheological factor

The yield stress can occasionally be an indicator of reducing the bearing torque at high speed when the same type thickener greases are used. The tendency cannot be applicable for different thickener greases. Regarding the grease channeling, the traction increase behaviors without grease supply could correlate the bearing torque behaviors at high speed conditions. The apparent viscosity itself cannot predict the bearing torque behaviors. (Hypothesis was partially confirmed)

2. Thickener structure

Thickener fiber structures were measured by TEM observation. The fibers of Li-complex were thinner and longer, in contrast the fibers of Li-St and Li-OHSt were thicker and shorter. Greases with the similar thickener structure showed different torque behaviors. In addition, film thickness behaviors were also different between

the greases. The fiber structures do not reflect the bearing torque behaviors. (Hypothesis was falsified)

3. Ability of film thickness and adaptability to surface conditions

Greases with Li-complex and Li-OHSt thickener showed higher film thickness especially at low speed. Contrary to expectations, the two type greases showed higher bearing torques at low speed conditions. The film thickness behavior of the Li-St thickened grease was similar to the base oil. The Li-St grease showed lower bearing torque at low speed. Regarding the film thickness behaviors on dented surfaces, Li-OHSt showed higher adaptability to the surface condition. However, the effect does not correlate with the torque behaviors. In contrast, the adaptability could be effective for grease replenishment to the contact. In addition, at high speed conditions, the dependence of the thickener types on the film thickness turns to be negligible and close to the base oils. Therefore, the correlation with the bearing torque at high speeds is weak. (Hypothesis was falsified)

4. Grease parameter correlation

Grease thickener entrainments influence on some grease properties, for instance, the film building up effect at low speeds, the formation of track patterns at the downstream of the contact, and the delay of the starvations. The behaviors of the film thickness and the track patterns were linked including the high speed history. The starvation is also related with the film thickness formation especially on dented surfaces, in other words, Li-OHSt thickened grease showed higher film thickness on the dented areas and the later starvation. (Hypothesis was confirmed)

9 LIST OF PUBLICATIONS

9.1 Papers published in Journals

SAKAI, K., D. KOSTAL, Y. SHITARA, M. KANETA, I. KRUPKA and M. HARTL. Influence of Li Grease Thickener Types on Film Thicknesses Formed between Smooth and Dented Surfaces. Tribology Online. 2017, 12(5), 262-273.
(Journal impact factor = 0.48)

NITTA, M., T. TSUDA, H. ARAI, K. SAKAMOTO and K. SAKAI. Effects of Transition Point of Viscoelasticity of Diurea Grease and Molecular Structure of Thickener on Running Torque of the Ball Bearing -Effects of the Alkyl Chain Length of Aliphatic Diurea-. Journal of Japanese Society of Tribologists. 2016, 61(10), 699-708 (in Japanese)
(Journal impact factor = 0.02)

SAKAI, K., Y. TOKUMO, Y. AYAME, Y. SHITARA, H. TANAKA and J. SUGIMURA. Effect of Formulation of Li Greases on Their Flow and Ball Bearing Torque. Tribology Online, 2016, 11(2), 168-173.
(Journal impact factor = 0.48)

SAKAI, K. and Y. SHITARA. Influence of Physical States of Amide Type Gel-Lubricants on their Tribological and Rheological Properties. Tribologia: Finnish Journal of Tribology. 2014, 32(2), 20-28.(Journal impact factor = 0.24)

SAKAI, K., Y. SHITARA, et al. Tribological Properties of Thermo-Reversible Gel-Lubricants Containing Solid Lubricants. Tribology Online, 2011, 6(1), 26-31.
(Journal impact factor = 0.48)

9.2 Conference abstracts

SAKAI, K., D. KOSTAL, Y. SHITARA, M. KANETA, I. KRUPKA and M. HARTL. Film Thickness Behaviors of Lithium Type Greases between Smooth and Dented Surfaces. The 18th Nordic Symposium on Tribology - NORDTRIB 2018. 2018, Uppsala, Sweden.

SAKAI, K., D. KOSTAL, Y. SHITARA, M. KANETA, I. KRUPKA and M. HARTL. An Experimental Study on the Film Thickness and Grease Flows of Lithium Type Greases. 2nd Czech-Japan Tribology Workshop. 2017, Takamatsu, Japan.

SAKAI, K., D. KOSTAL, Y. SHITARA, M. KANETA, I. KRUPKA and M. HARTL. The Experimental Study on the Relationship between Grease Film Thickness and Grease Flows. 6th European Conference on Tribology - ECOTRIB 2017. 2017, Ljubljana, Slovenia.

SAKAI, K., D. KOSTAL, Y. SHITARA, M. KANETA, I. KRUPKA and M. HARTL. Effects of Li Grease Components on Radial Ball Bearing Torque and the Grease Properties. 72nd STLE Annual Meeting & Exhibition. 2017, Atlanta, USA.

SAKAI, K., Y. TOKUMO, Y. AYAME, Y. SHITARA, H. TANAKA and J. SUGIMURA. Effect of Formulation of Li Greases on Their Flow and Ball Bearing Torque. 7th International Tribology Conference Tokyo 2015 -ITC Tokyo 2015. 2015, Tokyo, Japan.

SAKAI, K. and Y. SHITARA. Influence of Physical States of Amide Type Gel-Lubricants on their Tribological and Rheological Properties. The 16th Nordic Symposium on Tribology - NORDTRIB 2014. 2014, Aarhus, Denmark.

SAKAI, K., Y. SHITARA, et al. Tribological Properties of Thermo-Reversible Gel-Lubricants Containing Solid Lubricants. World Tribology Congress 2009 - WTC 2009. 2009, Kyoto, Japan.

10 REFERENCES

[1] HOLMBERG, K., P. ANDERSSON and A. ERDEMIR. Global Energy Consumption Due to Friction in Passenger Cars. *Tribology International*. 2012, **47**, 221-234.

[2] LUGT, P. M. A Review on Grease Lubrication in Rolling Bearings. *Tribology Transactions*. 2009, **52**, 470-480.

[3] COUSSEAU, T., B. GRACA, A. CAMPOS and J. SEABRA. Friction Torque in Grease Lubricated Thrust Ball Bearings. *Tribology International*. 2011, **44**, 523-531.

[4] COUSSEAU, T., B. GRACA, A. CAMPOS and J. SEABRA. Experimental Measuring Procedure for the Friction Torque in Rolling Bearings. *Lubrication Science*. 2010, **22**, 133-147.

[5] COUSSEAU, T., B. M. GRACA, A. V. CAMPOS and J. H. O. SEABRA. Influence of Grease Rheology on Thrust Ball Bearings Friction Torque. *Tribology International*. 2012, **46**, 106-113.

[6] GONCALVES, D., S. PINHO, B. GRACA, A. CAMPOS and J. SEABRA. Friction Torque in Thrust Ball Bearings Lubricated with Polymer Greases of Different Thickener Content. *Tribology International*. 2016, **96**, 87-96.

[7] WIKSTROM, V. and E. HOGLUND. Starting and Steady-State Friction Torque of Grease-Lubricated Rolling Element Bearings at Low temperatures—Part I: A Parameter Study. *Tribology Transactions*. 1996, **39**(3), 517-526.

[8] OIKAWA, E., N. INAMI, M. HOKAO, A. YOKOUCHI and J. SUGIMURA. Bearing Torque Characteristics of Lithium Soap Greases with Some Synthetic Base Oils. *Proc IMechE Part J: J Engineering Tribology*. 2012, **226**(6), 575-583.

[9] HOKAO, M., N. INAMI, E. WATABE, A. YOKOUCHI and J. SUGIMURA. A Study of the Structure Formed by Thickeners of Greases Using Atomic Force Microscope. *Tribology Online*. 2013, **8**(1), 76-82.

[10] DONG, D., T. KOMORIYA, T. ENDO and Y. KIMURA. Formation of EHL Film with Grease in Ball Bearings at Low Speeds. *Journal of Japanese Society of Tribologist*. 2012, **57**(8), 568-574 (in Japanese).

[11] HEYER, P. and J. LAUGER. Correlation between Friction and Flow of Lubricating Greases in a New Tribometer Device. *Lubrication Science*. 2009, **21**, 253-268.

[12] SAKAI, K., Y. TOKUMO, Y. AYAME, Y. SHITARA, H. TANAKA and J. SUGIMURA. Effect of Formulation of Li Greases on Their Flow and Ball bearing Torque. *Tribology Online*. 2016, **11**(2), 168-173.

[13] VENNER, C. H., M. T. van ZOELEN and P. M. LUGT. Thin Layer Flow and Film Decay Modeling for Grease Lubricated Rolling Bearings. *Tribology International*. 2012, **47**, 175-187.

[14] van ZOELEN, M. T., C. H. VENNER and P. M. LUGT. The Prediction of Contact Pressure–Induced Film Thickness Decay in Starved Lubricated Rolling Bearings. *Tribology Transactions*. 2010, **53**, 831-841.

[15] CANN, P. and A. A. LUBRECHT. An Analysis of the Mechanisms of Grease Lubrication in Rolling Element Bearings. *Lubrication Science*. 1999, **11**(3), 227-245.

[16] CANN, P. Starved Grease Lubrication of Rolling Contacts. *Tribology Transactions*. 1999, **42**(4), 867-873.

[17] LUBRECHT, T., D. MAZUYER and P. CANN. Starved Elastohydrodynamic Lubrication Theory: Application to Emalsions and Greases. *Comptes Rendus De L Academie Des Sciences Serie IV Physique Astrophysique*. 2001, **2**(5), 717-728.

[18] COUSSEAU, T., M. BJORLING, B. GRACA, A. CAMPOS, J. SEABRA and R. LARSSON. Film Thickness in a Ball-on-Disc Contact Lubricated with Greases, Bleed Oils and Base Oils. *Tribology International*. 2012, **53**, 53-60.

[19] GONCALVES, D., B. GRACA, A. V. CAMPOS, J. SEABRA, J. LECKNER and R. WESTBROEK. On the Film Thickness Behavior of Polymer Greases at Low and High Speeds. *Tribology International*. 2015, **90**, 435-444.

[20] LAURENTIS, N. D., A. KADIRIC, P. LUGT and P. CANN. The Influence of Bearing Grease Composition on Friction in Rolling/Sliding Concentrated Contacts. *Tribology International*. 2016, **94**, 624-632.

[21] KANETA, M., T. OGATA, Y. TAKUBO and M. NAKA. Effects of a Thickener Structure on Grease Elastohydrodynamic Lubrication Films. *Proc IMechE Part J: J Engineering Tribology*. 2000, **214**(4), 327-336.

[22] CEN, H., P. M. LUGT and G. MORALES-ESPEJEL. On the Film Thickness of Grease-Lubricated Contacts at Low Speeds. *Tribology Transactions*. 2014, **57**, 668-678.

[23] HUTTON, J. F. The Influence of Flow Elasticity on the Bearing Performance of Lubricating Grease. *Proc JSLE-ASLE International Lubrication Conference*. 1975, 707-714.

[24] LUGT, P. M. Modern Advancements in Lubricating Grease Technology. *Tribology International*. 2016, **97**, 467-477.

[25] NITTA, M., T. TSUDA, H. ARAI, K. SAKAMOTO and K. SAKAI. Effects of Transition Point of Viscoelasticity of Diurea Grease and Molecular Structure of Thickener on Running Torque of the Ball Bearing -Effects of the Alkyl Chain Length of Aliphatic Diurea-. *Journal of Japanese Society of Tribologists*. 2016, **61**(10), 699-708 (in Japanese).

[26] MORALES-ESPEJEL, G. E., P. M. LUGT, H. R. PASARIBU and H. CEN. Film Thickness in Grease Lubricated Slow Rotating Rolling Bearings. *Tribology International*. 2014, **74**, 7-19.

[27] HURLEY, S. and P. M. CANN. Starved Lubrication of EHL Contacts - Relationship to Bulk Grease Properties. *NLGI Spokesman*. 2000, **64**(2), 15-23.

[28] CEN, H., P. M. LUGT and G. MORALES-ESPEJEL. Film thickness of Mechanically Worked Lubricating Grease as Very Low Speeds. *Tribology Transactions*. 2014, **57**, 1066-1071.

[29] CANN, P. M. Grease Degradation in a Bearing Simulation Device. *Tribology International*. 2006, **39**, 1698-1706.

[30] CANN, P. M. Grease Lubrication of Rolling Element Bearings - Role of the Grease Thickener. *Lubrication Science*. 2007, **19**, 183-196.

[31] CANN, P. M. and H. A. Spikes. In Lubro Studies of Lubricants in EHD Contacts Using FTIR Absorption Spectroscopy. *Tribology Transactions*. 1991, **34**(2), 248-256.

[32] HOSHI, Y., K. TAKIWATARI, H. NANAO, H. YASHIRO and S. MORI. In Situ Observation of EHL Films of Greases by a Micro Infrared Spectroscopy. *Journal of Japanese Society of Tribologist*. 2015, **60**(2), 153-159(in Japanese).

[33] ASTROM, H., J. O. OSTENSEN and E. HOGLUND. Lubricating Grease Replenishment in an Elastohydrodynamic Lubrication Point Contact. *Journal of Tribology*. 1993, **115**(3), 501-506.

[34] CHEN, J., H. TANAKA and J. SUGIMURA. Experimental Study of Starvation and Flow Behavior in Grease-Lubricated EHD Contact. *Tribology Online*, 2015, **10**(1), 48-55.

[35] CANN, P. M. E. Thin-film Grease Lubrication. *Proc IMechE Part J: J Engineering Tribology*. 1999, **213**(5), 405-416.

[36] YOKOUCHI, A., M. HOKAO and J. SUGIMURA. Effect of Soap Fiber Structure on Boundary Lubrication of Lithium Soap Greases. *Tribology Online*. 2011, **6**(4), 219-225.

[37] CHANG, L., A. JACKSON and M. N. WEBSTER. Effects of 3-D Surface-Topography on the EHL Film Thickness and Film Breakdown. *Tribology Transactions*. 1994, **37**, 435-444.

[38] WEDEVEN, L. D. Influence of Debris Dent on EHD Lubrication. *ASLE Transactions*. 1978, **21**(1), 41-52.

[39] KANETA, M., T. KANADA and H. NISHIKAWA. Optical Interferometric Observations of the Effects of a Moving Dent on Point Contact EHL. *In: Elastohydrodynamics - '96 Fundamentals and Applications in Lubrication and Traction. Tribology Series.* 1997, **32**, 69-79.

[40] MOURIER, L., D. MAZUYER, A. A. LUBRECHT and C. DONNET. Transient Increase of Film Thickness in Micro-Textured EHL Contacts. *Tribology International*. 2006, **39**, 1745-1756.

[41] KRUPKA, I. and M. HARTL. Thin-Film Lubrication of Dented Surfaces. *Tribology Transactions*. 2007, **50**, 448-496.

[42] KRUPKA, I. and M. HARTL. The Effect of Surface Texturing on Very Thin Film EHD Lubricated Contacts. *Tribology Transactions*. 2009, **52**, 21-28.

[43] GONCALVES, D., B. GRACA, A. V. CAMPOS and J. SEABRA. On the Friction Behavior of Polymer Greases. *Tribology International*. 2016, **93**, 399-410.

[44] HARTL, M., I. KRUPKA, R. POLISCUK, M. LISKA, J. MOLIMARD, M. QUERRY and P. VERGNE. Thin Film Colorimetric Interferometry. *Tribology Transactions*. 2001, **44**, 270-276.

[45] BERTHE, L., A. ADAMS-CHAVES and A. A. LUBRECHT. Friction Measurement Indicating the Transition between Fully Flooded and Starved Regimes in Elasto-hydrodynamic Lubrication. *Proc IMechE Part J: J Engineering Tribology*. 2014, **228**(12), 1403-1409.

[46] CANN, P. M. Starvation and Reflow in a Grease-Lubricated Elastohydrodynamic Contact. *Tribology Transactions*. 1997, **39**(3), 698-704.

[47] HURLEY, S. and P. M. CANN. Grease Composition and Film Thickness in Rolling Contacts. *NLGI Spokesman*, 1999, **63**(4), 12-22.

LIST OF FIGURES AND TABLES